

OCRWM	DESIGN CALCULATION OR ANALYSIS COVER SHEET	1. QA: QA 2. Page 1
--------------	---	------------------------

3. System Uncanistered Spent Nuclear Fuel	4. Document Identifier 000-00C-DSU0-02800-000-00B
--	--

5. Title
 Commercial SNF Waste Package Design Report

6. Group
 Waste Package and Components

7. Document Status Designation

Preliminary
 Final
 Cancelled

8. Notes/Comments
 An AP-2.14Q review was completed on July 1, 2004.

Attachments	Total Number of Pages
None	

RECORD OF REVISIONS

9. No.	10. Reason For Revision	11. Total # of Pgs.	12. Last Pg. #	13. Originator (Print/Sign/Date)	14. Checker (Print/Sign/Date)	15. QER (Print/Sign/Date)	16. Approved/Accepted (Print/Sign)	17. Date
00A	Initial Issue This design report supercedes the previous document ANL-UDC-MD-000001 REV 00 to report the results for the latest Commercial SNF waste package designs. The changes are extensive and all pages are affected.	150	B-28	A.K. Scheider	T.A. Schmitt	D.J. Tunney	M.J. Anderson	03/11/2004
00B	Revised to include results of multiple calculations, revised requirement documents, and updated references.	156	B-24	A. K. Scheider <i>Adam K. Scheider</i> JUL 01, 2004	T. A. Schmitt <i>Tom Schmitt</i> 7/1/04	D. J. Tunney <i>Daniel J. Tunney</i> 7/1/2004	M. J. Anderson <i>M. J. Anderson</i>	7/1/04

CONTENTS

	Page
1. PURPOSE.....	9
2. QUALITY ASSURANCE.....	9
3. USE OF SOFTWARE.....	9
4. DESIGN INPUTS AND ASSUMPTIONS.....	9
5. GENERAL DESCRIPTION.....	10
5.1 GENERAL CONFIGURATION.....	10
5.1.1 GENERAL DESIGN BASIS FOR THE WASTE PACKAGE.....	12
5.1.2 Preclosure Design Performance Specifications.....	13
5.1.3 Postclosure Performance Specification.....	13
5.1.4 Design Descriptions.....	13
5.1.5 Waste Package Functions.....	14
5.2 COMMERCIAL SPENT NUCLEAR FUEL.....	14
5.2.1 Allocation of Commercial Spent Nuclear Fuel by Waste Package Configuration.....	15
5.2.2 Commercial Spent Nuclear Fuel Waste Package Configurations.....	16
5.3 JUSTIFICATION OF DESIGN FEATURES.....	17
5.3.1 Dimensions.....	21
5.3.2 Material Selection.....	21
5.3.3 ASME Code Position.....	24
6. SUMMARY OF DESIGN REQUIREMENTS.....	26
6.1 PRECLOSURE.....	26
6.1.1 Normal Operations.....	26
6.1.2 Event Sequence Evaluation.....	31
6.2 POSTCLOSURE.....	32
7. SATISFACTION OF DESIGN REQUIREMENTS.....	34
7.1 PRECLOSURE.....	34
7.1.1 Normal Operations.....	34
7.1.2 Event Sequences.....	49
7.2 POSTCLOSURE.....	102
7.2.1 Normal Operations.....	102
8. OPERATIONAL CONSIDERATIONS.....	103
8.1 INTERFACE REQUIREMENTS.....	103
8.2 INTERFACE WITH OTHER SYSTEMS.....	104
9. SUMMARY.....	104
10. REFERENCES.....	106
10.1 CITATIONS.....	106
10.2 CODES, STANDARDS, REGULATIONS, AND PROCEDURES.....	117
10.3 SOURCE DATA.....	118

APPENDIX A.....	A-1
A.1 POSTCLOSURE WASTE PACKAGE RESPONSE TO VIBRATORY GROUND MOTION DUE TO SEISMICITY.....	A-1
A.1.1 Preclosure Rock Fall on Waste Package.....	A-1
A.1.2 Embrittlement Due to Thermal Aging.....	A-1
A.1.3 Waste Package Response to Vibratory Ground Motion.....	A-1
A.2 TECHNICAL BASIS.....	A-1
A.2.1 Preclosure Rock Fall On Waste Package.....	A-1
A.2.2 Effects of Multiple Rock Falls.....	A-2
A.2.3 Waste Package Response to Vibratory Ground Motion.....	A-9
APPENDIX B.....	B-1
B.1 21-PWR WASTE PACKAGE.....	B-1
B.1.1 Design Basis Source.....	B-1
B.1.2 Average Source.....	B-8
B.1.3 Maximum Source.....	B-11
B.2 44-BWR.....	B-14
B.2.1 Average Source.....	B-14
B.2.2 Maximum Source.....	B-22

FIGURES

	Page
Figure 1. Schematic Illustration of the Emplacement Drift with Cutaway Views of Different Waste Packages.....	12
Figure 2. 21-PWR Surface and Cladding Temperatures in Surface Weld Cell.....	35
Figure 3. Peak Cladding Temperature—High Heat Load in Center.....	37
Figure 4. Peak Cladding Temperature—Loading Alternatives	39
Figure 5. Location of Stress on the Trunnion	41
Figure 6. Loading Curve and Projected Waste Stream, 21-PWR.....	47
Figure 7. Loading Curve and Projected Waste Stream, 44-BWR	48
Figure 8. Maximum Deformation at Room Temperature, 21-PWR.....	55
Figure 9. Maximum Deformation at 300°C, 21-PWR.....	56
Figure 10. Outer Corrosion Barrier at 600°F (Pa)	59
Figure 11. P_m Stresses at Varying Distance from the Location of Maximum Stress in the Outer Corrosion Barrier at Room Temperature	66
Figure 12. Relative Longitudinal (Y) Displacement (Raw and Filtered) of Waste Package with Respect to Emplacement Pallet for Annual Frequency of Occurrence $5*10^{-4}$ 1/yr.....	71
Figure 13. Relative Vertical (Z) Displacement (Raw and Filtered) of Waste Package with Respect to Emplacement Pallet for Annual Frequency of Occurrence $5*10^{-4}$ 1/yr.....	72
Figure 14. Relative Vertical (Z) Velocity (Raw and Filtered) of Waste Package with Respect to Emplacement Pallet for Annual Frequency of Occurrence $5*10^{-4}$ 1/yr.....	73
Figure 15. Stress Intensity (Raw and Filtered) for Waste Package Outer Barrier for Annual Frequency of Occurrence $5*10^{-4}$ 1/yr.....	74
Figure 16. Residual 1 st Principal Stress Plot in Outer Barrier (Top View) for Annual Frequency of Occurrence $5*10^{-4}$ 1/yr.....	75
Figure 17. Relative Longitudinal (Y) Displacement (Raw and Filtered) of Waste Package with Respect to Emplacement Pallet for Annual Frequency of Occurrence $1*10^{-4}$ 1/yr.....	76
Figure 18. Relative Vertical (Z) Displacement (Raw and Filtered) of Waste Package with Respect to Emplacement Pallet for Annual Frequency of Occurrence $1*10^{-4}$ 1/yr.....	77
Figure 19. Relative Vertical (Z) Velocity (Raw and Filtered) of Waste Package with Respect to Emplacement Pallet for Annual Frequency of Occurrence $1*10^{-4}$ 1/yr.....	78
Figure 20. Residual 1 st Principal Stress Plot in Outer Barrier (Top View) for Annual Frequency of Occurrence $1*10^{-4}$ 1/yr.....	79
Figure 21. Initial Stress Distribution across the Outer Corrosion Barrier Wall.....	89
Figure 22. Initial Stress (Pa) Distribution in X Direction in Outer Corrosion Barrier Caused by Annealing and Double-Sided Quenching	90

Figure 23. Initial Axial (Y-) Stress (Pa) Distribution in Outer Corrosion Barrier Caused by Annealing and Double-Sided Quenching	91
Figure 24. Effective-Strain Time History for Elements Characterized by the Peak Maximum Stress Intensity in the Inner Vessel (Elements 27077 and 27078) and Outer Corrosion Barrier (Element 10174).....	97
Figure 25. Relative Longitudinal (Y) Displacement (Raw – green and Filtered – red) of Waste Package with Respect to Emplacement Pallet for Annual Frequency of Occurrence $5*10^{-4}$ per year.....	98
Figure 26. Relative Vertical (Z) Displacement (Raw – green and Filtered – red) of Waste Package with Respect to Emplacement Pallet for Annual Frequency of Occurrence $5*10^{-4}$ per year.....	99
Figure 27. Waste Package Position at Maximum Potential Energy	100
Figure A-1. Simulation Setup for 6-MT Rock Fall with 50 cm Distance Between Impact Locations.....	A-3
Figure A-2. Finite Element Representation for 1-MT Rock Fall with 25 cm Distance Between Impact Locations.....	A-3
Figure A-3. Detail of Finite Element Representation Close to Impact Locations.....	A-4
Figure A-4. Detail of Finite Element Representation of Outer Corrosion Barrier	A-5
Figure A-5. Waste Package and Rock Deformation in Impact Region.....	A-6
Figure A-6. Elastic-Ideally-Plastic Constitutive Representation	A-7
Figure A-7. Cutaway View of Setup for Waste Package Vibratory Simulations.....	A-11
Figure A-8. Finite-Element Mesh for the Outer Corrosion Barrier of the Waste Package	A-11
Figure B-1. Surface Segments Used for Dose Rate Calculations	B-4
Figure B-2. Surface Segments Used for Dose Rate Calculations	B-18
Figure B-3. Segment of Bottom Surface of Outer Lid Used in Dose Rate Calculations	B-19

TABLES

	Page
Table 1. Standard Nomenclature for Waste Package Components	15
Table 2. Yield and Tensile Strengths of Alloy 22 (UNS N06022) and Stainless Steel Type 316.....	23
Table 3. Waste Package Handling Limits Performance Requirements	26
Table 4. Waste Package Closure Performance Requirements	26
Table 5. Preclosure Containment Performance Requirements	27
Table 6. Uncanistered SNF Quantities and Characteristics Performance Requirements	28
Table 7. Boiling Water Reactor Fuel	29
Table 8. Pressurized Water Reactor Fuel.....	30
Table 9. Postclosure Primary Performance Requirements	31
Table 10. Postclosure Confinement Performance Requirements	33
Table 11. Criticality Control Performance Requirements	33
Table 12. Fuel Cladding Temperature Results	36
Table 13. Peak Cladding Temperatures with High Heat Loads in Center.....	36

Table 14. Fuel Cladding Temperature Results	37
Table 15. Maximum Stress Intensities at Room Temperature.....	40
Table 16. Maximum Stress Intensities at 300°C.....	40
Table 17. Outer Corrosion Barrier Maximum Tangential Stress at the Outer Surface.....	42
Table 18. Outer Corrosion Barrier Maximum Tangential Stress at the Inner Surface	42
Table 19. Minimum Required Axial Gap Between the Inner and Outer Corrosion Barriers	43
Table 20. Resulting Gage Pressure with Respect to Ambient Pressure.....	44
Table 21. Calculation Results	44
Table 22. Non-dimensional Results.....	44
Table 23. Stresses in Degraded Waste Package (MPa)	45
Table 24. Cavity Design Dimensions	47
Table 25. 21-PWR Fire Calculation Case Descriptions.....	50
Table 26. Calculated Peak Temperatures for 21-PWR Fire Calculations	50
Table 27. Summarized Peak Cladding Temperature for 44-BWR	51
Table 28. Original 44-BWR Waste Package Fire Accident Evaluation Cases (800°C fire for 30 minutes).....	51
Table 29. 44-BWR Waste Package Fire Accident Evaluation Cases for Sensitivity Study	51
Table 30. Missile Impact Parameters for Three Different Case Studies.....	56
Table 31. Pressurized System Missile Impact Results for Different Waste Packages	57
Table 32. Maximum Wall Averaged Stress Intensity for 21-PWR Vertical Drop	58
Table 33. Maximum Stress for 44-BWR Vertical Drop.....	58
Table 34. Maximum Through-Wall Stress Intensity, Location Averages	60
Table 35. Maximum Wall Average Stress Intensities	60
Table 36. Allowable P_m Limits for OCB	61
Table 37. OCB P_m Evaluation.....	61
Table 38. Maximum Wall Average Stress Intensities	62
Table 39. Wall-Averaged Stress Intensity in the Outer Barrier.....	63
Table 40. Maximum Stress Intensities.....	63
Table 41. Maximum Stress Intensities (σ_{int}).....	64
Table 42. Wall-Averaged Stress Intensities.....	65
Table 43. Wall-Averaged Shear Stress of the Outer Corrosion Barrier at 300°C	65
Table 44. Component Based Membrane Stress Intensity in the Outer Corrosion Barrier at Room Temperature	67
Table 45. Wall-Averaged Stress Intensity in the Outer Corrosion Barrier.....	68
Table 46. Maximum Stress Intensity	68
Table 47. Maximum Stress Intensities in the Outer Corrosion Barrier	69
Table 48. Maximum Stress Intensities.....	70
Table 49. Maximum Stress Intensities for the 44-BWR Waste Package Swing Down	70
Table 50. Results for Three Different Initial Stress Approximations.....	92
Table 51. Strain-Rate Parameters	94
Table 52. Maximum Stress Intensity in Outer Corrosion Barrier and Inner Vessel for Three Different Levels of Strain-Rate Sensitivity.....	95
Table 53. Parameters Defining Strain-Rate Sensitivity for Inner Vessel and Outer Corrosion Barrier at the Time Characterized by Maximum Stress Intensity.....	95

Table 54. Ratio of Maximum Stress Intensity and True Tensile Strength in Outer Corrosion Barrier and Inner Vessel for Three Different Levels of Strain-Rate Sensitivity	96
Table 55. Resultant Impact Velocities by Parameter	101
Table 56. Resultant Maximum Stress Intensity by Parameter	102
Table 57. Waste Package Handling Limits Performance Requirements	103
Table 58. Waste Package Closure Performance Requirements	104
Table A-1. Relative Change of Stresses and Effective Plastic Strain for 0.1-MT Rock Fall for Three Different Impact Distances	A-7
Table A-2. Relative Change of Stresses and Effective Plastic Strain for 1-MT Rock Fall for Three Different Impact Distances	A-9
Table A-3. Relative Change of Stresses and Effective Plastic Strain for 6-MT Rock Fall for Three Different Impact Distances	A-9
Table A-4. Failed Area from Vibratory Ground Motion at a Peak Ground Velocity of 2.44 m/s	A-13
Table B-1. Dose Rates on Inner Surface of Inner Vessel: Design Basis PWR SNF (no Concrete)	B-1
Table B-2. Dose Rates on Waste Package Outer Radial Surface: Design Basis PWR SNF (no Concrete)	B-2
Table B-3. Dose Rates on Radial Surface 1 m from Waste Package: Design Basis PWR SNF (no Concrete)	B-2
Table B-4. Dose Rates on Radial Surface 2 m from Waste Package: Design Basis PWR SNF (no Concrete)	B-3
Table B-5. Dose Rates on Segments of Axial Surfaces: Design Basis PWR SNF (no Concrete)	B-3
Table B-6. Dose Rates on Inner Surface of Inner Vessel: Design Basis PWR SNF (Concrete)	B-5
Table B-7. Dose Rates on Waste Package Outer Radial Surface: Design Basis PWR SNF (Concrete)	B-5
Table B-8. Dose Rates on Radial Surface 1 m from Waste Package: Design Basis PWR SNF (Concrete)	B-6
Table B-9. Dose Rates on Radial Surface 2 m from Waste Package: Design Basis PWR SNF (Concrete)	B-6
Table B-10. Dose Rates on Segments of Axial Surfaces: Design Basis PWR SNF (Concrete)	B-7
Table B-11. Dose Rates on Inner Surface of Inner Vessel: Average PWR SNF (Concrete)	B-8
Table B-12. Dose Rates on Waste Package Outer Radial Surface: Average PWR SNF (Concrete)	B-8
Table B-13. Dose Rates on Radial Surface 1 m from Waste Package: Average PWR SNF (Concrete)	B-9
Table B-14. Dose Rates on Radial Surface 2 m from Waste Package: Average PWR SNF (Concrete)	B-9
Table B-15. Dose Rates on Segments of Axial Surfaces: Average PWR SNF (Concrete)	B-10
Table B-16. Dose Rates on Inner Surface of Inner Vessel: Maximum PWR SNF (Concrete)	B-11
Table B-17. Dose Rates on Waste Package Outer Radial Surface: Maximum PWR SNF (Concrete)	B-11

Table B-18. Dose Rates on Radial Surface 1 m from Waste Package: Maximum PWR SNF (Concrete)	B-12
Table B-19. Dose Rates on Radial Surface 2 m from Waste Package: Maximum PWR SNF (Concrete)	B-12
Table B-20. Dose Rates on Segments of Axial Surfaces: Maximum PWR SNF (Concrete)...	B-13
Table B-21. Dose Rates on Inner Surface of Inner Vessel: Average BWR SNF (no Concrete).....	B-14
Table B-22. Dose Rates on Waste Package Outer Radial Surface: Average BWR SNF (no Concrete).....	B-15
Table B-23. Dose Rates on Radial Surface 1 m from Waste Package: Average BWR SNF (no Concrete)	B-15
Table B-24. Dose Rates on Radial Surface 2 m from Waste Package: Average BWR SNF (no Concrete)	B-16
Table B-25. Dose Rates on Segments of Axial Surfaces: Average BWR SNF (no Concrete). B-17	
Table B-26. Dose Rates on Inner Surface of Inner Vessel: Average BWR SNF (Concrete) ...	B-19
Table B-27. Dose Rates on Waste Package Outer Radial Surface: Average BWR SNF (Concrete)	B-19
Table B-28. Dose Rates on Radial Surface 1 m from Waste Package: Average BWR SNF (Concrete)	B-20
Table B-29. Dose Rates on Radial Surface 2 m from Waste Package: Average BWR SNF (Concrete)	B-20
Table B-30. Dose Rates on Segments of Axial Surfaces: Average BWR SNF (Concrete).....	B-21
Table B-31. Dose Rates on Inner Surface of Inner Vessel: Maximum BWR SNF (Concrete)	B-22
Table B-32. Dose Rates on Waste Package Outer Radial Surface: Maximum BWR SNF (Concrete)	B-22
Table B-33. Dose Rates on Radial Surface 1 m from Waste Package: Maximum BWR SNF (Concrete)	B-23
Table B-34. Dose Rates on Radial Surface 2 m from Waste Package: Maximum BWR SNF (Concrete)	B-23
Table B-35. Dose Rates on Segments of Axial Surfaces: Maximum BWR SNF (Concrete)...	B-24

1. PURPOSE

A design methodology for the waste packages and ancillary components (i.e., the emplacement pallets and drip shields) has been developed to provide designs that satisfy the safety and operational requirements of the Yucca Mountain Project. This methodology is described in the *Waste Package Component Design Methodology Report* (Mecham 2004 [DIRS 169790]). To demonstrate the practicability of this design methodology, four waste package configurations have been selected to illustrate the application of the methodology. These four configurations are the 21-pressurized water reactor (PWR) absorber plate waste package, the 44-boiling water reactor (BWR) waste package, the 5-defense high-level radioactive waste (DHLW)/U.S. Department of Energy (DOE) spent nuclear fuel (SNF) codisposal short waste package, and the naval canistered SNF long waste package. Also included in this demonstration is the emplacement pallet and continuous drip shield.

The purpose of this report is to document how that design methodology has been applied to the waste package configurations intended to accommodate uncanistered commercial SNF. This demonstrates that the design methodology can be applied successfully to these waste package configurations and support the License Application for construction of the repository. In this document, the results of design calculations are summarized and used to show that the designs are in compliance with the applicable criteria in *DOE and Commercial Waste Package System Description Document* (BSC 2004 [DIRS 167273]) and *Project Design Criteria Document* (Doraswamy 2004 [DIRS 169548]).

2. QUALITY ASSURANCE

The Commercial SNF waste packages are classified as Safety Category items (BSC 2003 [DIRS 165179], Table A-2, p. A-3). Therefore, this document is subject to the requirements of *Quality Assurance Requirements and Description* (DOE 2004 [DIRS 168669]). This document was developed in accordance with AP-3.12Q, *Design Calculations and Analyses*.

3. USE OF SOFTWARE

No computer software or models were used in the generation of this report. Contributory calculations provide descriptions of software used.

4. DESIGN INPUTS AND ASSUMPTIONS

Generic design inputs and assumptions that are used in contributory calculations to this report may be found in *Waste Package Component Design Methodology Report* (Mecham 2004 [DIRS 169790], Sections 4 and 5). Specific design inputs and assumptions may be found in the supporting calculations.

5. GENERAL DESCRIPTION

5.1 GENERAL CONFIGURATION

Section 114(a)(1)(B) of the Nuclear Waste Policy Act of 1982 (NWPA), as amended (42 U.S.C. 10134(a)(1)(B)) [DIRS 101681], requires “a description of the waste form or packaging proposed for use at such repository, and an explanation of the relationship between such waste form or packaging and the geologic medium of the site.” This section describes the waste forms to be disposed, along with their packaging. An explanation of the important parameters considered in the design of the waste package is included in this section, as is a summary of the expected performance of the waste package design. This section:

- Presents an overview of the waste forms and the waste package design
- Describes the waste package, its design bases, and its functions
- Discusses in detail the waste forms, the parameters considered in designing the waste package (and its variations), and the evaluations performed on the design
- Describes the material selection of the waste package
- Presents the results of design evaluations of the waste package.

Waste Form Overview—Waste forms to be received and packaged for disposal include SNF from commercial power reactors, SNF owned by the DOE (including naval fuel), and canisters of solidified high-level radioactive waste from prior commercial and defense fuel reprocessing operations.

Section 114(d) of the NWPA (42 U.S.C. 10134(d) [DIRS 101681]) limits the first repository’s capacity to no more than 70,000 metric tons of heavy metal (MTHM) “...until such time as a second repository is in operation.” The types of waste that would be accepted at the repository have been allocated as follows (DOE 2002 [DIRS 155970], Chapter 2):

- 63,000 MTHM of commercial SNF
- 7,000 MTHM of DOE high-level radioactive waste, commercial high-level radioactive waste, and DOE SNF.

The waste forms received at a repository are in solid form. Materials that can ignite or react chemically at a level that compromises containment or isolation are not accepted by the repository. Neither the waste forms nor the waste packages contain free liquids that can compromise waste containment. Materials that are regulated as hazardous waste under the Resource Conservation and Recovery Act of 1976 (42 U.S.C. 6901 et seq. [DIRS 103936]) are not disposed in the repository (DOE 1999 [DIRS 105164], Section 4.2.3).

Waste Package Overview—The design of a waste package is based on the characteristics of the waste forms that it would hold. Because commercial and DOE high-level radioactive waste forms have similar characteristics, both may be placed into a waste package of the same design. This has allowed the DOE to design one waste package, with flexible configurations, that is capable of accommodating all types of SNF and high-level radioactive waste currently generated or anticipated in the United States, whether commercial or governmental.

The waste package has been designed, in conjunction with the natural and other engineered barriers, to ensure compliance with applicable U.S. Nuclear Regulatory Commission (NRC) regulations, to contribute to safe operations during the preclosure phase, to make efficient use of the potential repository area, and to preserve the option of retrieving the waste. To perform its containment and isolation functions, the waste package described in this report has been designed to take advantage of a location in the unsaturated zone.

The waste package design consists of two concentric cylinders in which the waste forms are placed. The inner cylinder is composed of stainless steel type 316. The outer cylinder is made of a corrosion-resistant nickel-based alloy (Alloy 22 [UNS N06022]). The waste package configurations for DOE SNF and high-level radioactive waste are larger in diameter and thicker than those for commercial SNF. The outer layer of corrosion-resistant material protects the underlying layer of structural material from corrosion, and the structural material supports the thinner material of the outer layer.

The waste package design has outer and inner lids. The outer (closure) lids are made of Alloy 22 (UNS N06022). The inner lids are made of stainless steel type 316. In addition to the inner and outer lids, an Alloy 22 (UNS N06022) lid on the closure end of the waste package (middle lid) provides additional protection against stress corrosion cracking in the closure weld area.

Before the double-walled waste package is sealed, helium is added as a fill gas (BSC 2004 [DIRS 167278], Section 3.1.1.7.3). The helium prevents oxidation of the waste form and helps transfer heat from the waste form to the wall of the inner vessel of the waste package. Transferring heat away from the waste form is an important means of controlling waste form temperatures. This helps preserve the integrity of the metal cladding on the fuel rods, thus extending the life of an existing barrier to water infiltration.

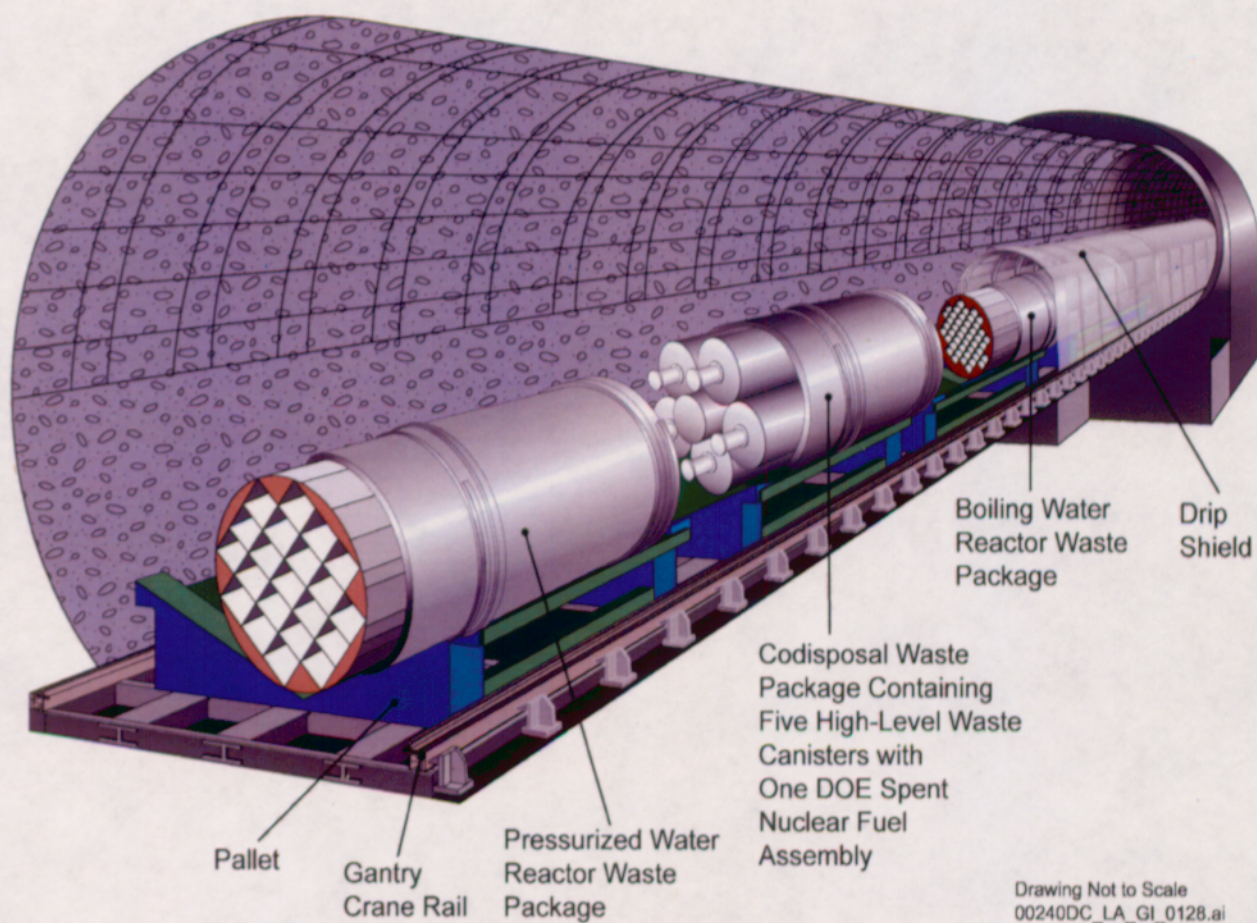
All waste package design configurations use a remote lifting-and-handling mechanism. The collar-sleeve-and-trunnion joint apparatus allows the necessary handling of the waste package before it is placed on an emplacement pallet and transferred to the designated drift. Each waste package also has a unique permanent identifying label (BSC 2003 [DIRS 167318], Section 6.4.2 and BSC 2003 [DIRS 167319], Section 6.4.2).

Although they share the features described previously, the waste package design configurations have different internal components to accommodate the different waste forms. For example, the waste package configurations for uncanistered commercial SNF has an internal basket assembly to support fuel assemblies. In other waste package configurations (e.g., for high-level radioactive waste and DOE SNF), the internal basket has a different design, or, as is the case

with naval SNF, the basket is contained inside the canister. Internal components are discussed in more detail in the respective waste package design sections.

5.1.1 GENERAL DESIGN BASIS FOR THE WASTE PACKAGE

The waste isolation system is an important element of the repository. The primary component of the system is the waste package. As defined in 10 CFR 63.2 [DIRS 158535], a waste package includes the waste form and any containers, shielding, packing, and other absorbent materials immediately surrounding it. The invert material does not immediately surround the waste package, so it is not considered part of the waste package. Figure 1 illustrates the waste package within the emplacement drift of the waste isolation system.



Source: Mecham 2004 [DIRS 169790], Figure 2

Figure 1. Schematic Illustration of the Emplacement Drift with Cutaway Views of Different Waste Packages

The waste package has been designed to use materials that perform well under the anticipated conditions at Yucca Mountain. The design analyses performed on the waste package include evaluations of structural integrity, thermal performance, criticality safety, and shielding properties.

5.1.2 Preclosure Design Performance Specifications

The performance specifications for the functionality of the waste package during the repository's preclosure phase are consistent with 10 CFR 63.112(b) (10 CFR 63 [DIRS 158535]). This regulation provides for the DOE analysis of the ability of the waste package structures, systems, and components to perform their intended safety functions during an accident or event sequences. For the waste package, event sequences are determined by identifying the functions of the waste package and evaluating the effects on its performance of given events that could occur during normal handling of the waste package or during a credible accident scenario (i.e., events that have at least 1 chance in 10,000 of occurring before permanent closure of the repository) 10 CFR 63.2 [DIRS 158535].

These event sequences and their effects on performance were defined by reviewing the results of BSC 2003 [DIRS 164128], Section 6 constituting a bounding list of preclosure event sequences that could affect the waste packages. Structural, thermal, and criticality analyses are performed according to this list.

5.1.3 Postclosure Performance Specification

10 CFR 63.113(b) [DIRS 158535] requires the entire repository system to meet specific dose limits for 10,000 years. The waste package is one of many barriers relied upon to meet this limit. The objective is to design a waste package that works in concert with the natural environment to meet performance standards while reducing the uncertainty associated with the current understanding of natural processes at the site.

5.1.4 Design Descriptions

An analysis was undertaken to determine the number of designs needed to handle the different waste forms that would constitute the anticipated waste stream in the most economical manner (CRWMS M&O 1997 [DIRS 100224]). The objective of the evaluation was to determine:

- The number of different waste package configurations needed
- The capacity of each waste package configuration (i.e., the amount of waste it would hold)
- The limits on SNF properties (e.g., age, thermal characteristics) that might apply to each waste package design.

The complete system of waste package configurations is intended to allow reliable disposal of those waste forms that a repository would accept while still enhancing overall efficiencies.

To determine the most efficient set of waste package configurations for commercial SNF, the DOE designed waste package configurations of various assembly-holding capacities and incorporated into the design methods for removing decay heat and preventing criticality. This resulted in the selection of a set of five waste package configurations as the most efficient means

of accommodating the anticipated waste stream of commercial SNF. These five are: 12-PWR waste package, 21-PWR waste package with absorber plate, 21-PWR waste package with control rods, 44-BWR waste package, and 24-BWR waste package.

5.1.5 Waste Package Functions

Waste containment begins when the waste form is sealed in the waste package. Once sealed, the waste package ensures a dry and stable physical and chemical environment for as long as it remains intact. The waste package is designed to work with the natural environment: the material for the outer barrier of the waste package was selected because of its resistance to corrosion in an environment such as the one expected at Yucca Mountain (CRWMS M&O 2000 [DIRS 138173]).

The waste package performs a number of other functions. System description documents define each function as the basis for a waste package performance specification (BSC 2004 [DIRS 167273], Section 2.1, Figure 1). The waste package, in conjunction with other systems, has been designed to:

- Provide preclosure containment
- Provide postclosure containment
- Control Criticality
- Maintain the Waste Form

5.2 COMMERCIAL SPENT NUCLEAR FUEL

In most nuclear fuel assemblies, the tubes containing the fuel pellets are made of Zircaloy, a zirconium-based material. The generic name for the metal that the tubes are composed of is "cladding." Zirconium-based cladding is used for 98.5 percent of PWR fuel assemblies and 99.8 percent of BWR fuel assemblies. The cladding on the remainder is made of stainless steel. Future fuel designs are not expected to change from mostly zirconium-based cladding (CRWMS M&O 1999 [DIRS 145022], Section 3.1.1).

In addition to standard commercial fuel assemblies, a small portion (less than 2 percent) of the SNF will arrive in canisters containing individual fuel rods. Utilities may repackage fuel rods that have damaged cladding in these canisters to confine radioactive materials during handling and shipment. To ensure that waste package designs have the flexibility to accommodate canistered fuel, the canisters have sizes within the range of dimensions that qualify as standard fuel. Thus, it is possible to handle and dispose of canistered fuel in the same way as uncanistered SNF assemblies (CRWMS M&O 1999 [DIRS 145022], Section 3.2). The 12-PWR waste package will be able to accommodate canisters containing DOE owned SNF of commercial origin (Section 11.3, DOE 2002 [DIRS 158398]). The maximum external dimensions of this canister are 9.00 in. by 9.00 in. (229 mm), and a length of 201.2 in. (5.110 m). These are within the design specifications of the 12-PWR waste package (see Section 7.1.1.4).

There are a number of major components that comprise the waste package. A standard nomenclature has been established for referring to these components. This nomenclature is shown in Table 1.

Table 1. Standard Nomenclature for Waste Package Components

Preferred Terminology	Acceptable for Clarity or Brevity	Description
Trunnion Sleeve	Trunnion Collar Sleeve	The welded attachment that accepts the trunnion collar
Trunnion Collar		The removable ring that mates with the trunnion sleeve
Outer Corrosion Barrier	Outer Barrier Alloy 22 Shell	The Alloy 22 (UNS N06022) shell (sides and the outer barrier bottom lid)
Outer Lid	Final Alloy 22 Lid	The outermost lid, Alloy 22 (UNS N06022)
Middle Lid		The first Alloy 22 (UNS N06022) lid, the middle of three lids
Spread Rings		The four-part ring that, when spread into position, mechanically holds the inner vessel lid in place
Inner Vessel Lid	Inner Lid	The stainless steel lid that seals the Inner Vessel
Inner Vessel	Stainless Steel Vessel	The inner vessel that is the ASME B&PV code-stamped pressure vessel
Shell Interface Ring		The stainless steel ring that sits between the support ring and the inner vessel
Inner Vessel Support Ring		The Alloy 22 (UNS N06022) ring that keeps the inner vessel off of the bottom of the outer corrosion barrier

Source: BSC 2003 [DIRS 167167], Appendix D

5.2.1 Allocation of Commercial Spent Nuclear Fuel by Waste Package Configuration

The characteristics of SNF assemblies (i.e., size, thermal output, and reactivity) are used to select the appropriate waste package configuration. The size of assemblies is used to determine the size and configuration of the fuel within the waste package, and to perform structural analyses to evaluate the integrity of the waste package during normal handling and event sequences. The thermal output and reactivity of the fuel is used to determine which waste package can accommodate each given fuel assembly.

5.2.1.1 Thermal Output

Commercial SNF arriving at the repository is expected to have a wide range of thermal outputs. The key factors used to determine the thermal output of SNF are its age (i.e., number of years out of the reactor), burnup (measured in gigawatt-days per metric ton of uranium), and initial enrichment of fissile material (i.e., uranium-235 or plutonium). To cover anticipated thermal outputs, the average characteristics are considered. Maximum characteristics are also evaluated to ensure that these fuel assemblies could be placed in the waste package.

Determining which waste package configuration can accommodate a particular SNF assembly thermally requires calculating the assembly's thermal output at the time it is emplaced in the repository. The appropriate waste package configuration is chosen to ensure that the maximum

thermal output limit is not violated. In the higher-temperature operating mode, this limit has been set at 11.8 kW (BSC 2004 [DIRS 167273], Section 3.1.1.5).

Of the five commercial waste package configurations, the 21-PWR waste package is the most limiting in thermal output as it is closest to 11.8 kW per waste package (BSC 2004 [DIRS 166941], Table 7). The characteristics of SNF assemblies loaded into this waste package type are carefully chosen to ensure that the thermal output limit is not violated.

The thermal output of the waste package can be reduced, if necessary, to accommodate either a range of thermal operating modes or potential changes in the characteristics of the waste stream. Reduction can be achieved by using one or more of the following waste package loading strategies: (1) fuel blending (i.e., combining low heat output fuel and high heat output fuel within a single waste package); (2) de-rating (i.e., loading fewer assemblies than the waste package is designed to hold); or (3) increasing the use of the 12-PWR waste package (i.e., placing high heat output fuel in smaller waste packages).

5.2.1.2 Criticality Control

Waste package configurations are evaluated to ensure that subcritical limits can be met, as well as the thermal limits described in the previous section. Loading curves are developed from commercial SNF parameters to determine the method of loading waste packages. This ensures that the reactivity of the fuel being loaded is below the level at which criticality could occur.

5.2.2 Commercial Spent Nuclear Fuel Waste Package Configurations

All the waste package configurations for commercial SNF have similar components that perform multiple functions. The internal components of commercial SNF waste package configurations are described in this section, along with their functions.

5.2.2.1 Internal Basket Design

Baskets are composed of interlocking plates, fuel tubes, thermal shunts, structural guides, and control rods in a small percentage of waste packages needing extra criticality control (BSC 2004 [DIRS 167273], Section 4.1.2.2).

Interlocking Plates—The interlocking plates set the pattern for how the fuel assemblies will be arranged inside the inner barrier of the waste package. The interlocking plates are made of SA 516 Grade 70 carbon steel or a neutron absorbing material.

The neutron absorber materials that prevent criticality can be placed directly into the plates using Ni-Gd Alloy (UNS N06464) (BSC 2004 [DIRS 169959]) or can take the form of separate control rods. Plates that include neutron absorber material vary in thickness and number of plates, depending on the design. For example, the 44-BWR waste package has more, thinner plates than the 21-PWR waste package.

The interlocking plates provide fuel basket structural strength, which is necessary to maintain the fuel geometry during event sequences.

Fuel Tubes—The fuel tubes are long, square containers that fit inside and support the structure created by the interlocking plates and hold the fuel assemblies in place. The fuel basket tubes help provide structural strength to the basket during event sequences. The fuel tubes for each waste package configuration are made of SA 516 Grade 70 carbon steel.

Thermal Shunts—All the waste package configurations for commercial SNF except the 24-BWR require thermal shunts. These shunts, which are made of SB 209 A96061 T4 (an aluminum alloy), are placed alongside the interlocking plates. The shunts are added to help transfer heat from the waste form to the walls of the waste package. Adding thermal shunts is a simple and effective method to improve heat conduction between the center of the waste package and the outer edge of the internal basket, providing a reliable means of keeping the temperature of the cladding within design limits. Limiting cladding temperatures helps protect the waste form by minimizing damage to the fuel cladding.

Structural Guides—The structural guides for each waste package configuration are made of 516 Grade 70 carbon steel and are placed inside the inner vessel of the waste package to hold the basket structure in place. They help maintain fuel geometry, which can prevent criticality during event sequences. The structural guides also help conduct heat from the waste form to the walls of the waste package, where it is transferred to the surrounding drift walls.

Control Rods—Absorber rods, similar to the absorber rods used in reactor applications, are used sparingly in the waste package design. They are used only in waste packages containing highly reactive fuel assemblies from PWRs, where long-term criticality control is required.

5.3 JUSTIFICATION OF DESIGN FEATURES

Accommodation of the fuel for all commercial waste package configurations was determined in *Sizing of Uncanistered Fuel Waste Package Cavity* (BSC 2003 [DIRS 163984], Attachment III). The size of the cavities for all commercial waste packages is summarized in BSC (2003 [DIRS 163984], Table 6-1). The cavity length for both waste package types is 180.5 in. (4.585 meters) from this table. The clear square insertion for the 21-PWR waste package is 8.80 in. (224 mm), while it is 6.00 in. (152 mm) for the 44-BWR waste package.

The outer lid is designed with a flat top. This is a result of the value engineering study in *Value Study Report—Waste Package Reevaluation* (BSC 2003 [DIRS 163185], Attachment III). With the middle lid present, it is unnecessary to use induction annealing on the final weld. Therefore, the final lid will be laser peened or controlled plasticity burnished to reduce residual stresses (BSC 2004 [DIRS 167278], Section 4.1.1.6).

The bottom trunnion sleeve will be extended past the outer barrier to act as an energy absorber in case of an accident. The part that extends will have a tapered surface to allow runoff when the waste package is horizontal.

For ease of assembly, the inner vessel and outer barrier will have a gap in between, both radially and axially. The axial gap will be at least 10 mm (0.39 in.) (BSC 2003 [DIRS 161691], Section 7), and the radial gap will be at least 1 mm (0.04 in.) (BSC 2001 [DIRS 152655], Section

6.1, Table 4). These distances account for differences in thermal expansion values for Alloy 22 (UNS N06022) and stainless steel type 316.

The shell interface ring is added as a measure to absorb energy during the corner drop load case. Its placement alleviates high stresses from occurring in the inner vessel bottom corner (CRWMS M&O 2000 [DIRS 157822], Section 6).

The support ring is added to prevent the weight of the fuel from creating a force in the middle of the bottom lid of the outer barrier when the waste package is in the vertical position. The support ring elevates the inner vessel and prevents it from contacting the outer barrier.

The middle lid design minimum thickness is 10 mm (0.39 in.). There is no stress mitigation on the fillet weld that closes the middle lid (BSC 2003 [DIRS 163185], Attachment III). Therefore, the throat of the weld must also be 10 mm (0.39 in.). The closest English equivalent size fillet weld to accommodate this criterion is a 9/16-in. (14.3-mm) fillet weld. A 1/2-in. (12.7-mm) lid is thicker and will deform less than a 10-mm (0.39-in.) thick lid under the stresses of a 9/16-in. (14.3-mm) fillet weld. Therefore, the actual lid thickness has been increased to 1/2 in..

21-PWR Waste Package Configuration with Absorber Plates

This waste package configuration will be the most common type (see Table 8 for verification of quantities and relevant dimensions). It holds the majority of the PWR SNF. Refer to Section 7.1.1.4 to find the cavity dimensions and maximum expected fuel assembly dimensions. This waste package is comprised of an Alloy 22 (UNS N06022) outer corrosion barrier, a stainless steel type 316 inner vessel, SA 516 Grade 70 carbon steel fuel tubes, guides, and stiffeners, and Aluminum A96061 T4 thermal shunts. The only difference between this waste package and the 21-PWR waste package with control rods is that the interlocking plates are made of neutron absorbing Ni-Gd Alloy (UNS N06464) (BSC 2004 [DIRS 169959]) instead of SA 516 Grade 70 carbon steel. It should be noted that all drawings referenced in Section 5.3 show the absorber plate material as Neutronit A978™. However, the material was changed to Ni-Gd Alloy (UNS N06464) in BSC 2004 [DIRS 169959]. The 21-PWR waste package may be seen in:

[DIRS 167393]

BSC 2004. *Design and Engineering, 21-PWR Waste Package Configuration*. 000-MW0-DSU0-00401-000-00C. Las Vegas, Nevada: Bechtel SAIC Company. ACC: ENG.20040202.0023.

[DIRS 166953]

BSC 2004. *Design and Engineering, 21-PWR Waste Package Configuration*. 000-MW0-DSU0-00402-000-00B. Las Vegas, Nevada: Bechtel SAIC Company. ACC: ENG.20040119.0004.

[DIRS 167394]

BSC 2004. *Design and Engineering, 21-PWR Waste Package Configuration*. 000-MW0-DSU0-00403-000-00C. Las Vegas, Nevada: Bechtel SAIC Company. ACC: ENG.20040202.0024.

21-PWR Waste Package Configuration with Control Rods

Refer to section 7.1.1.4 to find the cavity dimensions and maximum expected fuel assembly dimensions. This waste package configuration is comprised of an Alloy 22 (UNS N06022) outer corrosion barrier, a stainless steel type 316 inner vessel, SA 516 Grade 70 carbon steel fuel tubes, guides, and stiffeners, and Aluminum A96061 T4 thermal shunts. The only difference between this waste package and the 21-PWR waste package with absorber plates is that the interlocking plates are made of SA 516 Grade 70 carbon steel instead of neutron absorbing Ni-Gd Alloy (UNS N06464) (BSC 2004 [DIRS 169959]). This waste package may be seen in:

[DIRS 167393]

BSC 2004. *Design and Engineering, 21-PWR Waste Package Configuration.* 000-MW0-DSU0-00401-000-00C. Las Vegas, Nevada: Bechtel SAIC Company. ACC: ENG.20040202.0023.

[DIRS 166953]

BSC 2004. *Design and Engineering, 21-PWR Waste Package Configuration.* 000-MW0-DSU0-00402-000-00B. Las Vegas, Nevada: Bechtel SAIC Company. ACC: ENG.20040119.0004.

[DIRS 167394]

BSC 2004. *Design and Engineering, 21-PWR Waste Package Configuration.* 000-MW0-DSU0-00403-000-00C. Las Vegas, Nevada: Bechtel SAIC Company. ACC: ENG.20040202.0024.

12-PWR Waste Package Configuration

This waste package configuration accommodates the longest commercial SNF. It also will accept canisters containing DOE owned SNF (see Section 5.2). Refer to section 7.1.1.4 to find the cavity dimensions and maximum expected fuel assembly dimensions. This waste package is comprised of an Alloy 22 (UNS N06022) outer corrosion barrier, a stainless steel type 316 inner vessel, SA 516 Grade 70 carbon steel fuel tubes, guides, and stiffeners, and Aluminum A96061 T4 thermal shunts, and Ni-Gd Alloy (UNS N06464) (BSC 2004 [DIRS 169959]) interlocking plates. Any badly deformed fuel assemblies that will not fit into a standard 21-PWR waste package may be disposed of in the 12-PWR waste package. This is because the 12-PWR waste package can accommodate the largest cross section fuel assembly. Badly deformed BWR fuel will also be stored in the 12-PWR waste package. This waste package may be seen in:

[DIRS 164975]

BSC 2003. *Repository Design, 12-PWR Waste Package Configuration.* 000-MW0-DSU0-00301-000-00A. Las Vegas, Nevada: Bechtel SAIC Company. ACC: ENG.20030814.0004.

[DIRS 164976]

BSC 2003. *Repository Design, 12-PWR Waste Package Configuration.* 000-MW0-DSU0-00302-000-00A. Las Vegas, Nevada: Bechtel SAIC Company. ACC: ENG.20030815.0006.

[DIRS 164977]

BSC 2003. *Repository Design, 12-PWR Waste Package Configuration*. 000-MW0-DSU0-00303-000-00A. Las Vegas, Nevada: Bechtel SAIC Company. ACC: ENG.20030815.0007.

44-BWR Waste Package Configuration

This is the most common waste package configuration that will dispose of BWR fuel. Refer to section 7.1.1.4 to find the cavity dimensions and maximum expected fuel assembly dimensions. This waste package is comprised of an Alloy 22 (UNS N06022) outer corrosion barrier, a stainless steel type 316 inner vessel, SA 516 Grade 70 carbon steel fuel tubes, guides, and stiffeners, and Aluminum A96061 T4 thermal shunts, and Ni-Gd Alloy (UNS N06464) (BSC 2004 [DIRS 169959]) interlocking plates. This waste package may be seen in:

[DIRS 167550]

BSC 2004. *Design and Engineering, 44-BWR Waste Package Configuration*. 000-MW0-DSU0-00501-000-00B. Las Vegas, Nevada: Bechtel SAIC Company. ACC: ENG.20040213.0005.

[DIRS 166956]

BSC 2003. *Design and Engineering Organization, 44-BWR Waste Package Configuration*. 000-MW0-DSU0-00502-000-00A. Las Vegas, Nevada: Bechtel SAIC Company. ACC: ENG.20031021.0004.

[DIRS 167555]

BSC 2004. *Design and Engineering, 44-BWR Waste Package Configuration*. 000-MW0-DSU0-00503-000-00B. Las Vegas, Nevada: Bechtel SAIC Company. ACC: ENG.20040213.0006.

24-BWR Waste Package Configuration

This waste package configuration is intended for BWR fuel assemblies that need more criticality control than what the 44-BWR waste package may provide. Thomas 2004 [DIRS 170052] identifies the entire waste stream as being acceptable to store in the 44-BWR waste package. However, future waste streams may have enrichment greater than 4%, and therefore require a 24-BWR waste package. Refer to Section 7.1.1.4 to find the cavity dimensions and maximum expected fuel assembly dimensions. The 24-BWR waste package is comprised of an Alloy 22 (UNS N06022) outer corrosion barrier, a stainless steel type 316 inner vessel, SA 516 Grade 70 carbon steel fuel tubes, guides, and stiffeners, and Aluminum A96061 T4 thermal shunts, and Ni-Gd Alloy (UNS N06464) (BSC 2004 [DIRS 169959]) interlocking plates. This waste package may be seen in:

[DIRS 166929]

BSC 2004. *Design and Engineering, 24-BWR Waste Package Configuration*. 000-MW0-DSU0-00601-000-00A. Las Vegas, Nevada: Bechtel SAIC Company. ACC: ENG.20040119.0006.

[DIRS 166958]

BSC 2004. *Design and Engineering, 24-BWR Waste Package Configuration*. 000-MW0-DSU0-00602-000-00A. Las Vegas, Nevada: Bechtel SAIC Company. ACC: ENG.20040119.0007.

[DIRS 166959]

BSC 2004. *Design and Engineering, 24-BWR Waste Package Configuration*. 000-MW0-DSU0-00603-000-00A. Las Vegas, Nevada: Bechtel SAIC Company. ACC: ENG.20040119.0008.

5.3.1 Dimensions

Dimensions should be taken from the configuration drawings cited in the previous section.

5.3.2 Material Selection

The selection of materials from which reliable waste packages could be fabricated followed a multistep analysis and design process. It began by analyzing the critical functions of a particular waste package and its various components. In selecting a material for a component, both the material's availability and the critical functions the component would serve as part of the waste package were taken into consideration. They identified eight major components and eight performance criteria for selecting materials to fabricate them (CRWMS M&O 1997 [DIRS 100259], Section 3). The eight major components are:

- Structural inner vessel
- Corrosion-resistant barrier
- Fill gas
- Interlocking plates for commercial design configurations
- Fuel tubes for commercial designs
- Structural guides for commercial design configurations
- Guide tube for codisposal design configurations
- Thermal shunts for commercial design configurations

Not every waste package configuration requires all of these components; it varies according to the waste form each will hold. However, all eight of these components cover the major requirements of all ten waste package configurations (BSC 2004 [DIRS 169062], sheet 1).

The eight criteria that contribute to performance are:

- Mechanical performance (strength)
- Chemical performance (resistance to corrosion and microbial attack)
- Predictability of performance (understanding the behavior of materials)
- Compatibility with materials of the waste package and waste form
- Ease of fabrication using the material
- Previous experience (proven performance record)
- Thermal performance (heat distribution characteristics)
- Neutronic performance (criticality and shielding).

Reasonableness of cost was considered as a discriminator.

The first step in selecting the waste package materials was identifying the functional requirements for each component. Next, the characteristics of materials that would help meet the requirements were selected. Candidate materials were chosen from commonly available materials (or, in the case of fill gas, from common gases). The materials were then analyzed in terms of how they would perform their intended functions.

Corrosion-Resistant Materials—Corrosion performance has been determined to be the most important criterion for a long waste package lifetime. Essential performance qualities therefore include a material's resistance to general and localized corrosion, stress corrosion cracking, and hydrogen-assisted cracking and embrittlement. The effects of long-term thermal aging are also important. To address the performance requirements for the waste package, the DOE has initiated studies to gain a better understanding of the processes involved in predicting the rate of waste package material corrosion over the 10,000-year regulatory period.

Combinations and arrangements of materials as containment barriers were carefully considered from several perspectives. Relevant criteria includes (1) material compatibility (e.g., galvanic/crevice corrosion effects); (2) the material's ability to contribute to defense in depth (e.g., because it has a different failure mode from other barriers); (3) the material's ease of fabrication; and (4) the potential impact of thin, corrosion-resistant materials used as containment barriers on a repository's essential operations, such as waste package loading, handling, and emplacement.

The major objectives centered on understanding the temperature and humidity conditions that would exist at different times for a range of thermal operating modes in a particular unsaturated zone, then designing the waste packages accordingly. Since the properties of any material selected for a corrosion barrier would inevitably be influenced by the temperature and humidity conditions in a repository of a particular design at a particular site, selecting the right corrosion-resistant material became one of the most important priorities.

After assessing potential materials available for waste package corrosion barriers, nickel- and titanium-based alloys were selected as the most promising candidate materials for corrosion resistance in an oxidizing environment such as Yucca Mountain. Using a corrosion-resistant material as the outer barrier of the waste package will significantly lower the risk of waste package failure from corrosion. Alloy 22 (UNS N06022) was selected as the preferred material for the outer barrier because it has excellent resistance to corrosion in the environment expected at Yucca Mountain; it is easier to weld than titanium; and it has a better thermal expansion coefficient match to stainless steel type 316 than titanium. A structurally strong material (stainless steel) was chosen for the inner vessel of the waste package (CRWMS M&O 2000 [DIRS 138173], Section 7.6).

Alloy 22 (UNS N06022) also offers benefits in the areas of program and operating flexibility. It is extremely corrosion-resistant under conditions of high temperature and low humidity, such as those that would prevail for hundreds to thousands of years in a repository designed to allow a relatively high thermal output from the waste packages.

Structural Materials—The major functional requirement of the structural material for the inner layer of the waste package is to support the corrosion-resistant outer material. Stainless steel type 316 was selected for the structural layer (CRWMS M&O 2000 [DIRS 138173], Section 5.2). This material provides the required strength; has a better compatibility with Alloy 22 (UNS N06022) than SA 516 Grade 70 carbon steel; and provides an economical solution to functional requirements. Table 2 presents the yield and tensile strengths of stainless steel type 316 and Alloy 22 (UNS N06022).

Table 2. Yield and Tensile Strengths of Alloy 22 (UNS N06022) and Stainless Steel Type 316

		Alloy 22 (UNS N06022) (MPa)	Stainless Steel Type 316 (MPa)
Yield Strength (σ_y)	RT ^a	310	207
	100°C ^b	273	177
	300°C ^b	214	132
Engineering Tensile Strength	RT ^a	689	517
	100°C ^b	688	515
	300°C ^b	632	495
True Tensile Strength (σ_u)	RT ^b	971	703
	100°C ^b	977	664
	300°C ^b	910	619

^aASME 2001 [DIRS 158115], Section II, Part D, Tables Y-1 and U

^bBSC 2003 [DIRS 166184], Section 5

The configurations for commercial SNF and DOE codisposal waste packages include internal components (i.e., structural guides, interlocking plates, fuel tubes, and thermal shunts) that must be able to sustain the mechanical loads created by handling, emplacement, and, if necessary, retrieval. Thus, mechanical performance was a major selection criterion. Thermal performance was also an important selection criterion because these components provide an additional path for conducting heat from the waste form to the walls of the waste package. The fuel tubes contact both the waste form and the basket plates. If the material selected for the tubes causes the waste form to degrade, release rates could be increased; if it causes the plates to degrade, criticality control could be compromised. Therefore, compatibility with other materials was an important criterion. The waste package configuration does not rely on these components for postclosure performance, so corrosion-resistant materials are not needed. Two grades of carbon steel (SA 516 Grades 55 and 70) were found to be the best choices for these internal components, based on the criteria; the designers chose to use Grade 70 (CRWMS M&O 2000 [DIRS 138189], Section 4).

Neutron Absorber Interlocking Plates—The most important function of the neutron absorber is to reduce the potential for criticality. The neutron absorber material is typically an additive to a carrier material (e.g., stainless steel alloyed with a boron compound). The neutron absorber is used in the interlocking plates in the internal basket. Corrosion behavior is important in keeping the neutron absorber material in place and effective long after emplacement, so chemical performance in a variety of environments was an important selection criterion. Mechanical performance was an evaluation factor because the interlocking plates must be able to sustain the mechanical loads created by handling, emplacement, and, if necessary, retrieval. Compatibility

with other materials was considered, since the plates must not cause the waste form to degrade. The plates also provide an important path for conducting heat from the waste form to the walls of the waste package, so thermal performance was considered. The material of choice was Ni-Gd Alloy (UNS N06464) (BSC 2004 [DIRS 169959]). Its selection was based on its corrosion performance compared to the other candidate materials, as well as its neutron absorbing properties. The composition of Ni-Gd Alloy (UNS N06464) (BSC 2004 [DIRS 169959]) may be found in ASTM B 932-04 2004 [DIRS 168403], Table 1.

Thermal Shunts—The thermal shunts provide another important path for conducting heat from the waste form (in this case, commercial SNF) to the walls of the waste package. The thermal conductivity of the material is very important. The thermal shunts are in contact with the waste form, so compatibility with SNF is an important evaluation criterion. The thermal shunts are only needed during the early period of repository performance, when the decay heat from SNF is relatively high. The material selected does not need a high degree of corrosion resistance. The thermal shunts must have enough structural strength to withstand handling, emplacement, and possible retrieval operations. However, these service loads are not very large, so mechanical performance was not selected as an evaluation criterion. Aluminum alloys 6061 and 6063 were selected over copper because of concerns that, should a waste package be breached and water enter, copper may react with the chloride ions in the water. This could result in accelerated degradation of the Zircaloy cladding on the SNF, which would eventually release radionuclides from the waste (CRWMS M&O 2000 [DIRS 138192], Section 3.2.3).

Fill Gas—The fill gas can be a significant conductor of heat from the waste form to the internal basket, so thermal performance was deemed one of the most important criteria in choosing a gas. The fill gas should not degrade other components of the waste package, so compatibility with other materials was another important criterion. Helium is inert and is routinely used as the fill gas for fuel rods, which indicates that helium would have an excellent compatibility with SNF. Based on a review of data on thermal conductivity, it was chosen over other candidate gases, such as nitrogen, argon, and krypton (CRWMS M&O 2000 [DIRS 138192], Sections 3.3.1 through 3.3.3).

5.3.3 ASME Code Position

The basis for the selection and application of the American Society of Mechanical Engineers (ASME) Boiler and Pressure Vessel (B&PV) Code to the waste package is documented in the document entitled, *BSC Position on the Use of the ASME Boiler and Pressure Vessel Code for the Yucca Mountain Waste Packages* (BSC 2003 [DIRS 165058]). This section summarizes the salient points of that document with regard to the design of the waste packages.

Yucca Mountain Review Plan, Final Report (NRC 2003 [DIRS 163274]) provides specific guidance on the appropriateness of using the ASME B&PV Code (ASME 2001 [DIRS 158115]) in the design of the waste package (e.g., Section 2.1.1.7.2.3 (1)); however, it does not prescribe the exact implementation of the ASME B&PV Code.

In any discussion of the ASME B&PV Code, it is important to first note that it is a pressure vessel safety code and that its primary mission is to assure structural adequacy for pressure

loading. Any other use of the ASME B&PV Code, such as the use of the conservative material properties contained in it or failure limits for non-pressure loading, must be justified on insight into the structural phenomena that are postulated to occur. For the waste package, component sizing and thickness are not determined by pressure loads but rather by dynamic events that the waste package might experience. Therefore, the application of the ASME B&PV Code design rules for dynamic loading of the waste package must be carefully scrutinized to ensure that the rules are properly applied. It should be noted that the application of the ASME B&PV Code in terms of the preparation of the ASME Code Design Specification is beyond the scope of this report. The preparation of that document is described in *BSC Position on the Use of the ASME Boiler and Pressure Vessel Code for the Yucca Mountain Waste Packages* (BSC 2003 [DIRS 165058]).

For the application of the ASME B&PV Code, Section III, Division I, Subsection NC (ASME 2001 [DIRS 158115]), has been selected by Bechtel SAIC Company (BSC) for the Code-compliant design and fabrication of the waste packages. It is important to differentiate the parts of the waste package to which the ASME B&PV Code apply. There are four major assembled components of the waste package. These are (1) the stainless steel inner vessel, (2) the Alloy 22 (UNS N06022) outer corrosion barrier, (3) the internal basket assemblies, and (4) the removable trunnion collar that is used for lifting and handling purposes. With regard to the ASME B&PV Code design, the only one of these parts that is considered an ASME B&PV Code pressure vessel is the stainless steel inner vessel.

With regard to the hermeticity of the inner vessel and integrity of the same against pressure loads, no currently postulated dynamic structural event involves simultaneous over-pressurization of the inner vessel. For over-pressurization, the capability of the spread ring and seal weld combination to retain the design pressure is assured by a helium leak check. While the seal welds are anticipated to be sound welds, no credit for resistance against dynamic events is taken as these are partial-penetration welds. Therefore, for dynamic structural events where the inner vessel in the vicinity of the seal welds may be reasonably anticipated to experience significant loads, these welds will not be credited to maintain the hermeticity of the inner vessel. In such cases, it must be shown that the outer corrosion barrier does not breach to maintain containment of the waste form.

For the other components of the waste package, the ASME B&PV Code is only used as guidance, either through the use of conservative material properties or conservative stress limits. For credible preclosure event sequences, and the assessment of those event sequences, the code and supporting code interpretations are used to formulate layered defensible material failure criteria. The basis for these failure criteria is discussed in Section 7.1.2.3.

It should be noted that if a waste package suffers a nontrivial dynamic event (i.e., drop, tip over, etc.), the waste form would be repackaged in a new waste package and the original waste package permanently removed from service.

6. SUMMARY OF DESIGN REQUIREMENTS

Preclosure and postclosure requirements are discussed in this section. Functional requirements are taken from BSC 2004 [DIRS 167273].

6.1 PRECLOSURE

6.1.1 Normal Operations

Functional Requirement Number: 3.1.3.1

Functional Requirement Title: Waste Package Handling Limits

Functional Requirement Text: Waste package handling shall not introduce any surface defect in the corrosion barrier exceeding those identified by performance assessment and on interface exchange drawings. Surface defects include, but are not limited to, scratches, nicks, dents, and permanent changes to the surface stress condition (Table 3).

Table 3. Waste Package Handling Limits Performance Requirements

Performance Requirement Number	Performance Requirement Text	Applicability
1	This issue is under investigation and will be resolved prior to construction authorization. A closure weld defect is the area of most concern and shall be limited to 1.6 mm (1/16 inch) (BSC 2004 [DIRS 164475], p. 59-60).	Yes

Functional Requirement Number: 3.1.3.2

Functional Requirement Title: Waste Package Closure

Functional Requirement Text: Sealing operations shall be performed on the waste package (Table 4).

Table 4. Waste Package Closure Performance Requirements

Performance Requirement Number	Performance Requirement Text	Applicability
1	Waste package sealing operations shall meet the requirements for the waste package as specified in the SDD for the waste package closure system.	Yes

6.1.1.1 Thermal

Thermal design requirements for normal operations include:

- Maximum cladding temperature of 350°C (Doraswamy 2004, Section 5.1.3.2 [DIRS 169548]) (this requirement is for both preclosure and postclosure)
- Maximum waste package heat output of 11.8 kW at emplacement (BSC 2004, Section 3.1.1.5 [DIRS 167273])

6.1.1.2 Structural

Functional Requirement Number: 3.1.1.1

Functional Requirement Title: Preclosure Containment

Functional Requirement Text: The waste package contains the waste form within its boundary for the preclosure period (Table 5).

Table 5. Preclosure Containment Performance Requirements

Performance Requirement Number	Performance Requirement Text	Applicability
1	The sealed waste package shall not breach during normal operations or during credible preclosure event sequences.	Yes
2	The waste package shall be designed and constructed to the codes and standards specified in Doraswamy 2004, [DIRS 169548], Section 5.1.1.	Yes
3	Normal operations and credible event sequence load combinations are defined in Mecham 2004 [DIRS 169790], Section 6.2.2. Note: The normal operations and credible event sequence load combinations are in Mecham 2004 [DIRS 169790], Section 6.2.2 and are not present in Doraswamy 2004 [DIRS 169548].	Yes
4	The waste package shall be designed to permit retrieval during the preclosure period until the completion of a performance confirmation program and NRC review of the information obtained from such a program.	Yes
5	The waste package shall be designed to permit retrieval during the preclosure period so that any or all of the emplaced waste could be retrieved on a reasonable schedule starting at any time up to 50 years after waste emplacement operations are initiated, unless a different time period is approved or specified by the NRC.	Yes
6	The waste package shall be designed to meet the full range of preclosure operating conditions for up to 300 years after the final waste emplacement.	Yes

The waste package shall be designed to account for residual stresses and differential thermal expansion (Mecham 2004 [DIRS 169790], Section 6.2.2.2).

The waste package shall be designed to account for internal pressure resulting thermally (i.e., differential thermal expansion) and due to fuel cladding rupture (Mecham 2004 [DIRS 169790], Section 6.2.2.3).

6.1.1.3 Shielding

Shielding analyses evaluate the effects of ionizing radiation on personnel, equipment, and materials. The primary sources for waste package radiation are gamma rays and neutrons emitted from SNF and high-level radioactive waste. Loading, handling, and transporting of waste packages would be carried out remotely to keep personnel exposure as low as reasonably achievable (e.g., having the human operators behind radiation shield walls, using remote manipulators, viewing operations with video cameras). The general shielding requirements are stated in Section 4.9.1 of Doraswamy 2004 [DIRS 169548]. Table 4.9.1-2 of Doraswamy 2004 [DIRS 169548] does not list any shielding requirements on the waste package. The transporter and building will provide shielding.

6.1.1.4 Waste Form Accommodation

Functional Requirement Number: 3.1.2.2

Functional Requirement Title: Uncanistered SNF Quantities and Characteristics

Functional Requirement Text: The waste package shall accommodate intact fuel assemblies from commercial SNF (Table 6).

Table 6. Uncanistered SNF Quantities and Characteristics Performance Requirements

Performance Requirement Number	Performance Requirement Text	Applicability
1	Table 7 and Table 8 identify parameters (size, weight, and inventory) that may be used for design.	Yes

Table 7. Boiling Water Reactor Fuel

Assembly Class	Length ^a in. (cm)	Channeled Width ^a in. (cm)	Unchanneled Width ^b in. (cm)	Assembly Weight (lb)	Non-Fuel Component (NFC) Weight (lb)	Total Weight (lb)	Number of Stored Assemblies 12/31/1994	Projected Number of Assemblies 12/31/2040
Big Rock Point	84.8 (215)	6.81 (17.3)	6.52 (16.6)	465	101	566	421	600
Humboldt Bay	96 (244)	4.8 (12.2)	4.67 (11.9)	276	23	299	390	400
LaCrosse	103.5 (263)	5.91 (15.0)	5.62 (14.3)	386	69	455	333 ^c	333 ^c
Dresden 1	135.7 (345)	4.57 (11.6)	4.28 (10.9)	328	30	358	892	900
GE BWR 2, 3	173 (439)	5.61 (14.2)	5.36 (13.6)	619	80	699	18,813	35,000
GE BWR 4-6	177.8 (452)	5.61 (14.2)	5.36 (13.6)	588	80	668	39,295	130,000

NOTES: ^aDimensions are post-irradiation. Widths include fuel channels, but make no allowance for channel spacer buttons and attachment clips.

^bDimensions are post-irradiation.

^cStainless steel clad assemblies.

GE = General Electric; NFC = non-fuel component; BWR = Boiling Water Reactor.

Source: BSC 2004 [DIRS 167273], Table 2.

Table 8. Pressurized Water Reactor Fuel

Assembly Class	Length w/o NFC ^a in. (cm)	Length w/ NFC ^a in. (cm)	Width ^a in. (cm)	Assembly Weight (lb)	NFC Weight (lb)	Total Weight (lb)	Number of Stored Assemblies 12/31/94	Projected Number of Assemblies 12/31/2040
Yankee Rowe	112.9 (286.8)	112.9 (286.8)	7.61 (19.3)	797	N/A	797	533 (76 ^b)	700 (76 ^b)
San Onofre 1	138.4 (351.5)	139.9 (355.3)	7.76 (19.7)	1,247	107	1,354	665 (665 ^b)	1000 (822 ^b)
Haddam Neck	138.4 (351.5)	139.9 (355.3)	8.5 (21.6)	1,255	166	1,421	892 (888 ^b)	1500 (945 ^b)
Indian Point 1	139.1 (353.3)	139.1 (353.3)	6.27 (15.9)	437	N/A	437	160 (160 ^b)	200 (160 ^b)
Fort Calhoun	147.7 (375.2)	158.5 (402.6)	8.12 (20.6)	1,220	67	1,287	570	1100
Palisades	148.9 (378.2)	148.9 (378.2)	8.31 (21.1)	1,360	N/A	1,360	793	1500
CE 14x14	158.8 (403.4)	169.6 (430.8)	8.11 (20.6)	1,270	77	1,347	4565	9800
St. Lucie 2	159.7 (405.6)	170.6 (433.3)	8.13 (20.7)	1,300	66	1,366	544	1900
WE 15x15	161.4 (410.0)	166.9 (423.9)	8.42 (21.4)	1,472	165	1,637	7,490	15,000
WE 14x14	161.4 (410.0)	166.3 (422.4)	7.76 (19.7)	1,302	130	1,432	4,093	7800
WE 17x17	161.4 (410.0)	168.8 (428.8)	8.42 (21.4)	1,482	180	1,662	15,295	59,000
B&W 17x17	167.4 (425.2)	173.5 (440.7)	8.54 (21.7)	1,505	149	1,654	4	3100
B&W 15x15	167.4 (425.2)	173.5 (440.7)	8.54 (21.7)	1,515	165	1,680	5,435	10,000
CE 16x16	178.6 (453.6)	190.8 (484.6)	8.14 (20.7)	1,430	72	1,502	2,340	8100
CE System 80	180 (457.2)	194.8 (494.8)	8.16 (20.7)	1,430	N/A	1,430	1,132	8100
South Texas	201.1 (510.8)	201.1 (510.8)	8.4 (21.3)	1,720	200	1,920	424	3000

NOTES: ^aDimensions are post-irradiation.

^bNumber of stainless steel clad assemblies. Remainders are zircaloy alloy clad.

B&W = Babcock & Wilcox; CE = Combustion Engineering; WE = Westinghouse Electric; NFC = non-fuel component.

Source: BSC 2004 [DIRS 167273], Table 3.

6.1.1.5 Criticality

The preclosure safety analysis must include consideration of means to prevent and control criticality (10 CFR 63.112(e)(6) [DIRS 158535]). In addition to any criticality countermeasures that might be included with a DOE SNF waste form in the standardized canister, and the inherent sub-critical neutron multiplication of the vitrified high-level waste, avoidance of criticality is ensured by moderator exclusion from the waste package during preclosure (Doraswamy 2004 [DIRS 169548], Sections 4.9.2.2.3 and 4.9.2.2.6).

Section 5.1.2 of BSC 2003 [DIRS 164128] assumes that waste packages are designed such that they can be loaded with any combination of commercial SNF assemblies that are acceptable for disposal without leading to a preclosure nuclear criticality provided that moderator exclusion is in effect. Following this assumption, criticality is not a credible event for the preclosure.

6.1.2 Event Sequence Evaluation

6.1.2.1 Thermal

Functional Requirement Number: 3.1.1.5

Functional Requirement Title: Postclosure Primary Performance

Functional Requirement Text: The waste package shall be designed so that working in combination with natural barriers and other engineered barriers the radiological exposures to the reasonably maximally exposed individuals are within the limits established through 10 CFR 63.113(b) [DIRS 156605], and the release of radioculides into the accessible environments are within limits established through 10 CFR 63.113(c) [DIRS 158535] (Table 9).

Table 9. Postclosure Primary Performance Requirements

Performance Requirement Number	Performance Requirement Text	Applicability
1	The maximum waste package power at emplacement is 11.8 kW.	Yes

During a fire, maximum cladding temperature must not exceed 570°C (Doraswamy 2004 [DIRS 169548], Section 5.1.3.2). It should be noted that the fire event is the only relevant preclosure thermal event. The 11.8 kW power at emplacement pertains to normal operations, and sets the initial conditions of the fire event.

6.1.2.2 Structural

The waste package shall not breach during normal operation or during credible preclosure sequence events (BSC 2004 [DIRS 167273], Section 3.1.1.1). These include the following:

Rockfall on Waste Package – the waste package is at rest on the emplacement pallet in the drift without a drip shield, when rock(s) fall and impacts the waste package surface (Mecham 2004 [DIRS 169790], Section 6.2.2.4).

Object Drop on Waste Package – the waste package is at rest in a vertical position and a equipment failure (i.e., gantry crane) falls and impacts the top of the waste package (Mecham 2004 [DIRS 169790], Section 6.2.2.4).

Missile Impact on Waste Package – the waste package is at rest and a small object at high velocity impacts the waste package surface (Mecham 2004 [DIRS 169790], Section 6.2.2.4).

Waste Package Vertical Drop – the waste package is being lifted in a vertical orientation at a height of 2.0 m (6.6 ft) when the lifting device inadvertently drops it. The waste package impacts the ground squarely on its base (Mecham 2004 [DIRS 169790], Section 6.2.2.5).

Waste Package Tipover – the waste package is at rest on the ground in a vertical position and an external force (such as a seismic event) causes the waste package to tip over and impact the ground. A tipover from an elevated surface is also considered (Mecham 2004 [DIRS 169790], Section 6.2.2.5).

Waste Package Horizontal Drop – the waste package is being lifted in a horizontal orientation at a height of 2.4 m (7.9 ft) when the lifting device inadvertently drops it. The waste package impacts the ground squarely on its side (Mecham 2004 [DIRS 169790], Section 6.2.2.5).

Horizontal Drop with Emplacement Pallet – the emplacement pallet with waste package is being lifted in a horizontal orientation when the lifting device inadvertently drops it. The emplacement pallet with waste package impacts the ground along its horizontal axis. This is also done as a horizontal drop onto the emplacement pallet. The emplacement pallet is the object considered that may puncture the waste package (Mecham 2004 [DIRS 169790], Section 6.2.2.5).

Waste Package Corner Drop – the waste package is being lifted in a vertical orientation at a height of 2.0 m (6.6 ft) when the lifting device inadvertently drops it. A corner of the waste package impacts the ground first (Mecham 2004 [DIRS 169790], Section 6.2.2.5).

Waste Package 10-Degree Oblique Drop with Slap Down – the waste package is being lifted in a horizontal orientation at a height of 2.4 m (7.9 ft) when the lifting device inadvertently releases one end. After the bottom end has rotated 10 degrees, the lifting device holding the top of the waste package fails and the entire waste package falls due to gravity and impacts the ground (This criteria is not in Mecham 2004 [DIRS 169790], but is considered a useful event by structural engineers).

Waste Package Swing Down – the waste package is being lifted in a horizontal orientation at a height of 2.4 m (7.9 ft) when the lifting device inadvertently releases one end. One end of the waste package remains held by the lifting device while the other end swings down and impacts the ground (Mecham 2004 [DIRS 169790], Section 6.2.2.5).

Waste Package Exposed to Vibratory Ground Motion – the waste package is subjected to vibratory ground motion in the underground for a seismic evaluation for an annual frequency of exceedance of 5×10^{-4} per year and 1×10^{-4} per year (Mecham 2004 [DIRS 169790], Section 6.2.2.6).

6.2 POSTCLOSURE

Functional Requirement Number: 3.1.1.2

Functional Requirement Title: Postclosure Confinement

Functional Requirement Text: The sealed waste package shall restrict the transport of radionuclides to the outside of the waste package boundary after repository closure (Table 10).

Table 10. Postclosure Confinement Performance Requirements

Performance Requirement Number	Performance Requirement Text	Applicability
1	In conjunction with natural barriers and other engineered barriers, the sealed waste package shall limit transport of radionuclides in a manner sufficient to meet long-term repository performance requirements.	Yes
2	The waste package shall be designed and constructed to the codes and standards specified in the Doraswamy 2004, [DIRS 169548], Section 5.1.1.	Yes
3	Normal operations and event load combinations are defined in Mecham 2004 [DIRS 169790], Section 6.2.2. Note: The normal operations and credible event sequence load combinations are in Mecham 2004 [DIRS 169790], Section 6.2.2 and are not present in Doraswamy 2004 [DIRS 169548].	Yes

Functional Requirement Number: 3.1.1.3

Functional Requirement Title: Criticality Control

Functional Requirement Text: The sealed waste package shall provide criticality control (Table 11).

Table 11. Criticality Control Performance Requirements

Performance Requirement Number	Performance Requirement Text	Applicability
1	The methodology defined in the <i>Disposal Criticality Analysis Methodology Topical Report</i> (YMP 2003 [DIRS 165505]) shall be used to demonstrate acceptable criticality control for waste packages.	Yes
2	The waste package shall meet criteria 4.9.2.2.2 from Doraswamy (2004 [DIRS 169548], Section 4.9.2).	Yes

The criteria given in Section 4.9.2 of *Project Design Criteria Document* (Doraswamy 2004 [DIRS 169548]) does not apply to fuel after it is placed in the waste package. *Project Requirements Document* (Canori and Leitner 2003 [DIRS 166275]) gives the requirements and rationale for waste package criticality. These are given in Section 3 of the document, PRD-013/T-016 and PRD-013/T-038. The methodology for waste package criticality analyses is provided in YMP 2003 [DIRS 165505].

7. SATISFACTION OF DESIGN REQUIREMENTS

7.1 PRECLOSURE

The waste package must satisfy defined performance specifications to protect the public and workers and to meet the performance objectives of a repository. An example of a performance specification is the ability of a waste package to withstand a tipover event without breaching. Performance specifications are discussed in the following sections, where they are categorized by relevant engineering discipline (i.e., thermal, criticality, structural, and shielding). Detailed discussions of performance specifications are available in System Description Documents (e.g., BSC 2004 [DIRS 167273]).

7.1.1 Normal Operations

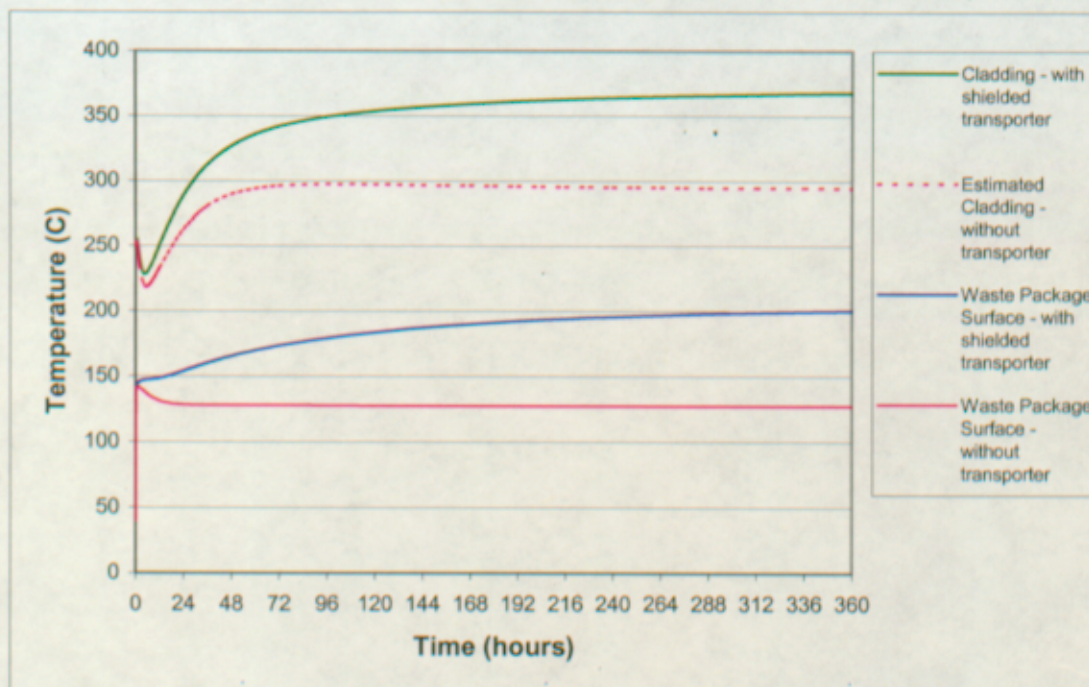
7.1.1.1 Thermal

The thermal calculations for normal operations are performed continuously through preclosure and postclosure times. During preclosure, peak temperatures are far below the limit due to the significant heat removal by the ventilation system. Highest temperatures occur a few decades after closure.

Thermal Performance in the Surface Facility

Thermal conditions for a loaded 21-PWR waste package sitting in the surface facility weld cell have been calculated in BSC 2003 [DIRS 164075]. Most of the cases in these calculations were for a waste package in a shielded trolley, but one case had no trolley. The design now does not use the shielded trolley. Conservative assumptions were used including radiative cooling only, a high initial assembly temperature of 250°C, instantaneous loading of all assemblies in the waste package, and room temperature at 40°C. Figure 2 shows the waste package surface temperatures and maximum cladding temperatures for cases with and without the shielded trolley. For the case without shielding, the cladding temperature was estimated by adding the temperature difference (cladding minus surface) of the shielded case to the waste package surface temperature.

The lower temperatures represent the current design and show peak cladding temperatures remain below 300°C at all times, even if steady-state thermal conditions are achieved. If shielding were used, the higher cladding temperatures remain below 400°C at all times and below 350°C for several days.



Source: BSC 2003 [DIRS 164075] data files

Figure 2. 21-PWR Surface and Cladding Temperatures in Surface Weld Cell

Bounding, two-dimensional, thermal calculations for 11.8 kW 21-PWR and 44-BWR waste packages are reported in BSC 2004 [DIRS 166695] and BSC 2003 [DIRS 166899].

The temperature boundary conditions applied to the waste package outer surface for the two-dimensional calculations are taken from a three dimensional (pillar) calculation of a representative drift segment (BSC 2003 [DIRS 164726], Section 6).

PWR Thermal Results—Solutions were found using a finite element representation in ANSYS. Table 12 shows peak fuel cladding temperatures for three PWR loading alternatives, each having a total waste package heat output of 11.8 kW. For the three cases shown here, the peak cladding temperature does not exceed the 350°C limit. As long as the hot assemblies are placed in the outer positions, a margin of about 35°C was maintained. If more heat is concentrated in the center of the waste package, cladding temperature limits would be exceeded, so it may be necessary to know and control the loading patterns in the waste package.

Table 12. Fuel Cladding Temperature Results

ANSYS V5.6.2 Case Name and Loading Configuration	21pwrcase6			21pwrcase5			21pwuni		
	C	M	O	C	M	O	C	M	O
Zone	C	M	O	C	M	O	C	M	O
Number of Assemblies	0.5	4	6	7	1	2.5	N/A	N/A	N/A
Initial Heat Output /Assembly (W)	2100	485	485	15	545	2100	561.9	561.9	561.9
Maximum Fuel Cladding Temperature (°C)	350			317			312		

NOTE: C = center-zone ■; M = middle-zone ▣; O = outer-zone □.

Source: BSC 2004 [DIRS 166695], Table 21 and Table 22

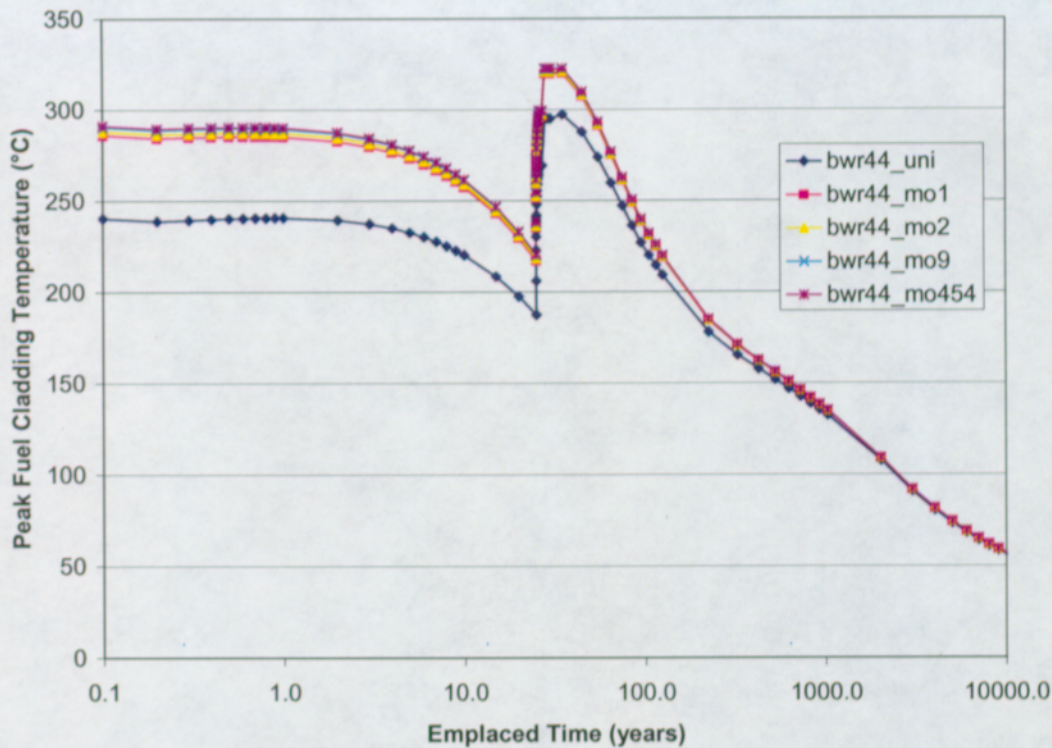
BWR Thermal Results—Solutions were found using a finite element representation in ANSYS. The thermal calculations for an 11.8 kW 44 BWR waste package included a uniform heat distribution, four cases with a single high heat assembly in the center of the waste package, twelve cases with multiple high heat assemblies in the center of the waste package, and a single case with multiple high heat assemblies in the outer region of the waste package.

Table 13 and Figure 3 show the calculated temperatures for cases with uniform loading and a single high heat assembly in the center of the waste package. The results show, as expected, that cladding temperatures are higher if the higher-heat fuel assemblies are concentrated towards the center of the waste package. In all cases the peak temperatures are 30°C to 50°C below the 350°C limit.

Table 13. Peak Cladding Temperatures with High Heat Loads in Center

	Center Zone	Middle Zone	Outer Zone	ANSYS Case Name	Maximum Fuel Cladding Temperature (°C)
Number of Cells	6	10	6		
Heat Output per Fuel Assembly (W)	600	143.75	143.75	bwr44_6106_mo1	320.3
	600	176.92	88.46	bwr44_6106_mo2	321.4
	600	215.63	23.96	bwr44_6106_mo9	322.6
	600	227	5	bwr44_6106_mo454	322.9
	268.18	268.18	268.18	bwr44_uni	297.5

Source: BSC 2003 [DIRS 166899], Table 21



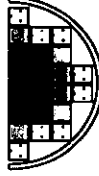
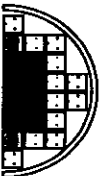
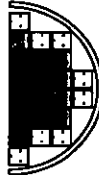
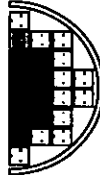
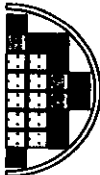
Source: BSC 2003 [DIRS 166899], Figure 1

Figure 3. Peak Cladding Temperature—High Heat Load in Center

Table 14 and Figure 4 show calculated fuel cladding temperatures for cases with multiple high heat assemblies. The maximum fuel cladding temperature was near 325°C for all cases with high heat in the center. Placing the high heat assemblies in the outer portion of the waste package reduces the maximum fuel cladding temperature by about 40°C.

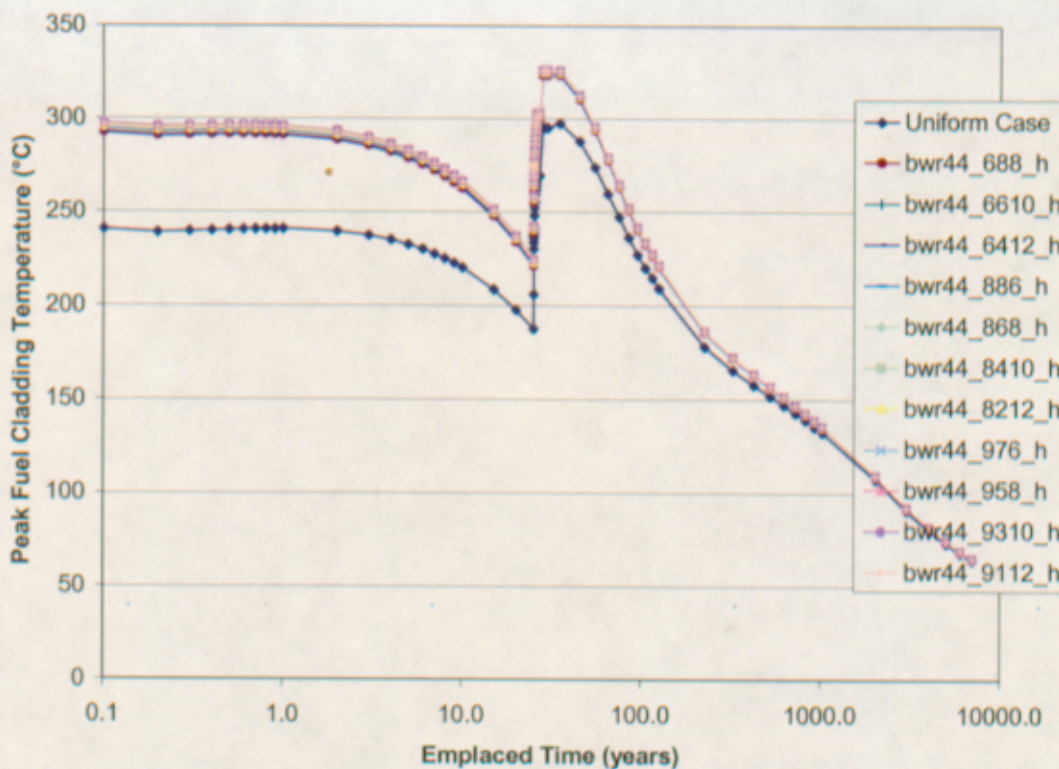
Table 14. Fuel Cladding Temperature Results

ANSYS Case Name and Loading Configuration	bwr44_6106_h			bwr44_688_h			bwr44_6610_h			bwr44_6412_h		
	C	M	O	C	M	O	C	M	O	C	M	O
Number of Fuel Assemblies	6	10	6	6	8	8	6	6	10	6	4	12
Heat Output / Fuel Assembly (W)	600	227	5	600	282.5	5	600	375	5	600	560	5
Maximum Fuel Cladding Temperature (°C)	322.9			323.6			324.8			323.4		

ANSYS Case Name and Loading Configuration	bwr44_886_h 			bwr44_868_h 			bwr44_8410_h 			bwr44_8212_h 			
	Zone	C	M	O	C	M	O	C	M	O	C	M	O
	Number of Fuel Assemblies	8	8	6	8	6	8	8	4	10	8	2	12
	Heat Output / Fuel Assembly (W)	600	133.75	5	600	176.67	5	600	262.5	5	600	520	5
	Maximum Fuel Cladding Temperature (°C)	324.9			325.2			325.7			325.7		
ANSYS Case Name and Loading Configuration	bwr44_976_h 			bwr44_958_h 			bwr44_9310_h 			bwr44_9112_h 			
	Zone	C	M	O	C	M	O	C	M	O	C	M	O
	Number of Fuel Assemblies	9	7	6	9	5	8	9	3	10	9	1	12
	Heat Output / Fuel Assembly (W)	600	67.1	5	600	92	5	600	150	5	600	440	5
	Maximum Fuel Cladding Temperature (°C)	326.0			326.1			326.3			325.9		
ANSYS Case Name and Loading Configuration	bwr44_9310_r 												
	Zone	C	M	O									
	Number of Fuel Assemblies	10	3	9									
	Heat Output / Fuel Assembly (W)	5	150	600									
	Maximum Fuel Cladding Temperature (°C)	285.9											

Source: BSC 2003 [166899], Table 22

Note: C = center-zone ■; M = middle-zone ■; O = outer-zone □.



Source: BSC 2003 [DIRS 166899], Figure 2

Figure 4. Peak Cladding Temperature—Loading Alternatives

Two-Dimensional Repository Calculations—Calculations have been performed with a two dimensional representation of the repository (BSC 2003 [DIRS 165093]). These calculations use line heat loads, and consider waste packages as a continuous infinite cylindrical heat source. Solutions of the finite element representation are found using ANSYS. Such calculations can be performed rapidly and the numerous results are used to generate response surfaces. That is, surfaces of constant peak waste package surface temperature as a function of waste package spacing, ventilation efficiency, and ventilation time. Different sets of response surfaces are generated for varied line heat loads. By holding all but one variable constant on a given response surface, operating curves can be generated that show the variation of waste package temperature due to variation in the remaining variable. The repository two-dimensional temperatures cannot be strictly applied to waste packages, but the change in temperature in the small locus of points provides the designer with a good method to determine the impact that changes in design will have on waste package temperatures. Hence, the results of bounding calculations presented in this report can be used with the operating curves from *Two-Dimensional Repository Thermal Design Calculations* (BSC 2003 [DIRS 165093]) to estimate thermal margins resulting from design variations.

7.1.1.2 Structural

7.1.1.2.1 Lifting

The waste package must be able to be lifted using the twist-on trunnion collars for normal operations. The waste package will be lifted by the top trunnion collar when in the vertical orientation, and by both the top and bottom trunnion collars when in the horizontal orientation. Since the top trunnion collar lifts the entire waste package in the vertical orientation and the Naval SNF Long waste package has the greatest mass, this scenario was analyzed (BSC 2003 [DIRS 166827]). The results of various waste package components at room temperature and 300°C are presented in Tables 15 and 16, respectively.

Table 15. Maximum Stress Intensities at Room Temperature

	σ_{int} (MPa)	σ_y (MPa)	σ_u (MPa)	σ_{int} / σ_y	σ_{int} / σ_u	$1/3 \sigma_y$	$1/5 \sigma_u$
Outer Corrosion Barrier	56	310	689	0.18	0.08	103	138
Trunnion Sleeve	280	310	689	0.90	0.41	103	138
Trunnion Sleeve Bottom Weld	44	310	689	0.14	0.06	103	138
Trunnion Collar	320	1170	1310	0.27	0.24	390	262
Trunnion	158	1170	1310	0.14	0.12	390	262

Source: BSC 2003 [DIRS 166827], Table 6-3

Table 16. Maximum Stress Intensities at 300°C

	σ_{int} (MPa)	σ_y (MPa)	σ_u (MPa)	σ_{int} / σ_y	σ_{int} / σ_u	$1/3 \sigma_y$	$1/5 \sigma_u$
Outer Corrosion Barrier	54	214	688	0.25	0.08	71	138
Trunnion Sleeve	360	214	688	1.68	0.52	71	138
Trunnion Sleeve Bottom Weld	44	214	688	0.21	0.06	71	138
Trunnion Collar	320	965	1100	0.33	0.29	322	220
Trunnion	156	965	1100	0.16	0.14	322	220

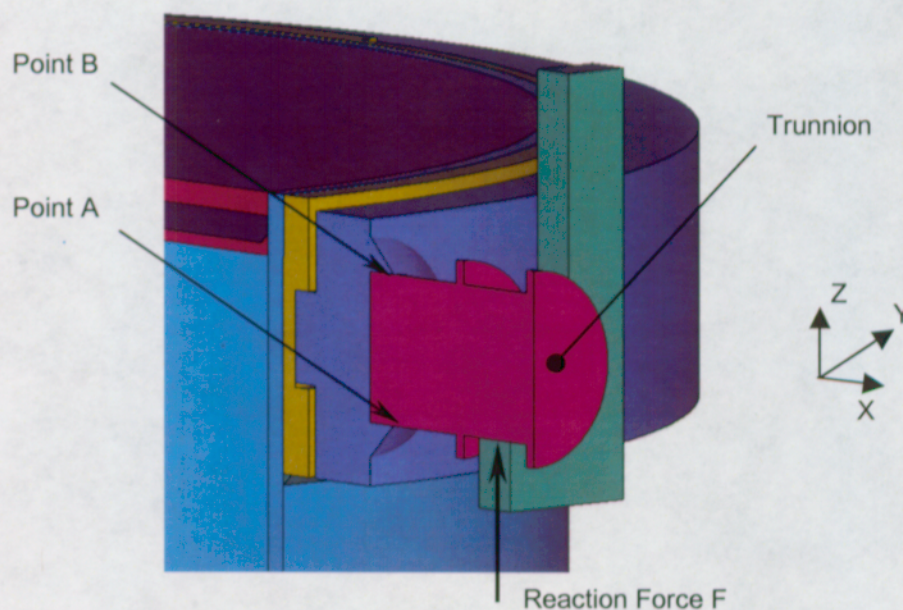
Source: BSC 2003 [DIRS 166827], Table 6-4

Tables 15 and 16 show that the maximum stresses in the components of the waste package are less than 1/3 the yield strength and 1/5 the tensile strength (ANSI N14.6-1993 [DIRS 102016], Section 4.2.1.1). However, the trunnion sleeve and the trunnion collar have maximum stress intensities above those limits. BSC (2003 [DIRS 166827], Section 6) shows the maximum stress in the trunnion sleeve is a localized contact stress between the trunnion sleeve and the trunnion collar. Furthermore, BSC 2003 [DIRS 166827], Section 6 shows that the stresses are far below the requirements in the surrounding areas and through the thickness of the engagement. In addition the trunnion collars and trunnion sleeve have rounded corners and chamfered corners that would alleviate stresses in the corners and edges.

The trunnion undergoes repeated bending stress from the engagement of the hooks. From Tables 15 and 16, the tensile stress at Point A will cycle from zero to approximately 160 MPa.

Since the trunnion collars are reusable and can be used either on the top end of the waste package or the bottom end of the waste package, Point A may cycle from zero to 160 MPa in tension or zero to 160 MPa in compression. Point B lies on the exact opposite surface of the direction of bending, and the stress is exactly the same. Except, it is in compression when Point A is in tension and in tension when Point A is in compression. Since fatigue failure occurs faster in tension-compression than in tension-tension (ASM 1980 [DIRS 104317], Figure 10), Point B of Figure 5 will be considered. Since Point B lies on the exact opposite surface of the direction of bending, the stress will be exactly the same, only it will be in compression instead of tension.

Therefore, Points A and B will undergo cycles from 0 to 160 MPa. Meaning the mean stress is 80 MPa and the alternating stress is also 80 MPa.



Source: BSC 2003 [DIRS 166827], Figure 6-1

Figure 5. Location of Stress on the Trunnion

From ASM 1980 [DIRS 104317], Figure 10, it is seen that the stress is approximately seven times less than the fatigue limit for 10^7 cycles. Although the yield and tensile strength of the material for this Constant-life diagram is slightly higher, considering the trunnion collar will never undergo 10^7 cycles and its cycling is not constant, the design of the trunnion collar is adequately designed for any possible fatigue. Therefore the trunnion collars are appropriately designed for normal handling operations.

7.1.1.2.2 Radial Thermal Expansion Stress

The necessary radial gap due to elevated temperatures is explored in BSC 2001 [DIRS 152655]. The objective of this activity is to determine the tangential stresses of the outer corrosion barrier, due to uneven thermal expansion of the inner vessel and outer corrosion barrier of the current

waste package design. The tangential stresses are significantly larger than the radial stresses associated with thermal expansion, and at the waste package outer surface the radial stresses are equal to zero. The scope of this activity is limited to determining the tangential stresses in the waste package outer corrosion barrier resulting from two different coefficients of thermal expansions. The inner vessel has a greater coefficient of thermal expansion than the outer corrosion barrier, producing a pressure between the two shells. The temperature range for this calculation is 20 °C to 239 °C. Closed form solutions are used to obtain the results.

Tables 17 and 18 show that there will be zero tangential stress due to thermal expansion if the radial gap is 1 mm (0.04 in.) or greater. Therefore, the minimum gap is determined to be 1 mm (0.04 in.).

Table 17. Outer Corrosion Barrier Maximum Tangential Stress at the Outer Surface

Waste Package Type	Maximum Tangential Stress at the Outer Surface, σ_{os} (MPa)										
	Gap Size (mm)										
	0.0	0.1	0.2	0.3	0.4	0.5	0.6	0.7	0.8	0.9	1.0
21-PWR	140.9	122.1	103.2	84.4	65.6	46.8	27.9	9.1	0.0	0.0	0.0
44-BWR	140.9	122.4	103.9	85.5	67.0	48.5	30.1	11.6	0.0	0.0	0.0
24-BWR	141.3	117.4	93.5	69.6	45.8	21.9	0.0	0.0	0.0	0.0	0.0
12-PWR	140.8	117.2	93.6	69.9	46.3	22.7	0.0	0.0	0.0	0.0	0.0
5 DHLW/DOE SNF - Short	131.4	117.9	104.4	90.9	77.4	63.9	50.4	36.9	23.4	9.9	0.0
2-MCO/2-DHLW	130.9	115.0	99.2	83.4	67.5	51.7	35.8	20.0	4.2	0.0	0.0
Naval SNF Long	130.4	115.7	101.1	86.4	71.7	57.0	42.4	27.7	13.0	0.0	0.0

Source: BSC 2001 [DIRS 152655], Table 4

Table 18. Outer Corrosion Barrier Maximum Tangential Stress at the Inner Surface

Waste Package Type	Maximum Tangential Stress at the Inner Surface, σ_{is} (MPa)										
	Gap Size (mm)										
	0.0	0.1	0.2	0.3	0.4	0.5	0.6	0.7	0.8	0.9	1.0
21-PWR	144.6	125.3	106.0	86.6	67.3	48.0	28.7	9.4	0.0	0.0	0.0
44-BWR	144.5	125.6	106.6	87.7	68.7	49.8	30.8	11.9	0.0	0.0	0.0
24-BWR	146.1	121.4	96.7	72.0	47.3	22.7	0.0	0.0	0.0	0.0	0.0
12-PWR	145.6	121.1	96.7	72.3	47.8	23.4	0.0	0.0	0.0	0.0	0.0
5 DHLW/DOE SNF - Short	134.8	120.9	107.1	93.2	79.4	65.5	51.7	37.9	24.0	10.2	0.0
2-MCO/2-DHLW	134.8	118.5	102.2	85.9	69.5	53.2	36.9	20.6	4.3	0.0	0.0
Naval SNF Long	134.1	119.0	103.9	88.8	73.7	58.6	43.5	28.5	13.4	0.0	0.0

Source: BSC 2001 [DIRS 152655], Table 5

7.1.1.2.3 Axial Thermal Expansion Stress

Four different potential waste package design configurations are evaluated in BSC 2003 [DIRS 161691], Section 7: the 21-PWR, Naval SNF Long, 44-BWR, and 5 DHLW/DOE SNF Long. For each one of these potential waste package design configurations, a parametric study is performed to calculate the interference produced by the thermal expansion of the inner vessel and outer corrosion barrier to determine the required axial gap. Because the inner vessel

undergoes a greater change in temperature and has a larger coefficient of thermal expansion as compared to those of the outer corrosion barrier, this interference is calculated as the inner vessel length minus the outer corrosion barrier cavity length subsequent to thermal expansion. The length of this interference is equal to the required axial gap created during fabrication (i.e., at room temperature and prior to fuel loading) to avoid contact between the inner vessel and outer corrosion barrier during thermal expansion. The maximum interference between the inner vessel and outer corrosion barrier produced from thermal expansion is equal to the minimum required waste package axial gap. These minimum axial gaps are presented in Table 19.

Table 19. Minimum Required Axial Gap Between the Inner and Outer Corrosion Barriers

Waste Package Type	Maximum Interference	
	(mm)	(in.)
21-PWR	8.1	0.32
Naval SNF - Long	7.6	0.30
44-BWR	8.0	0.32
5 DHLW/DOE SNF- Long	6.8	0.27

Source: BSC 2003 [DIRS 161691], Table 4

Table 19 shows that the maximum interference occurs in the 21-PWR waste package and is 8.1 mm (0.32 in.). For consistency amongst the waste package design configurations the minimum axial gap is determined to be 10 mm (0.39 in.).

7.1.1.2.4 Internal Pressurization Due To Thermal Expansion

This calculation determines the resulting tangential (hoop) and longitudinal stresses in the outer corrosion barrier produced by an internal pressure increase due to elevated temperatures and a decreasing volume from thermal expansion. From BSC 2001 [DIRS 152655], Tables 4 and 5 the required radial gap between the waste package inner vessel and outer corrosion barrier to avoid contact is 1 mm (0.04 in.). This calculation assumes that the waste package inner vessel and outer corrosion barrier have a 1-mm (0.04-in.) gap between them, and this gap collapses completely; consequently, the gas volume between the inner vessel and outer corrosion barrier decreases, increasing the internal pressure.

Table 20 below provides the resulting gage pressure with respect to ambient pressure for each waste package. The results are summarized in Table 21 and the non-dimensional results in, Table 22, comparing the tangential (hoop) and longitudinal stress to the yield stress (BSC 2003 [DIRS 167005], Section 6).

Table 20. Resulting Gage Pressure with Respect to Ambient Pressure

Waste Package	Gage Pressure with Respect to Ambient, p_{gage}		
	(atm)	(KPa)	(psi)
21-PWR	2.65	268	38.9
Naval SNF - Long	2.24	227	32.9
44-BWR	2.59	263	38.1
5 DHLW/DOE SNF - Long	2.09	212	30.7

Source: BSC 2003 [DIRS 167005], Table 2

Table 21. Calculation Results

Waste Package	Tangential Stress, σ_h		Longitudinal Stress, σ_l	
	(MPa)	(ksi)	(MPa)	(ksi)
21-PWR	10.2	1.48	5.12	0.742
Naval SNF - Long	10.3	1.50	5.17	0.750
44-BWR	10.2	1.48	5.12	0.742
5 DHLW/DOE SNF - Long	10.5	1.52	5.26	0.762

Source: BSC 2003 [DIRS 167005], Table 3

Table 22. Non-dimensional Results

Waste Package	σ_h/σ_y (%)	σ_l/σ_y (%)
21-PWR	4.51	2.26
Naval SNF - Long	4.55	2.28
44-BWR	4.51	2.25
5 DHLW/DOE SNF - Long	4.63	2.32

Source: BSC 2003 [DIRS 167005], Table 4

Based on the results of Table 22, the outer corrosion barrier is subjected to a stress that is less than 5% of its yield strength in the hoop direction and less than 3% in the axial direction, making the effect of internal pressure insignificant.

7.1.1.2.5 Static Weight on the Emplacement Pallet

Table 23 is reprinted from BSC (2002 [DIRS 165492], Table 6-2). The objective of this calculation is to determine the structural response of the outer corrosion barrier of four different waste packages while statically resting on an emplacement pallet at 400°F. Degraded thicknesses are used to account for possible corrosion of the outer corrosion barrier. LS-DYNA is used to solve the finite element representation of the problem.

Table 23. Stresses in Degraded Waste Package (MPa)

Waste Package	4 mm Radial Gap	10 mm Radial Gap	15 mm Radial Gap
21-PWR	90	80	90
44-BWR	86	80	116
Naval Long	74	84	76
5 DHLW/DOE SNF-Short	20	42	52

Source: BSC 2002 [DIRS 165492], Table 6-2.

The stresses reported are less than the yield stress of Alloy 22 (UNS N06022), and indicate significant margin to failure for a range of gap sizes. The yield stress of Alloy 22 (UNS N06022) may be found in Table 2. Therefore, the waste package is able to withstand the stresses of its own self-weight even after 10,000 years of degradation. Since this is a bounding case, the results show that the non-degraded waste package will also meet the criteria. Consequently, no breach of the waste package is expected.

7.1.1.3 Shielding

Table 4.9.1-2 of *Project Design Criteria Document* (Doraswamy 2004 [DIRS 169548]) does not list any shielding requirements on the waste package. The transporter and building will provide shielding.

Although there are no shielding criteria outlined for the waste package, the following results are presented for information only. BSC 2003 [DIRS 164533] is the dose rate calculation for the 21-PWR waste package, and BSC 2003 [DIRS 166596] is the dose rate calculation for the 44-BWR waste package. The specific dose rates are reported in Appendix B.

7.1.1.3.1 21-PWR Waste Package Conclusions and Recommendations

This entire section, 7.1.1.3.1, is taken from BSC 2004 [DIRS 169593], Section 6.5.

Dose rates, including gamma and neutron contributions, have been calculated inside the waste package, on the surface of the waste package, and at various distances away from the waste package and are suitable to support the waste package and repository facility design.

Calculations with the design basis source (4.0 wt % initial ^{235}U enrichment, 60 GWd/MTU burnup, and 10 year cooling time) are performed for both the waste package surrounded by a concrete structure 3 m away and the waste package without the structure. It is noted that the dose rate increased about 3-10 % on the external waste package surface, depending on location, when the concrete structure is present due to scattering radiation (the closer to the concrete wall, the higher the increase in dose rates).

The calculations show that secondary gamma rays have very little impact on the total dose rate, as the primary gamma source is the predominant contributor for an unshielded waste package.

Three various source terms from a controlled source were utilized. The maximum source term is revised to utilize 5.0 wt% initial ^{235}U enrichment, 80 GWd/MTU burnup, and 5 year cooling

time. As expected, the maximum source produced the highest dose rates followed by the design basis and average source. The revised maximum source term produced approximately 10% higher dose rates in the radial direction while the dose rates in the axial direction are virtually unaffected.

Corresponding neutron intensity peaking factors are calculated for the three various source terms to accurately depict the neutron contribution. The maximum source features the highest peaking factor (2.47), followed by the average source (2.38) and the design basis source (2.24).

Radiation effects on the ground control material (stainless steel type 316) are determined to be insignificant, as the cumulative neutron fluence over 300 years is well below the threshold for the mechanical property changes. Gamma radiation has no effect on stainless steel type 316.

7.1.1.3.2 44-BWR Conclusions and Recommendations

This entire section, 7.1.1.3.2, was taken from BSC 2003 [DIRS 166596], Section 6.3.

Dose rates, including gamma and neutron contributions, are calculated inside the waste package, on the surface of the waste package, and at various distances away from the waste package and are suitable to support the waste package and repository facility design.

Calculations with the average source (3.5 wt% initial ^{235}U enrichment, 40 GWd/MTU burnup, and 25-year cooling time) are performed for both the waste package surrounded by a concrete structure 3 meters (9.8 ft) away and the waste package without the structure. It is noted that the dose rate increased approximately 3 to 10 percent on the waste package external surfaces (depending on location) when the concrete structure is present due to scattering radiation.

The calculations showed that secondary gamma rays have very little impact on the total dose rate, as the primary gamma source is the predominant contributor for an unshielded waste package. However, secondary gamma ray contribution may become important in shielded cases.

Two various source terms (BSC 2003 [DIRS 164364]) from a controlled source are utilized in this calculation. As expected, the maximum source produced the highest dose rates compared to the average source.

Corresponding neutron intensity peaking factors are calculated for the two various source terms to accurately depict the neutron contribution. The maximum source features the highest peaking factor (2.82) compared to the average source (2.62).

7.1.1.4 Waste Form Accommodation

Table 24 (BSC 2003 [DIRS 163984] Section 6, Table 6-1) gives the dimensions of the waste package cavity that are to be used to accommodate the fuel assemblies listed in Tables 7 and 8. These dimensions may be verified on the configuration drawings.

Table 24. Cavity Design Dimensions

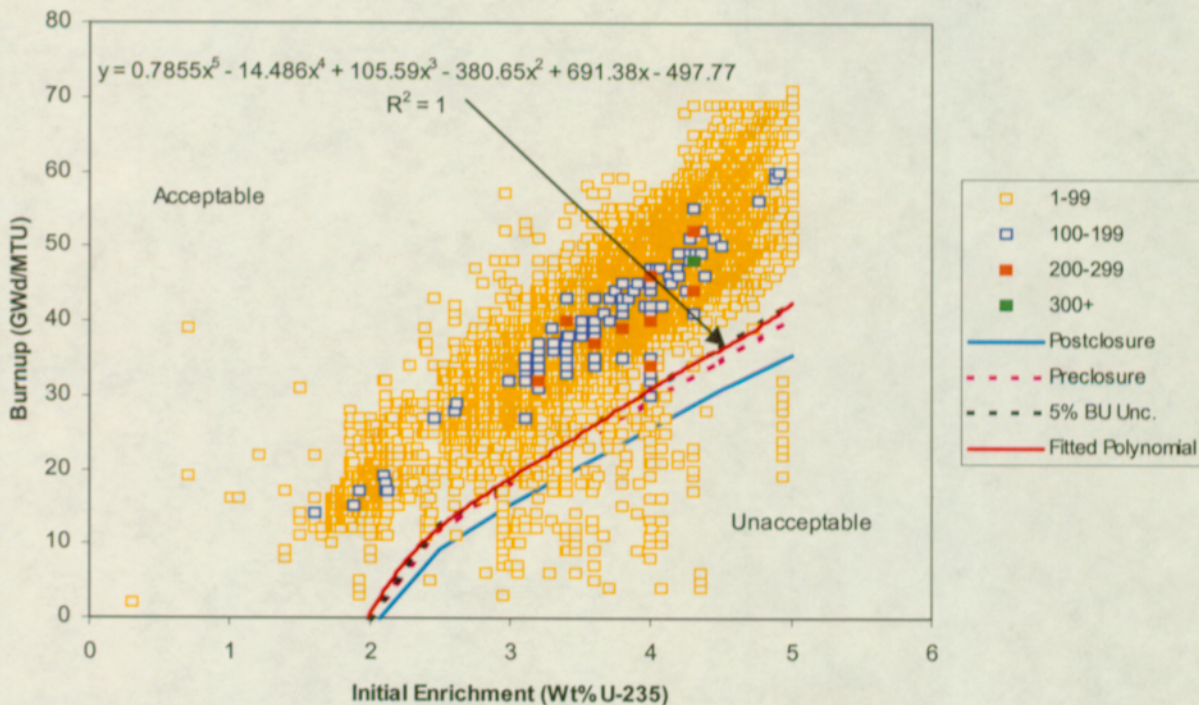
Waste Package	10 CFR 961 Appendix E Max Length Dimension	10 CFR 961 Appendix E Max Width Dimension	Max Fuel Assembly Width	Max Fuel Assembly Length	Design Cavity Length (minimum)	Design Clear Square Insertion (minimum)
21-PWR	178	9	8.536	180	180.5	8.80
12-PWR	178	9	8.4	201.1	201.6	9.00
44-BWR	179	6	5.91	177.8	180.5	6.00
24-BWR	179	6	5.91	177.8	180.5	6.00

NOTE: all dimensions are in inches, the DIRS number for 10 CFR 961 is 118049.
 Source: BSC 2003 [DIRS 163984], Table 6-1.

7.1.1.5 Criticality

21-PWR

BSC 2003 [DIRS 166610] is used to evaluate the reactivity limit, defined by minimum burnup as a function of initial enrichment, that would permit loading of PWR SNF assemblies into the 21-PWR waste package configuration with absorber plate. This calculation is performed using the baselined MCNP code. Note that in Section 7.1.1.5 (including Figure 6 and Figure 7), BU stands for Burn Up, Unc. stands for Uncertainty, and LC stands for Loading Curve.



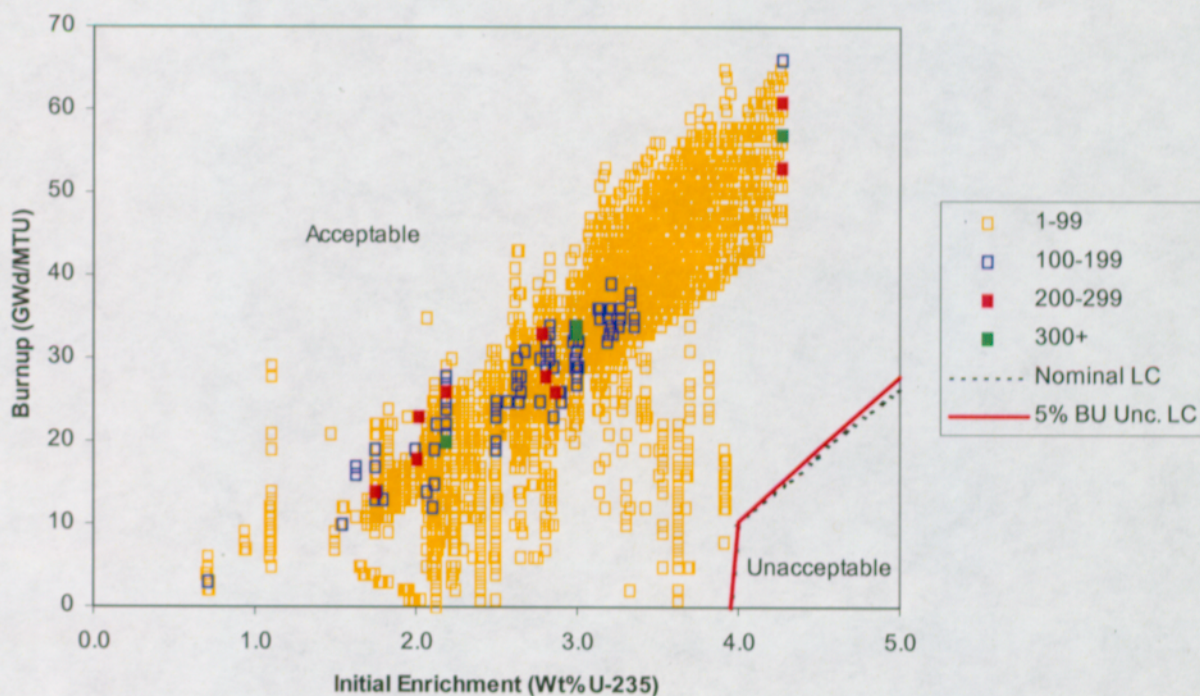
Source: BSC 2003 [DIRS 166610], Figure 40.

Figure 6. Loading Curve and Projected Waste Stream, 21-PWR

The squares above the fitted polynomial in Figure 6 show that approximately 98 percent of the current PWR SNF projected waste stream may be disposed in a 21-PWR waste package with absorber plate (BSC 2003 [DIRS 166610], Section 6.3). Note the squares in the legend indicate the number groupings of assemblies at a particular burnup and enrichment (e.g., 100-199 indicates that there are 100 to 199 assemblies at a listed burnup and enrichment). A different waste package configuration, such as a 21-PWR waste package configuration with control rod, could be used for disposing of the remaining 2 percent of the projected PWR SNF waste stream. Alternatively, predetermined loading patterns could be used to blend assemblies that are below the design basis reactivity limit with assemblies that have sufficiently low reactivity to compensate. It is also important to note that BSC (2003 [DIRS 166610]) uses Neutronit A978TM as the neutron absorbing material. Refer to Section 5.3 for the current design description.

44-BWR

Preliminary results have been transmitted to the Waste Package and Components group via Thomas 2004 [DIRS 170052]. Figure 7 shows the criticality loading curve plotted against the waste stream inventory. The squares in the legend have the same meaning as those in the 21-PWR figure. *Nominal LC* is the loading curve based on the nominal required minimum burnup; and *5% BU Unc. LC* is the loading curve adjusted to accommodate five percent uncertainty associated with the reported assembly burnups. These results are for optimum moderation conditions.



Source: Dan Thomas 2004 [DIRS 170052], Figure 1.

Figure 7. Loading Curve and Projected Waste Stream, 44-BWR

The criticality loading curve results indicate that 100 percent of the current BWR projected waste stream may be disposed of in the 44-BWR waste package with Ni-Gd Alloy (UNS N06464) absorber plates.

Separate results documented in the loading curve calculation indicate that the 44-BWR waste package with Ni-Gd Alloy (UNS N06464) absorber plates will not go critical with commercial fuel assemblies if there is no moderator present within the waste package. Other results cited in Thomas 2004 [DIRS 170052] indicate that there is no significant package-to-package interaction, so the waste packages may be stored together in large arrays.

7.1.2 Event Sequences

7.1.2.1 Thermal

Conditions used in fire calculations (BSC 2003 [DIRS 165968]) represented a parametric range, up to and including the full transportation fire (800°C for 30 minutes).

Tables 25 and 26 have been reprinted from *Thermal Response of the 21-PWR to a Fire Accident* (BSC 2003 [DIRS 165968], Tables 6-1 and 6-2). Fourteen cases were analyzed. All but one case had no gap between the stainless steel inner vessel and Alloy 22 outer barrier, which maximizes internal temperatures. Thermal conductivity for PWR SNF was evaluated at both minimum (14x14 assembly) and maximum (15x15 assembly) values. A nominal heat transfer coefficient, h , was used for natural convection around a horizontal cylinder in air. Fire duration was varied at 10, 20, and 30 minutes, and fire temperature was varied at 600°C, 700°C, and 800°C. Flame emissivity was constant at 1.0 and waste package surface emissivity was varied conservatively for initial, fire, and postfire time periods. Solutions were found using a finite element representation in ANSYS.

The results of the 21-PWR waste package fire calculation show that for all cases, even for the full transportation fire, peak cladding temperatures are far below 570°C. The lowest margin is 125°C and the margin for 10-minute fires is at least 300°C.

Table 25. 21-PWR Fire Calculation Case Descriptions

Case No.	Model Type	Thermal Conductivity of SNF	Fire Duration (min)	Fire Temperature (°C)	Natural Convection During Fire	Outer Surface Emissivity Initial/Fire/Postfire
1	No Gap	Kmin	30	800	h	0.87 / 0.87 / 0.87
2	Gap	Kmin	30	800	h	0.87 / 0.87 / 0.87
3	No Gap	Kmax	30	800	h	0.87 / 0.87 / 0.87
4	No Gap	0.5 Kmax	30	800	h	0.87 / 0.87 / 0.87
5	No Gap	Kmin	30	800	3 h	0.87 / 0.87 / 0.87
6	No Gap	Kmin	30	800	h	0.5 / 1.0 / 0.5
7	No Gap	Kmin	30	700	h	0.87 / 0.87 / 0.87
8	No Gap	Kmin	30	600	h	0.87 / 0.87 / 0.87
9	No Gap	Kmin	20	800	h	0.87 / 0.87 / 0.87
10	No Gap	Kmin	20	700	h	0.87 / 0.87 / 0.87
11	No Gap	Kmin	20	600	h	0.87 / 0.87 / 0.87
12	No Gap	Kmin	10	800	h	0.87 / 0.87 / 0.87
13	No Gap	Kmin	10	700	h	0.87 / 0.87 / 0.87
14	No Gap	Kmin	10	600	h	0.87 / 0.87 / 0.87

Source: BSC 2003 [DIRS 165968], Table 6-1.

Table 26. Calculated Peak Temperatures for 21-PWR Fire Calculations

Case No.	Peak Temperature of Component (°C)					
	PWR Cladding	Basket	Neutron Absorber	Thermal Shunt	Inner Vessel	Outer Barrier
1	407.5	409.9	393.5	386.2	510.7	551.3
2	327.4	335.6	313.5	311.5	372.2	685.7
3	407.0	409.4	393.2	385.9	510.7	551.2
4	410.8	413.0	394.9	387.8	510.8	551.3
5	427.6	430.3	411.9	404.0	535.5	575.8
6	465.8	468.2	450.5	443.3	564.1	602.0
7	336.5	338.1	328.1	323.3	412.9	446.1
8	280.3	281.3	276.7	273.7	333.4	358.6
9	334.5	336.2	326.9	321.6	428.4	479.2
10	283.6	284.6	280.0	276.6	350.9	390.6
11	273.5	256.0	256.0	255.9	289.1	318.1
12	275.4	258.0	258.0	257.9	322.3	386.5
13	269.3	251.5	251.5	251.4	274.0	321.8
14	264.4	246.3	246.3	246.2	236.6	270.3

Source: BSC 2003 [DIRS 165968], Table 6-2.

Fire calculations for the 44-BWR waste package are reported in *Thermal Response of the 44-BWR Waste Package to Hypothetical Fire Accident* (BSC 2003 [DIRS 162007]). Table 27 summarizes the maximum cladding temperatures for all the cases analyzed (BSC 2003 [DIRS 162007], Section 6). The various fire conditions are described by Tables 28 and 29 (BSC 2003 [DIRS 162007], reproduced from Tables 5-2 and 5-20).

Table 27. Summarized Peak Cladding Temperature for 44-BWR

Case	Max. Temp (°C)	Case	Max. Temp (°C)
1	338.3	3 - 4	351.4
2	336.8	3 - 5	317.4
3	430.4	3 - 6	285.8
4	429.7	3 - 7	277.6
5	438.8	3 - 8	273.5
6	438.1	3 - 9	269.5
3 - 1	428.2	3 - 10	426.2
3 - 2	378.9	3 - 11	428.5
3 - 3	333.6		

Source: BSC 2003 [DIRS 162007], Section 6.

Table 28. Original 44-BWR Waste Package Fire Accident Evaluation Cases (800°C fire for 30 minutes)

Item	BWR SNF Fuel Representation	Configuration	BWR Thermal Load	Description
Case 1	With Channel	With Gaps	Max. Design	Base configurations
Case 2	No Channel	With Gaps	Max. Design	
Case 3	With Channel	No Gaps	Max. Design	Eliminating gaps should increase fire accident effects
Case 4	No Channel	No Gaps	Max. Design	
Case 5	With Channel	No Gaps	1.2 x Max. Design	Evaluate sensitivity of BWR peak cladding temperature to increased thermal load
Case 6	No Channel	No Gaps	1.2 x Max. Design	

Source: BSC 2003 [DIRS 162007], Table 5-2.

Table 29. 44-BWR Waste Package Fire Accident Evaluation Cases for Sensitivity Study

Load Case	Time (min.)	Temperature (°C)	Absorber Properties
3-1	30	800	Normal
3-2	30	700	Normal
3-3	30	600	Normal
3-4	20	800	Normal
3-5	20	700	Normal
3-6	20	600	Normal
3-7	10	800	Normal
3-8	10	700	Normal
3-9	10	600	Normal
3-10	30	800	Diffusivity, >5000% of Normal
3-11	30	800	Diffusivity, 5% of Normal

Source: BSC 2003 [DIRS 162007], Table 5-20.

The results of the 44-BWR fire calculation shows the maximum cladding temperature for the 44-BWR waste package is far below 570°C, even for the full transportation fire. There is a 150°C margin for the transportation fire and a margin of over 300°C for the 10-minute fires.

7.1.2.2 Structural

The preclosure safety analysis considers the probability of potential hazards, taking into account the range of uncertainty associated with the data that support probability calculations. Event sequences are defined in Meham 2004 [DIRS 169790], Section 5.2.8 and Section 6.1.2.2, and these sequences of human-induced and natural events are used as inputs to calculate the consequences of potential failures of structures, systems, and components in terms of worker safety and dose to workers and the public during the preclosure period of a repository at Yucca Mountain.

The waste package is a component identified as important to safety (BSC 2003 [DIRS 165179], Table A-2, p. A-3) since it provides containment for the waste forms. The waste package is credited to prevent a release, in terms of dose to workers and the public during the preclosure period. Therefore, the waste package is designed to a set of criteria to ensure that the waste package will not breach as a result of credible event sequences.

The waste package design is evaluated using a finite element analysis based on numerical simulations of waste package dynamic events including, but not limited to, vertical and horizontal drops, slapdowns, drops onto objects, collisions, and equipment drops onto the waste package.

The failure criterion used is explained in detail in Section 7.1.2.3.1.2 and is broken into a tiered screening criteria shown below. The easiest to apply and most conservative criteria are applied initially. If these can not be met, less conservative screening criteria are imposed that require more calculations. These screening criteria in decreasing order of conservatism are (an element's total stress intensity is equal to twice the element's maximum shear stress (ASME 2001 [DIRS 158115], Section III, Division 1, NB-3000)):

Maximum $\sigma_{int} < 0.7\sigma_u$?	Yes: Meets P_m and P_L limits without the need for wall averaging.
No: Maximum $\sigma_{int} < 0.77\sigma_u$?	Yes: Meets P_L limit without the need for wall averaging but the stress field must not be uniform around the entire circumference (only a concern for vertical drop events).
No: Maximum wall-averaged $\sigma_{int} < 0.7 \sigma_u$?	Yes: Meets P_m and P_L limits.
No: Maximum wall-averaged $\sigma_{int} < 0.77\sigma_u$?	Yes: Meets P_L limit if the stress fields are not uniform around the entire circumference (only a concern for vertical drop events).

No:

Maximum wall-averaged $\sigma_{int} < 0.84 \sigma_u$

and

wall-averaged $\sigma_{int} < 0.77 \sigma_u$ at $\sqrt{R \cdot t}$

surrounding maximum location?

Yes: Meets P_L and average primary shear limit

No:

Maximum wall-averaged $\sigma_{int} < 0.9 \sigma_u$

and

wall-averaged $\sigma_{int} < 0.77 \sigma_u$ at $\sqrt{R \cdot t}$

surrounding maximum location?

and

wall-average of each shear stress on the stress classification line

$(\tau_{xy}, \tau_{yz} \text{ and } \tau_{xz}) < 0.42 \sigma_u$?

Yes: Meets P_L and average primary shear limit

(x,y,z are element (not global) directions

orthogonal to the stress classification line)

No: Fails simplified screening criterion.

If the wall-averaged σ_{int} limits can not be met, perform a less conservative rigorous Code evaluation using all six stress components (and solve a cubic equation for principle stress direction values) and/or use multiple stress classification lines to extrapolate to governing wall locations when they have significant non-membrane primary stress intensity contributions.

If the average primary shear limit can not be met, then review appropriateness of using a stress classification plane rather than a stress classification line.

7.1.2.2.1 Preclosure Rock Fall Evaluations

Rock falls may occur both in the preclosure and postclosure periods. For the preclosure period, the drip shields have not yet been emplaced, so rocks may fall onto the emplaced waste packages. Four waste package configurations for license application (21-PWR waste package, 44-BWR waste package, 5-DHLW/DOE SNF codisposal short waste package, and Naval Canistered SNF long waste package) are investigated to determine their structural response to rock fall dynamic loads (Mecham 2004 [DIRS 169790], Section 6.2.2.4, and BSC 2004 [DIRS 167182], Section 6). Using the commercially available LS-DYNA finite element code, a finite element analysis is performed. Four different axial locations of impact are evaluated in this study. The first impact location is selected at the waste package bottom-end, directly above the trunnion-to-bottom lid fillet-weld region; second, at mid-length; third, directly above the emplacement pallet support; and fourth, at the waste package upper-end, directly above the closure-weld region. These locations are critical to the waste package design and provide bounding results for structural evaluations.

One waste package configuration is used to determine the most damaging location of impact among the four impact locations. For this purpose, LS-DYNA simulations of the 44-BWR waste package are developed for all four impact locations. The results of these calculations suggest that the most damaging results are obtained when the axial location of the initial impact zone is directly above the trunnion collar sleeve, at the bottom lid fillet-weld region. Consequently, the rock fall calculations for the remaining waste package configurations are performed for this impact location, which is the most damaging simulation setup used.

For single rock fall evaluations, a total of eleven three-dimensional half-symmetry finite element representations of the waste package emplaced on the emplacement pallet, and the rock, are developed in LS-DYNA for one bounding rock size and initial impact speed (6.8 MT, 6 m/s). One additional simulation is also performed to determine the effect of the greatest initial impact speed (1.3 MT, 14 m/s). The results show that the rock with the greatest mass causes higher stresses than the rock with the greatest initial impact speed.

One additional simulation is also performed to determine the response of the waste package components to multiple rock falls onto the same location. The main purpose of this study is to determine the effect of two rocks on the stress intensity history when they impact the same location on the waste package. For this purpose, a representative 21-PWR waste package configuration is selected. This waste package is subjected to the highest stress intensity for the bounding impact location. Therefore, the results of this case are bounding for all waste package configurations.

For the simulation of the rock fall onto corroded waste package, the thickness of the Alloy 22 (UNS N06022) components is appropriately reduced based on the calculation of the depth of corroded layer presented in BSC 2004 [DIRS 167182], Section 5.3.

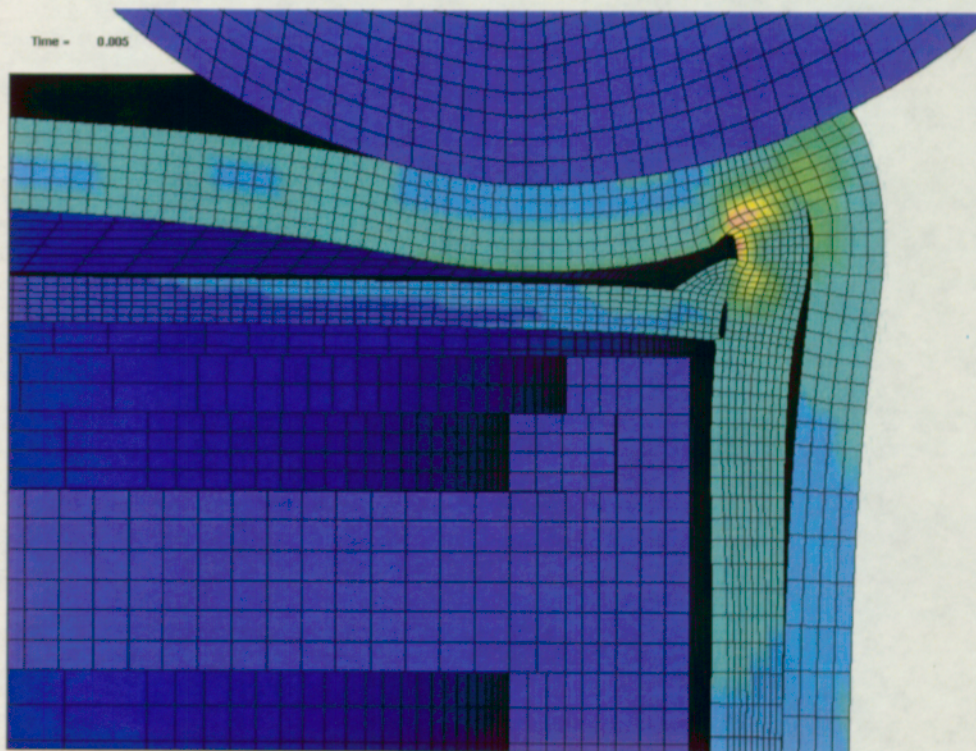
The results of the rock fall evaluations indicate that for all rock impact simulations, the maximum stress intensity in the outer corrosion barrier and outer lids is less than 0.7 times the tensile strength of Alloy 22 (UNS N06022) at maximum temperatures during their presence in the repository (BSC 2004 [DIRS 167182], Section 6). Therefore, the waste package is not anticipated to fail due to a preclosure rock fall event.

7.1.2.2.2 Object Drop

The Object Drop consists of raising a hook that is used to lift the waste package directly above a vertically standing waste package. The hook is raised to a maximum height of 30 ft (9.1 m). After which the lifting device, with the hook attached, fails and the hook falls due to gravity. The hook then impacts the waste package top surface. The simulation is performed using LS-DYNA finite element software. The simulation is performed at RT and 300°C to bound potential waste package operational temperatures. The results (BSC 2003 [DIRS 166943], Section 6) presented in this subsection are obtained by using the maximum hook elevation of 30 ft (9.1 m) and a hook mass of 2,000 lb (BSC 2003 [DIRS 164128], Assumption 5.3.41):

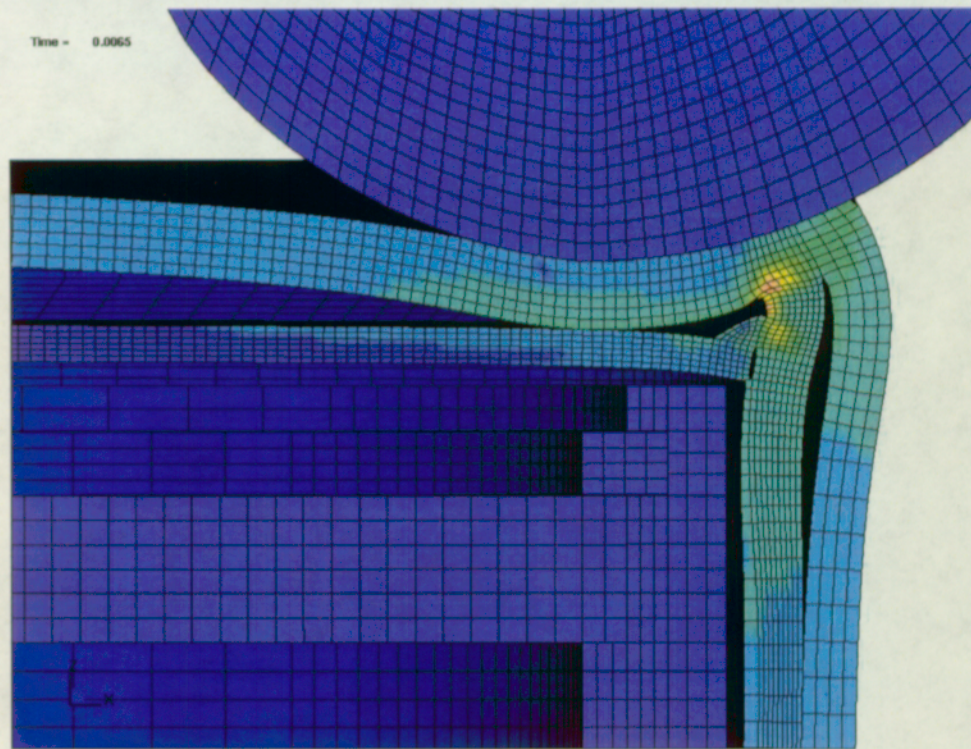
The maximum stresses in the components of the outer corrosion barrier are mostly beyond the acceptable range. However, the stresses in this calculation are reported for the outer corrosion barrier only. This is because even under maximum deformation, the outer corrosion barrier never touches the inner vessel. Therefore, the inner vessel remains at its initial condition throughout the simulation. Therefore, no release of radionuclides is expected to result from this event. Figures 8 and 9 showing the maximum deformation, taken from BSC 2004 [DIRS 166943], Section 6 are reprinted below.

The results presented are appropriate for both the 21-PWR and 44-BWR waste packages.



Source: BSC 2003 [DIRS 166943], Section 6, Figure 8.

Figure 8. Maximum Deformation at Room Temperature, 21-PWR



Source: BSC 2003 [DIRS 166943], Section 6, Figure 9.

Figure 9. Maximum Deformation at 300°C, 21-PWR

7.1.2.2.3 Missile Impact on Waste Package

Four different waste package configurations are evaluated in CRWMS M&O 2000 [DIRS 149351]: 21-PWR, 44-BWR, 5-DHLW/DOE SNF-Short, and Naval SNF Long waste packages. For each one of these waste package configurations, a parametric study is performed by reporting the results for different missile diameter, mass, and velocities. These parameters are given in Table 30.

Table 30. Missile Impact Parameters for Three Different Case Studies

	Case 1	Case 2	Case 3
Missile diameter	10 mm	20 mm	30 mm
Missile mass	0.5 kg	1.0 kg	1.5 kg
Missile velocity	5.7 m/s	6.0 m/s	6.3 m/s

Source: CRWMS M&O 2000 [DIRS 149351], Table 5.2-1

The effect of dynamic impact on the waste package outer barrier is determined using the empirical relations developed for perforation of plates by a rigid mass. The literature on dynamic impact analyses shows that various empirical equations have been developed for the perforation of ductile metal plates (specifically, mild steel plates). The waste package outer barrier has circular geometry formed from plates rolled into cylinders; however, the effect of shell curvature is small, yet conservative due to convexity, considering the missile diameter, the radius of curvature of the waste package shells, and the shell thickness. Therefore, the empirical relations of flat plates are used for the purpose of evaluating the missile impact problem.

The perforation of a plate by a projectile involves a complex mechanism of impact and subsequent failure if the projectile has a large amount of kinetic energy. Thus, there is no complete theoretical model that incorporates all of the relevant phenomena and that is capable of predicting accurately all of the aspects of an impact perforation event. However, there are some empirical equations developed for the low-velocity impact analysis. One of these relations used widely in design is the Ballistics Research Laboratory equation (Jones 1994 [DIRS 137700], page 53). No limitations are associated with this equation in terms of the missile velocity range or the ratio of the target span to the missile diameter. Hence, the use of Ballistics Research Laboratory equation is more general compared to other equations provided. A second reason for using the Ballistics Research Laboratory equation is that this equation gives reasonable agreement with the experimental results.

The structural response of the waste package to dynamic impact of a pressurized system missile is reported in terms of the minimum velocities required for a pressurized system missile to cause perforation of the waste package outer barrier. The calculation results are summarized in Table 31.

Table 31. Pressurized System Missile Impact Results for Different Waste Packages

Waste Package	Minimum required velocity of projectile to cause perforation (m/s)		
	Case 1	Case 2	Case 3
21-PWR	322	383	424
44-BWR	322	383	424
5 DHLW/DOE SNF - Short	339	403	446
Naval SNF - Long	339	403	446

Source: CRWMS M&O 2000 [DIRS 149351], Table 6-1

At this point in time, there is no credible source for anything at the site to be moving at velocities greater than 300 m/s. In fact, measures are taken to ensure that such velocities are unobtainable. Additionally, the air pressure system and the pneumatics within the infrastructure are not capable of propelling blown valves or other debris at speeds greater than 300 m/s. Therefore, the probability is incredible, and the waste package is not anticipated to breach due to this type of event.

7.1.2.2.4 Vertical Drop

The vertical drop consists of raising the waste package vertically to a maximum height of 2.0 m (6.6 ft) (see Mechem 2004 [DIRS 169790], Section 5.2.8). After which, the lifting device carrying the waste package fails and the waste package falls. The waste package then impacts an unyielding surface. The simulation is performed using LS-DYNA finite element software. The simulation is performed at room temperature, 400°F, and 600°F for the 44-BWR, and room temperature and 300°C for the 21-PWR, to bound potential waste package operational temperatures.

21-PWR Waste Package

The vertical drop results for the 21-PWR waste package are shown in Table 32. The finite element representation is solved using LS-DYNA. In the calculation, the waste package is

dropped 2.0 m (6.6 ft) onto an unyielding surface while in the vertical position. Solutions for room temperature and 300°C are presented in Table 32.

Table 32. Maximum Wall Averaged Stress Intensity for 21-PWR Vertical Drop

Part	Temperature	Max Stress Intensity (σ_{int})	σ_{int} / σ_u
Outer Barrier	RT	611 MPa	0.629
Inner Vessel	RT	404 MPa	0.575
Outer Barrier	300 °C	549 MPa	0.603
Inner Vessel	300 °C	422 MPa	0.683

NOTE: RT = room temperature.

Source: BSC 2004 [DIRS 169647], Table 6-2.

The wall average stress intensities in the outer corrosion barrier and inner vessel are below seven-tenths of the true tensile strengths of Alloy 22 (UNS N06022) and 316 SS, respectively. Therefore, both the outer corrosion barrier and the inner vessel meet the plastic analysis criteria.

44-BWR Waste Package

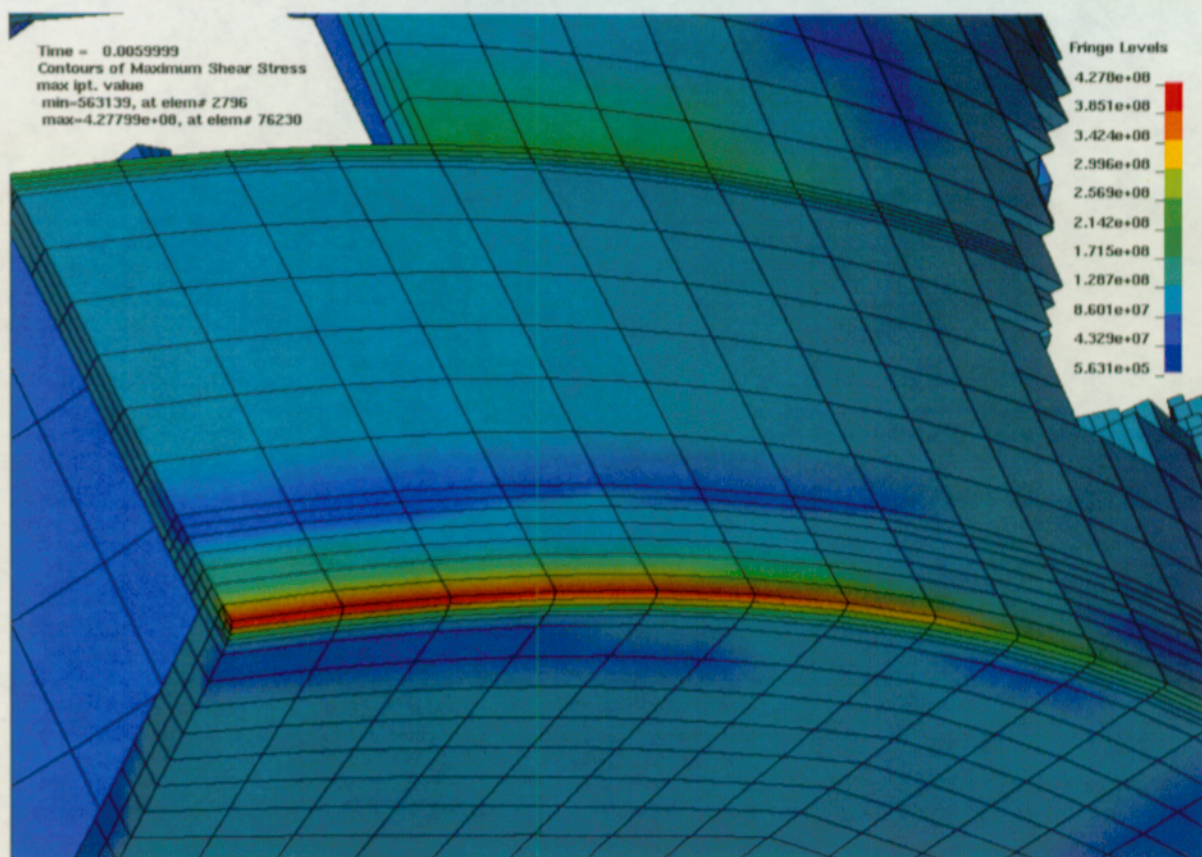
Table 33. Maximum Stress for 44-BWR Vertical Drop

Part	Temperature	Max Stress Intensity	σ_{int} / σ_u
Inner Vessel	RT	398 MPa	0.566
Outer Corrosion Barrier	RT	1030 MPa	1.06
Inner Vessel	400 °F	385 MPa	0.570
Outer Corrosion Barrier	400 °F	884 MPa	0.954
Inner Vessel	600 °F	381 MPa	0.566
Outer Corrosion Barrier	600 °F	850 MPa	0.963
Inner Vessel	600 °F	400 MPa	0.646
Outer Corrosion Barrier	600 °F	856 MPa	0.936

NOTE: RT = room temperature.

Source: BSC 2002 [DIRS 162692], Table 6-2.

At the time that the calculation providing the results in Table 33 was originated, the tiered approach to ASME B&PV Code limits had not yet been fully formulated; however, a close inspection of the stress fields near the maximum stress intensity may be examined to provide visual confirmation that a detailed calculation of the stress field would satisfy the one or more tiers of the stress limit hierarchy



Source: BSC 2002 [DIRS 162692], Figure 6-9

Figure 10. Outer Corrosion Barrier at 600°F (Pa)

Figure 10 shows that the elements with maximum stress are in the weld section of the outer corrosion barrier. Hechmer and Hollinger 1998 [DIRS 166147] provides guidance for analyzing through wall stress away from welds or discontinuities (such as corners). By utilizing the color legend, the average shear stress adjacent to the weld would be no greater than 300 MPa, or 600 MPa if using stress intensity. The first limit of through wall stress in the tiered approach is $0.7\sigma_u$, which is 638 MPa for Alloy 22 (UNS N06022) at 600 °F. Therefore, the tiered criterion is met, and the 44-BWR waste package is not anticipated to fail due to a vertical drop. It should also be noted that for a flat vertical drop that the seal welds at the top of the inner vessel should not be compromised by the drop. The seal welds are over 4.57 meters (180 in.) away from the impact location and should be structurally unaffected by the event.

7.1.2.2.5 Tip Over from Elevated Surface

21-PWR Waste Package

A tip over from elevated surface event is bounding for a tip over with slap down event. Therefore, only the tip over from elevated surface needs to be presented. This event sequence simulates what happens when a 21-PWR waste package is resting while being supported at an elevation of 2.0 m (6.6 ft) (BSC 2004 [DIRS 167024], Assumption 3.10) above an unyielding

surface, and gets tipped over. Results for this calculation are found at room temperature and at 300 °C. The finite element solution is found using LS-DYNA. Table 34 is reprinted from BSC 2004 [DIRS 167024].

Table 34. Maximum Through-Wall Stress Intensity, Location Averages

Outer Corrosion Barrier Location	Temp. (°C)	Approximate Stress Intensity (MPa)	$0.77\sigma_u$
Side 2	RT	623	748
Side 1	RT	687	748
Top 1	RT	600	748
Side 2	300 °C	534	701
Side 1	300 °C	613	701
Top 1	300 °C	604	701

NOTE: RT = room temperature.

Source: BSC 2004 [DIRS 167024], Table 6-3

Table 34 shows the average stress intensity through the wall of the outer corrosion barrier (used to define P_1) is less than $0.77\sigma_u$. Inspecting the stress patterns reveals that the stress does not extend around the circumference. Therefore, the outer corrosion barrier meets the appropriate criteria, and is not expected to breach.

44-BWR Waste Package

The 44-BWR waste package tip over from elevated surface is identical in nature to the 21-PWR waste package tip over, except for the change of waste package. Results are reported for room temperature and 100°C. Table 35 is reprinted from BSC 2004 [DIRS 169705].

Table 35. Maximum Wall Average Stress Intensities

Section	Temperature	Max Wall Average Stress Intensity (σ_{int})	σ_{int} / σ_u
Wall Section 1	RT	714 MPa	0.74
Wall Section 2	RT	664 MPa	0.68
Wall Section 1	100 °C	658 MPa	0.67
Wall Section 2	100 °C	620 MPa	0.63

NOTE: RT = room temperature.

Source: BSC 2004 [DIRS 169705], Table 6-3.

The wall averages, which are $<0.77\sigma_u$, indicate that the tip-over drop meets the limits when bending stresses are secondary with wall averaged stress intensity used as a conservative general primary membrane stress intensity. Therefore, the 44-BWR waste package is not expected to breach during this event.

7.1.2.2.6 Horizontal Drop

21-PWR Waste Package

Table 36 shows allowable P_m limits for the outer corrosion barrier made from Alloy 22 (UNS N06022). The horizontal drop results for the 21-PWR waste package are shown in Table 37. The finite element representation is solved using LS-DYNA. In the calculation, the waste package is dropped 2.4 m (7.9 ft) (see Mecham 2004 [DIRS 169790], Section 5.2.8) onto an unyielding surface while in the horizontal position. Solutions for room temperature and 100°C are presented in the tables below.

Table 36. Allowable P_m Limits for OCB

Temperature	Allowable P_m (MPa)
RT	$0.7 \times 971 = 680$
100°C	$0.7 \times 977 = 684$

NOTE: RT = room temperature

Source: BSC 2004 [DIRS 167718], Table 6-1.

Table 37. OCB P_m Evaluation

Temperature	P_m (MPa)	P_m Damage Fraction
RT	612	0.90
100°C	574	0.84

NOTE: RT = room temperature

Source: BSC 2004 [DIRS 167718], Table 6-3.

Table 36 shows the allowable P_m , which is equal to 70 percent of σ_u . Table 37 shows that the wall averaged stress intensity, used as P_m , is less than the allowable P_m . Therefore, the tiered criteria is met, and the 21-PWR waste package is not anticipated to fail during the horizontal drop event.

44-BWR Waste Package

The conditions of the 44-BWR horizontal drop are identical to those used for the 21-PWR waste package. The source calculation for this event sequence is BSC 2004 [DIRS 169707]. The simulation is performed using LS-DYNA finite element software. The simulation is performed at room temperature and 300°C to bound potential waste package operational temperatures. The results for the horizontal drop of the 44-BWR waste package are shown in Table 38.

Table 38. Maximum Wall Average Stress Intensities

Wall Section	Temperature	Max Wall Average Stress Intensity (σ_{int})	σ_{int} / σ_u
1	RT	685 MPa	0.71
2	RT	701 MPa	0.72
3	RT	710 MPa	0.73
1	300 °C	571 MPa	0.63
2	300 °C	586 MPa	0.64
3	300 °C	596 MPa	0.65

NOTE: RT = room temperature.

Source: BSC 2004 [DIRS 169707], Table 5.

The wall averages, which are $< 0.77\sigma_u$, indicate that the tip-over drop meets the limits when bending stresses are secondary with wall averaged stress intensity used as a conservative general primary membrane stress intensity. Given that the stresses do not extend around the circumference, the 44-BWR waste package is not expected to breach during the horizontal drop event.

7.1.2.2.7 Horizontal Drop with Emplacement Pallet21-PWR Waste Package

The drop with emplacement pallet consists of raising the waste package while on the emplacement pallet horizontally to a maximum height of 2.0 m (6.6 ft) (see Mecham 2004 [DIRS 169790], Section 5.2.8). After which the lifting device carrying the waste package and emplacement fails and the two fall due to gravity. The waste package then impacts with the emplacement pallet, which impacts an unyielding surface. The simulation is performed using LS-DYNA finite element software. The simulation is performed at room temperature and 300°C to bound potential waste package operational temperatures. The results for the drop with the emplacement pallet of the 21-PWR waste package are shown in Table 39 (BSC 2004 [DIRS 167030], Section 6).

Table 39. Wall-Averaged Stress Intensity in the Outer Barrier

	Wall-Averaged Stress Intensity (P_m)	$0.7\sigma_u$	$P_m/0.7\sigma_u$
RT	624 MPa	680 MPa	0.92
300°C	523 MPa	637 MPa	0.82

NOTE: RT = room temperature.

Source: BSC 2003 [DIRS 167030], Table 6-3.

Since the through wall average stress intensity is less than $0.7\sigma_u$, the outer corrosion barrier meets the tiered criterion presented at the beginning of this section, and is not anticipated to fail during this event sequence.

44-BWR Waste Package

The conditions of the 44-BWR horizontal drop with emplacement pallet are identical to those used for the 21-PWR waste package. The source calculation for this event sequence is BSC 2004 [DIRS 167372]. The simulation is performed using LS-DYNA finite element software. The simulation is performed at room temperature and 300°C to bound potential waste package operational temperatures. The results for the drop with the emplacement pallet of the 44-BWR waste package are shown in Table 40.

Table 40. Maximum Stress Intensities

Temperature	σ_{INT}	$0.7 \sigma_u$	$\sigma_{INT}/0.7\sigma_u$
RT	656 MPa	680 MPa	0.96
300°C	575 MPa	637 MPa	0.90

NOTE: RT = room temperature.

Source: BSC 2004 [DIRS 167372], Table 6-2

If the maximum at any element is less than $0.7\sigma_u$, then the average across the thickness must also be less than $0.7\sigma_u$. Since the maximum stress intensity at a point is less than $0.7\sigma_u$, the outer corrosion barrier meets the tiered criterion presented at the beginning of this section, and is not anticipated to fail during this event sequence.

7.1.2.2.8 Corner Drop

The Corner Drop consists of raising the waste package vertically to a maximum height of 2.0 m (6.6 ft) (see Mecham 2004 [DIRS 169790], Section 5.2.8). The lifting device carrying the waste package fails when the waste package is at the point where the center of gravity is vertically aligned with the bottom corner of the waste package. The waste package then falls due to gravity and the waste package impacts an unyielding surface. The simulation is performed using LS-DYNA finite element software. The simulation is performed at room temperature and 300°C to bound potential waste package operational temperatures.

21-PWR

The maximum shear stress in the outer corrosion barrier occurs at the junction of the lower trunnion sleeve upper weld and the outer corrosion barrier. The maximum shear stress in the inner vessel occurs in the bottom corner. Table 41 lists the maximum stress intensities at a point in the inner vessel and outer corrosion barrier at room temperature and 300 °C.

Table 41. Maximum Stress Intensities (σ_{int})

	Outer Corrosion Barrier and Lids	σ_u	σ_{int}/σ_u	Inner Vessel and Lids	σ_u	σ_{int}/σ_u
RT	3204 MPa	971 MPa	2.30	443 MPa	703 MPa	0.63
300°C	2365 MPa	910 MPa	2.60	402 MPa	619 MPa	0.65

NOTE: RT = room temperature.

Source: BSC 2004 [DIRS 170059], Table 6-2

From Table 41, the stress intensities in the outer corrosion barrier are greater than $0.7\sigma_u$ of Alloy 22 (UNS N06022). However, the stress intensity in the inner vessel and lids are below $0.77\sigma_u$ of stainless steel type 316 and do not extend around the circumference of the inner vessel. Therefore, the inner vessel meets the plastic analysis criteria. However, according to Table 41, the maximum stress intensities in the outer corrosion barrier are higher than $0.77\sigma_u$ of Alloy 22 (UNS N06022). To verify that this maximum stress intensity does not cause a failure in the outer corrosion barrier requires a more detailed investigation into the source of the stress.

Table 42 contains the wall-averaged total stress intensities and their ratios of P_m allowables. Also, since the stress intensity in the inner vessel is close to $0.77\sigma_u$, the through wall stress in the inner vessel wall and lid is examined. Recall the maximum stress intensity in the inner vessel occurred at the bottom corner of the inner vessel wall and lower lid juncture. For this reason the through-wall average stress intensities of the wall and lid are examined.

Table 42. Wall-Averaged Stress Intensities

		Wall-Averaged Stress Intensity (P_m)	P_m/σ_u
RT	Outer Corrosion Barrier	1081 MPa	1.12
300°C		773 MPa	0.85
RT	Inner Vessel Wall	285 MPa	0.41
300°C		221 MPa	0.36
RT	Inner Vessel Lower Lid	308 MPa	0.44
300°C		250 MPa	0.41

NOTE: RT = room temperature.

Source: BSC 2004 [DIRS 170059], Table 6-3

From Table 42, the P_m stresses in the inner vessel and lower lid are below $0.7\sigma_u$ of stainless steel type 316. Consequently, the stresses are below $0.77\sigma_u$ and do not extend for the entire circumference of the waste package. Therefore, the inner vessel meets the plastic analysis criteria. However, the P_m stresses in the outer corrosion barrier are above $0.9\sigma_u$ of Alloy 22 (UNS N06022) at room temperature. At 300°C, the P_m stresses are above $0.77\sigma_u$ but are below $0.9\sigma_u$. This passes the first step of the last tier of the simplified plastic analysis criteria. The P_m stress at a distance of $\sqrt{R \cdot t} = 127$ mm (where R = the midsurface radius of the outer corrosion barrier and t = the thickness of the outer corrosion barrier) is 574 MPa, which is less than $0.7\sigma_u$. Therefore the second step of the last tier of the simplified plastic analysis criteria is met.

Finally, the average shear stress in each of the three planes are presented in Table 43.

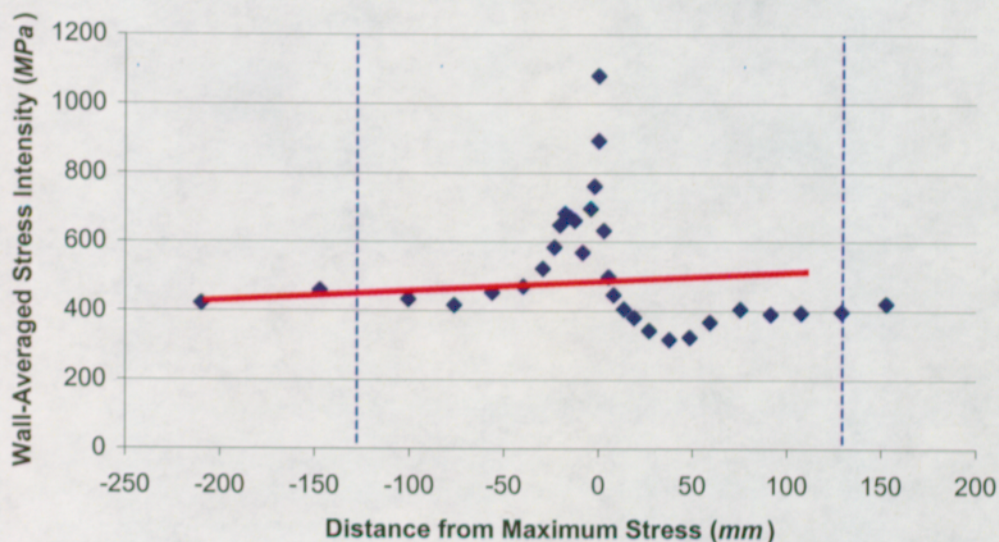
Table 43. Wall-Averaged Shear Stress of the Outer Corrosion Barrier at 300°C

Shear Stress Plane	Wall-Averaged Shear Stress	$0.42\sigma_u$	Wall-Averaged Shear Stress / $0.42\sigma_u$
τ_{xy}	13 MPa	382 MPa	0.03
τ_{yz}	198 MPa	382 MPa	0.52
τ_{zx}	71 MPa	382 MPa	0.19

Source: BSC 2004 [DIRS 170059], Table 6-4

Thus, at 300°C the outer corrosion barrier meets the plastic analysis criteria. Since the P_m stresses in the outer corrosion barrier are above $0.9\sigma_u$ of Alloy 22 (UNS N06022) at room temperature, the outer corrosion barrier fails the simplified screening criteria and further analysis is needed to determine if the outer corrosion barrier is safe from breach.

The highest P_m stresses occur in the line of elements that contain the element with the maximum stress intensity. This element is being severely distorted due to the single corner node at the juncture of the lower trunnion sleeve and the outer corrosion barrier. This discontinuity is heavily influencing the P_m stress in this line of elements. It is important to recognize that in accordance with the discussion in 7.1.3.3.1.2, the bending component of the stress intensity presented should be classified as secondary stress (i.e., $P_b = 0$), and should not be taken into account in the failure assessment. In a region of the local and gross discontinuities it is appropriate to calculate the P_m stresses at distances away from the discontinuity and then interpolating linearly back to the discontinuity in the failure assessment. Figure 11 presents the P_m stresses at distances away from the discontinuity.



Source: BSC 2004 [DIRS 170059], Figure 6-1

Figure 11. P_m Stresses at Varying Distance from the Location of Maximum Stress in the Outer Corrosion Barrier at Room Temperature

In Figure 11, P_m stresses are shown at distances above (indicated as negative) and below (indicated as positive) the stress classification line that contained the element with the maximum stress intensity, plotted at point 0. The dashed blue lines indicate a distance of $\sqrt{R \cdot t} = 127 \text{ mm}$ from the stress classification line at point 0. The solid red line indicates the linear relationship the stress fields have and how a singularity has such a large impact on the overall results. Singularities like this one impose severe mesh requirements on finite element analyses. A more realistic result can be achieved by following the solid red line to point 0. The result here is 500

MPa. From Table 42, this is below $0.7\sigma_u$ of Alloy 22 (UNS N06022). Therefore the outer corrosion barrier meets the plastic analysis criteria.

To further support these results, the identification of stress component (signed σ_x , σ_y , σ_z , τ_{xy} , τ_{yz} , τ_{zx}) fields across the wall is performed. These fields are averaged to create wall-averaged stress components, and then translated to principle stress directions for calculating the difference between the maximum (σ_1) and minimum (σ_3) principle stress direction values. This calculation results in a P_L value, provided that the outer corrosion barrier and trunnion sleeve weld juncture with P_L exceeding 1.1 times the P_m limit does not extend for greater than $\sqrt{R \cdot t}$. Table 44 shows the stress component fields in the stress classification line of the outer corrosion barrier of the standard mesh case at RT with the highest maximum stress defined in Table 42. This stress classification line is examined at the time the maximum wall average shear stress occurs.

Table 44. Component Based Membrane Stress Intensity in the Outer Corrosion Barrier at Room Temperature

Stress Direction	Wall-Averaged Stress
σ_x	520.6 MPa
σ_y	372.1 MPa
σ_z	660.8 MPa
τ_{xy}	-17.7 MPa
τ_{xz}	-76.1 MPa
τ_{yz}	-258.3 MPa

Source: BSC 2004 [DIRS 170059], Table 6-5

$$x^3 - I_1 \cdot x^2 + I_2 \cdot x - I_3 = 0$$

The roots of x are:

$$x = 823 \text{ MPa}, 519 \text{ MPa}, \text{ and } 211 \text{ MPa}$$

These are the membrane principle stresses (σ_1 , σ_2 , and σ_3). Recalling the membrane stress intensity is equal to the first principle stress minus the third principle stress, we get:

$$P_L = 823 \text{ MPa} - 211 \text{ MPa} = 612 \text{ MPa}$$

Comparing this with Table 42, this is below $0.7\sigma_u$ of Alloy 22 (UNS N06022) at room temperature. Therefore the outer corrosion barrier meets the plastic analysis criteria.

The results presented are conservative and the 21-PWR waste package meets the plastic analysis criteria. The 21-PWR waste package is not anticipated to breach during the corner drop event.

44-BWR

The results for the corner drop of the 44-BWR waste package at room temperature and 300°C are shown in Table 45 (BSC 2003 [DIRS 167031]).

Table 45. Wall-Averaged Stress Intensity in the Outer Corrosion Barrier

	Wall-Averaged Stress Intensity (P_m)	$0.7\sigma_u$	$P_m/0.7\sigma_u$
RT	560 MPa	680 MPa	0.82
300°C	440 MPa	637 MPa	0.69

NOTE: RT = room temperature.

Source: BSC 2003 [DIRS 167031], Table 6-3

Since the through wall average stress intensity is less than $0.7\sigma_u$, the outer corrosion barrier meets the tiered criterion presented at the beginning of this section, and is not anticipated to fail during this event sequence.

7.1.2.2.9 Oblique Drop with Slap Down

21-PWR Waste Package

The 10-degree oblique drop with slap down consists of raising the waste package horizontally to a maximum height of 2.4 m (7.9 ft) (see Mecham 2004 [DIRS 169790], Section 5.2.8). After which the lifting device carrying the bottom half of the waste package fails and the bottom half of the waste package begins to fall due to gravity. After the bottom end has rotated 10 degrees, the lifting device holding the top of the waste package fails and the entire waste package falls due to gravity. The waste package then impacts an unyielding surface with the bottom edge first followed by the top end. The simulation is performed using LS-DYNA finite element software. The simulation is performed at room temperature and 300°C to bound potential waste package operational temperatures. The results for the 10-degree oblique drop with slap down of the 21-PWR waste package are shown in Table 46 (BSC 2004 [DIRS 167032]). σ_{int}/σ_u represents the ratio of the stress intensity and the true tensile strength.

Table 46. Maximum Stress Intensity

Part	Temperature	Max Stress Intensity (σ_{int})	σ_{int} / σ_u
Outer Barrier	RT	679 MPa	0.699
Inner Vessel	RT	396 MPa	0.563
Outer Barrier	300 °C	553 MPa	0.608
Inner Vessel	300 °C	401 MPa	0.648

NOTE: RT = room temperature.

Source: BSC 2004 [DIRS 167032], Table 6-2

The previous table shows that for each temperature condition, the maximum stress intensities in the outer corrosion barrier and lids, and the inner vessel and lids did not exceed seven-tenths of the true tensile strength of Alloy 22 (UNS N06022) and stainless steel type 316. Therefore, there is no further analysis needed. The tiered criterion at the beginning of this section is satisfied, and the 21-PWR waste package is not anticipated to fail during this event sequence.

44-BWR Waste Package

The conditions of the 44-BWR oblique drop are identical to those used for the 21-PWR waste package. The source calculation for this event sequence is BSC 2004 [DIRS 169706]. The simulation is performed using LS-DYNA finite element software. The simulation is performed at room temperature and 300°C to bound potential waste package operational temperatures. The results for the oblique drop of the 44-BWR waste package are shown in Table 47.

Table 47. Maximum Stress Intensities in the Outer Corrosion Barrier

Temperature	Max Stress Intensity, σ_{int} (MPa)	σ_{int} / σ_u
RT	738	0.760
300 °C	661	0.726

NOTE: RT = room temperature

Source: BSC 2004 [DIRS 169706], Table 4.

The above table shows that, for both temperature conditions, the maximum stress intensity is less than $0.77\sigma_u$ of Alloy 22 (UNS N06022). This leads to the conclusion that the 44-BWR waste package oblique drop meets the code limits, when the peak stress is not uniform around the circumference of the waste package. Therefore, the outer corrosion barrier does not breach during a 10° oblique drop at room temperature and 300 °C.

7.1.2.2.10 Swing Down

21-PWR Waste Package

The source calculation for this event sequence is BSC 2004 [DIRS 167392]. In this calculation, the waste package is held horizontally 2.4 m (7.9 ft) (see Mecham 2004 [DIRS 169790], Section 5.2.8) over an unyielding surface while one end is free to swing down due to gravity. The simulation is performed using LS-DYNA finite element software. The simulation is performed at room temperature and 300°C to bound potential waste package operational temperatures. The results for the swing down of the 21-PWR waste package are shown in Table 48.

Table 48. Maximum Stress Intensities

	Outer Barrier (σ_{int})	σ_u	σ_{INT} Ratio (σ_{int}/σ_u)
RT	537.3 MPa	971 MPa	0.55
300 °C	444.1 MPa	911 MPa	0.49

NOTE: RT = room temperature.

Source: BSC 2004 [DIRS 167392], Table 6-2

Table 48 shows that the outer barrier and lids are below 70 percent of σ_u for both room temperature and 300°C and meet the tiered criterion presented at the beginning of this section. Therefore, the waste package is not expected to breach during this event sequence.

44-BWR Waste Package

The stress intensities resulting from BSC 2003 [DIRS 166291] are shown in Table 49. The conditions of the 44-BWR swing down are identical to those of the 21-PWR waste package swing down. The finite element representation is solved using LS-DYNA. Solutions for room temperature and 300°C are presented below.

Table 49. Maximum Stress Intensities for the 44-BWR Waste Package Swing Down

	Outer Barrier and Lids (σ_{int}/σ_u)
RT	0.59
300°C	0.60

NOTE: RT = room temperature.

Source: BSC 2003, [DIRS 166291], Table 5.

Table 49 shows that the outer barrier and lids are below 70 percent of σ_u for both room temperature and 300°C and meet the tiered criterion presented at the beginning of this section. Therefore, the waste package is not expected to breach during this event sequence.

7.1.2.2.11 Evaluation of a 21-PWR Waste Package Exposed to Vibratory Ground Motion

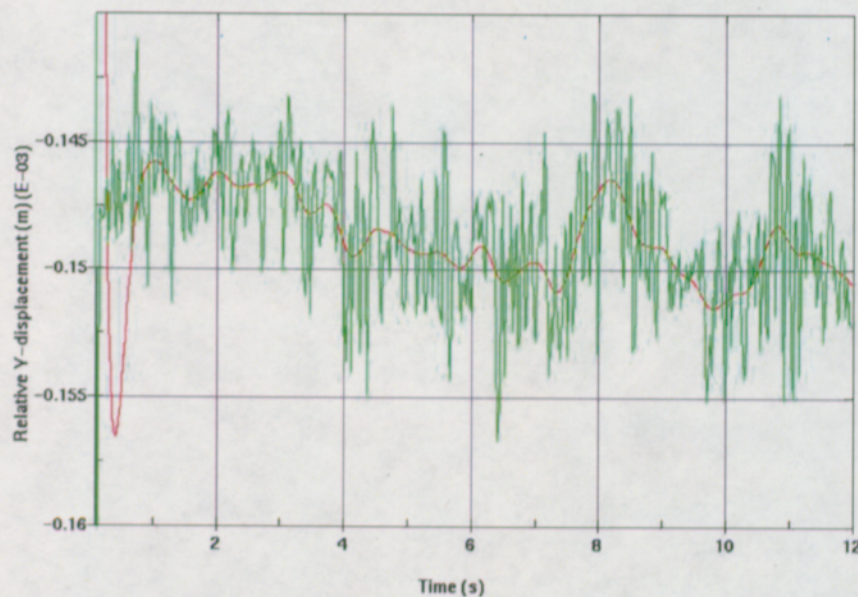
This entire section, 7.1.2.2.11, is taken from Section 6 of BSC 2004 [DIRS 167083].

ANNUAL FREQUENCY OF OCCURRENCE $5 \cdot 10^{-4}$ 1/yr

The event with an annual frequency of occurrence $5 \cdot 10^{-4}$ 1/yr is evaluated by using the same finite element representation previously used for most of the $1 \cdot 10^{-6}$ 1/yr realizations (with the exception of the realization number 6) (BSC 2004 [DIRS 167083]). The simulation is performed at a temperature of 150°C. The simulation started at 3.0 s of the ground motion time history (corresponding to 5 percent of energy of ground motion), and the ending time is 15 s

(corresponding to 65 percent of energy of ground motion). This duration covered the most intense period of the ground motion time history.

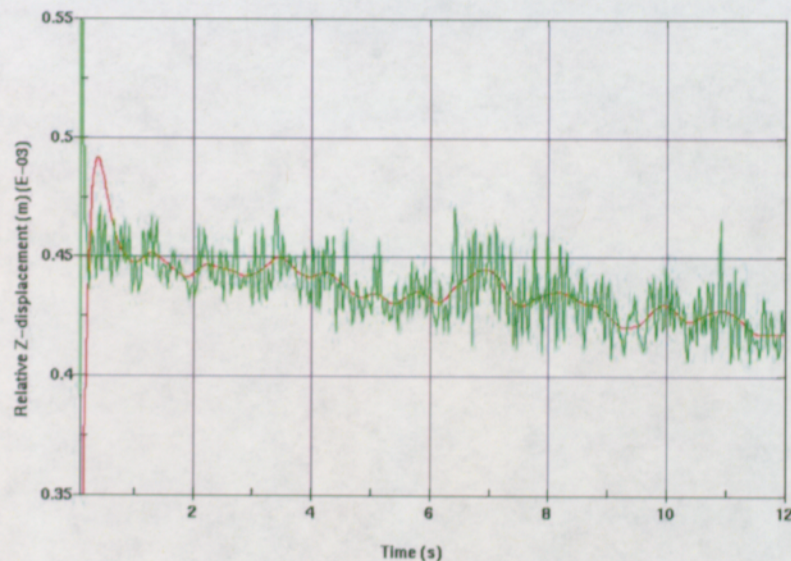
The ground motion with an annual frequency of occurrence $1 \cdot 10^{-4}$ 1/yr is much less intense than its $1 \cdot 10^{-6}$ 1/yr counterparts. Consequently, the rigid-body motion during the $1 \cdot 10^{-4}$ 1/yr vibratory simulation is extremely small. Specifically, the relative motion of the waste package with respect to the emplacement pallet in longitudinal (Y) and vertical (Z) direction is practically nonexistent. Figure 12 indicates that – once the initial gap between waste package and emplacement pallet is closed (see BSC 2004 [DIRS 167083], Section 6.3.1) – the relative displacement of two waste package and emplacement pallet nodes is less than ± 0.01 mm (± 0.0004 in.) even for the raw (unfiltered) plot (i.e., it varies within the range 0.15 ± 0.01 mm [0.0059 ± 0.0004 in.]). The filtered plot is more meaningful since the noise – very pronounced due to the high-frequency excitation and the lack of damping – is eliminated. A Butterworth filter with cutoff frequency of 1000 Hz is used for that purpose throughout this section.



Source: BSC 2004 [DIRS 167083], Figure 10

Figure 12. Relative Longitudinal (Y) Displacement (Raw and Filtered) of Waste Package with Respect to Emplacement Pallet for Annual Frequency of Occurrence $5 \cdot 10^{-4}$ 1/yr.

The relative displacement in vertical (Z) direction of the waste package with respect to the emplacement pallet is also small as indicated in Figure 13. Values range between 0.44 ± 0.03 mm [0.017 ± 0.001 in.], after the initial transient.



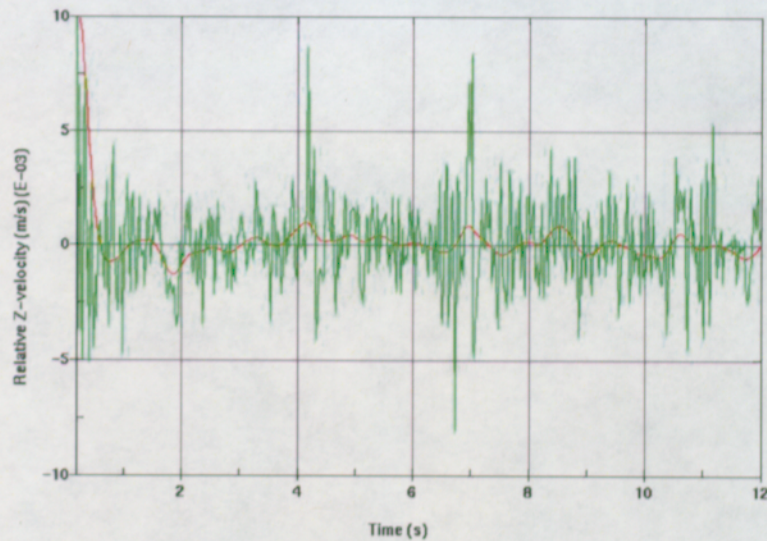
Source: BSC 2004 [DIRS 167083], Figure 11

Figure 13. Relative Vertical (Z) Displacement (Raw and Filtered) of Waste Package with Respect to Emplacement Pallet for Annual Frequency of Occurrence $5 \cdot 10^{-4}$ 1/yr.

As a consequence of the limited rigid-body motion, there is no contact between the waste package and the longitudinal boundary in the course of the $5 \cdot 10^{-4}$ 1/yr simulation. For the same reason, there is no contact between the waste package and the drip shield either, at any time during the simulation. Thus, the only remaining interaction, relevant for the objective of this analysis, is the one between the waste package and the emplacement pallet.

As far as the waste package-emplacment pallet interaction is concerned, another important consequence of limited rigid-body motion (especially in the vertical direction) is the very small impact velocity characterizing that interaction. As Figure 14 indicates, the impact velocity between the waste package and the emplacement pallet rarely exceeds 0.005 m/s even for the raw (unfiltered) plot. The maximum impact velocity (between waste package and the emplacement pallet) based on the filtered plot (Figure 14) does not exceed 0.0015 m/s.

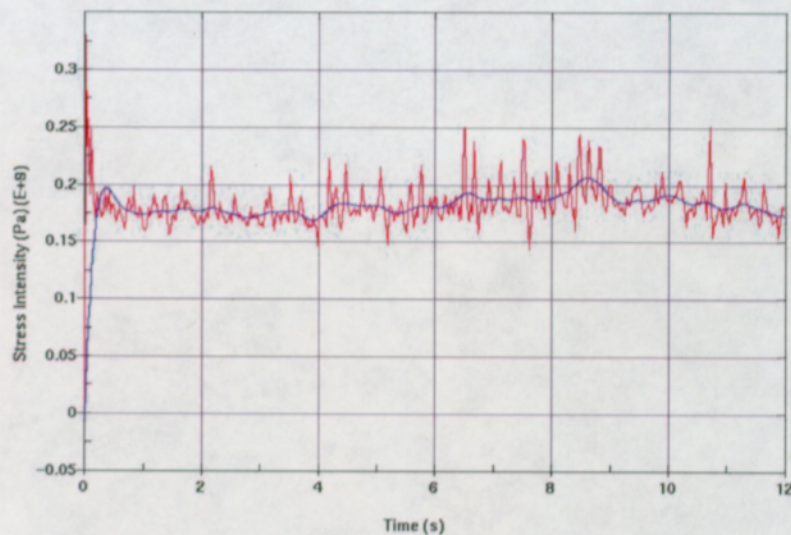
The vibratory part of the simulation is performed without either the system damping or the contact damping (see Section 5.2 of BSC 2004 [DIRS 167083]). The claim that the rigid-body motion is negligible at this annual frequency of occurrence is supported by the results presented in Figures 12 through 14.



Source: BSC 2004 [DIRS 167083], Figure 12

Figure 14. Relative Vertical (Z) Velocity (Raw and Filtered) of Waste Package with Respect to Emplacement Pallet for Annual Frequency of Occurrence $5 \cdot 10^{-4}$ 1/yr.

Figure 15 presents the stress intensity plot for the vibratory part of the simulation. The maximum peak stress intensity remains below the yield strength (310 MPa at 150°C, see Section 5.1.1 of BSC 2004 [DIRS 167083]) in the course of vibratory simulation. The peak value of the maximum stress intensity is 208 MPa based on the filtered plot (Figure 15). Thus, the waste package deformation is elastic during the vibratory ground motion. An apparent exception occurring only for the raw plot and a very brief period of time (less than 0.05 s) – is the beginning of the event, which is demonstrated in Section 6.3.1 of BSC 2004 [DIRS 167083] to be unrelated to the physics of the problem.



Source: BSC 2004 [DIRS 167083], Figure 13

Figure 15. Stress Intensity (Raw and Filtered) for Waste Package Outer Barrier for Annual Frequency of Occurrence 5×10^{-4} 1/yr.

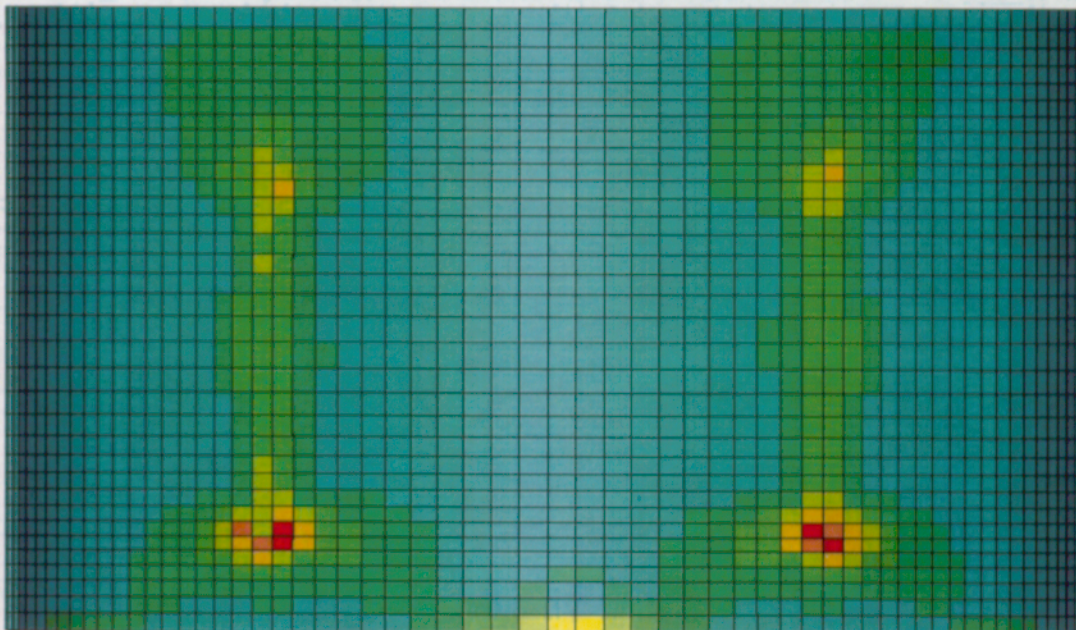
Finally, the maximum residual 1st principal stress (77 MPa, see Figure 16) is below the stress limit (80%-90% of yield strength) by a large margin. It should be noted that since the deformation of the waste package outer barrier is elastic throughout the ground motion the residual stresses due to that motion should be theoretically zero, and the actual residual stresses approach the static emplacement solution.

Therefore, the waste package outer barrier remains undamaged throughout the 5×10^{-4} 1/yr event (i.e., the outer barrier area exceeding established stress limits is zero).

Time = 12.3
 Contours of Maximum Prin Stress
 max ipt. value
 min=-4.00862e+07, at elem# 16004
 max=7.74270e+07, at elem# 20673

Fringe Levels

7.743e+07
 6.568e+07
 5.393e+07
 4.217e+07
 3.042e+07
 1.867e+07
 6.919e+06
 -4.832e+06
 -1.658e+07
 -2.833e+07
 -4.009e+07



Source: BSC 2004 [DIRS 167083], Figure 14

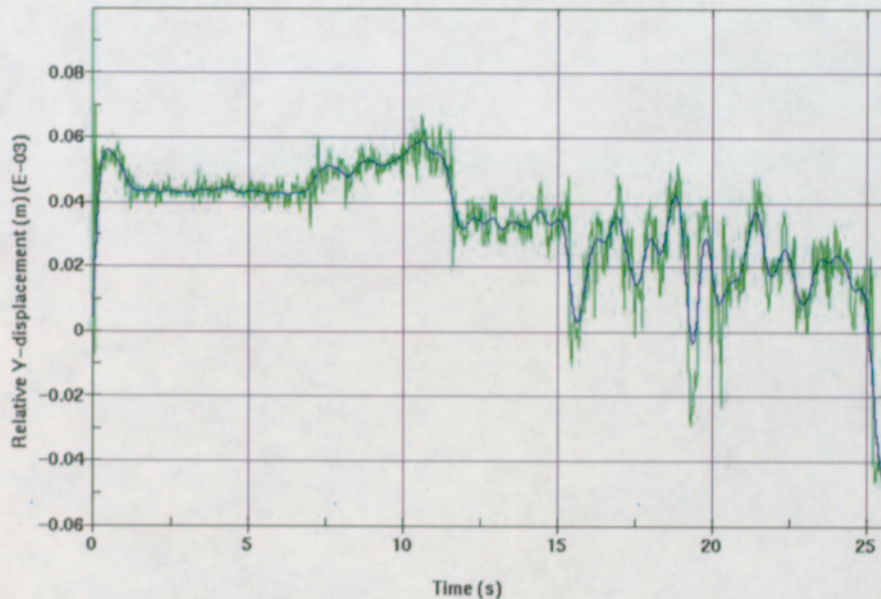
Figure 16. Residual 1st Principal Stress Plot in Outer Barrier (Top View) for Annual Frequency of Occurrence 5×10^{-4} 1/yr.

ANNUAL FREQUENCY OF OCCURRENCE 1×10^{-4} 1/yr

The event with an annual frequency of occurrence 1×10^{-4} 1/yr is evaluated by using the same finite element representation previously used for the 5×10^{-4} 1/yr realization and most of the 1×10^{-6} 1/yr realizations (with the exception of realization number 6). The simulation is performed at a temperature of 150°C. The simulation started at 9.7 s of the ground motion time history (corresponding to 5 percent of energy of ground motion), and the ending time is 34.9 s (corresponding to 65 percent of energy of ground motion). This duration covered the most intense period of this ground motion time history.

The rigid-body motion during the 1×10^{-4} 1/yr vibratory simulation is very small due to the small intensity of the ground motion. Figure 17 indicates that—once the initial gap between waste package and emplacement pallet is closed—the relative displacement of two typical waste package and emplacement pallet nodes is less than ± 0.07 mm (± 0.003 in.) even for the raw plot.

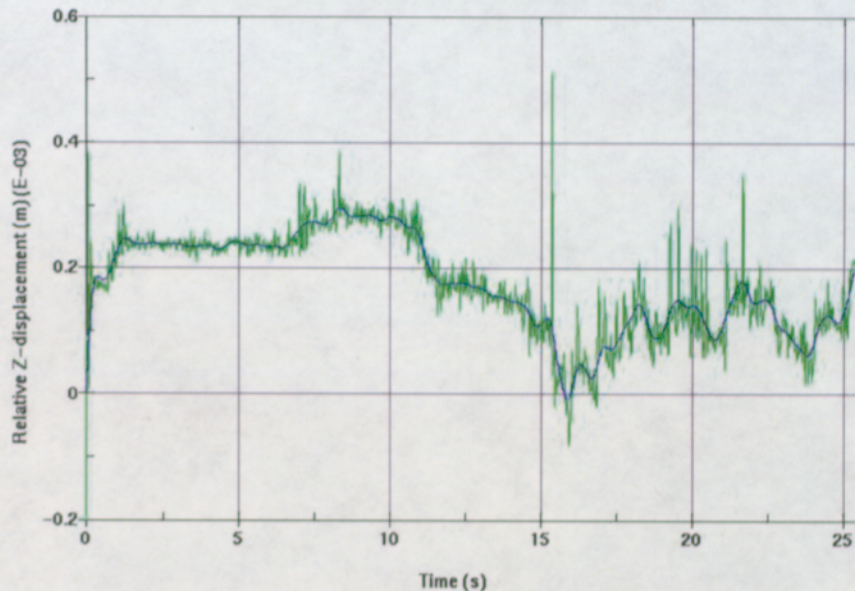
The filtered plot is more meaningful since the high-frequency noise—very pronounced due to the high-frequency excitation and the absence of damping—is eliminated. A Butterworth filter with cutoff frequency of 1000 Hz is used for that purpose throughout this section.



Source: BSC 2004 [DIRS 167083], Figure 20

Figure 17. Relative Longitudinal (Y) Displacement (Raw and Filtered) of Waste Package with Respect to Emplacement Pallet for Annual Frequency of Occurrence 1×10^{-4} 1/yr.

The relative displacement in the vertical (Z) direction of the waste package with respect to the emplacement pallet is also small as indicated in Figure 18. Most of the time it varies within the range from 0 to 0.3 mm (0 to 0.01 in.). (Note the spikes in Figures 17 and 18 at the onset of simulations.)



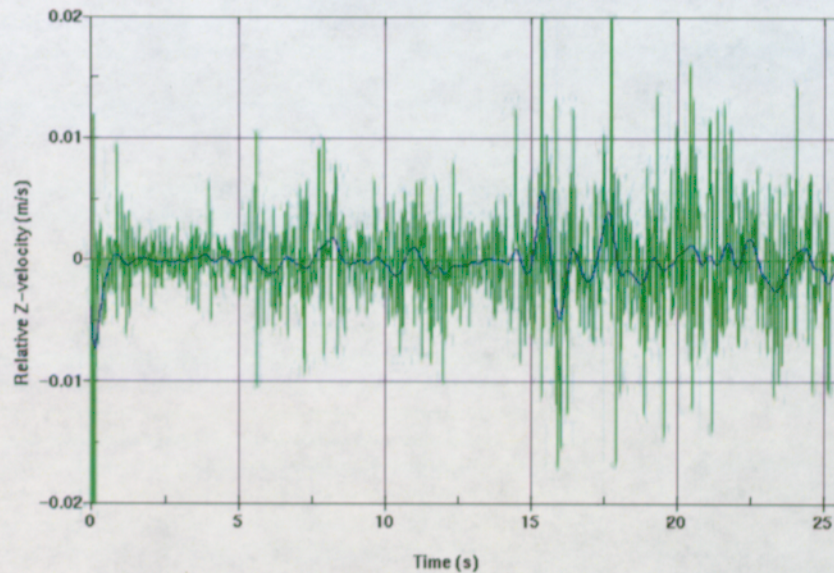
Source: BSC 2004 [DIRS 167083], Figure 21

Figure 18. Relative Vertical (Z) Displacement (Raw and Filtered) of Waste Package with Respect to Emplacement Pallet for Annual Frequency of Occurrence $1 \cdot 10^{-4}$ 1/yr.

As a consequence of the limited rigid-body motion, there is no contact between the waste package and the longitudinal boundary in the course of the $1 \cdot 10^{-4}$ 1/yr simulation. For the same reason, there is no contact between the waste package and the drip shield either. Thus, the only remaining interaction, relevant for the objective of this analysis, is the one between the waste package and the emplacement pallet.

As far as the waste package-emplacment pallet interaction is concerned, another important consequence of limited rigid-body motion (especially in the vertical direction) is the very small impact velocity characterizing that interaction. As Figure 19 indicates, the impact velocity between the waste package and the emplacement pallet rarely exceeds 0.005 m/s (for the filtered plot). The maximum impact velocity (between the waste package and the emplacement pallet) based on the filtered plot (blue curve in Figure 19) does not exceed 0.006 m/s.

The vibratory part of the simulation is performed without either system damping or the contact damping. Therefore, the claim that the rigid-body motion is negligible at this annual frequency of occurrence is supported by the results presented in Figures 17 through 19.

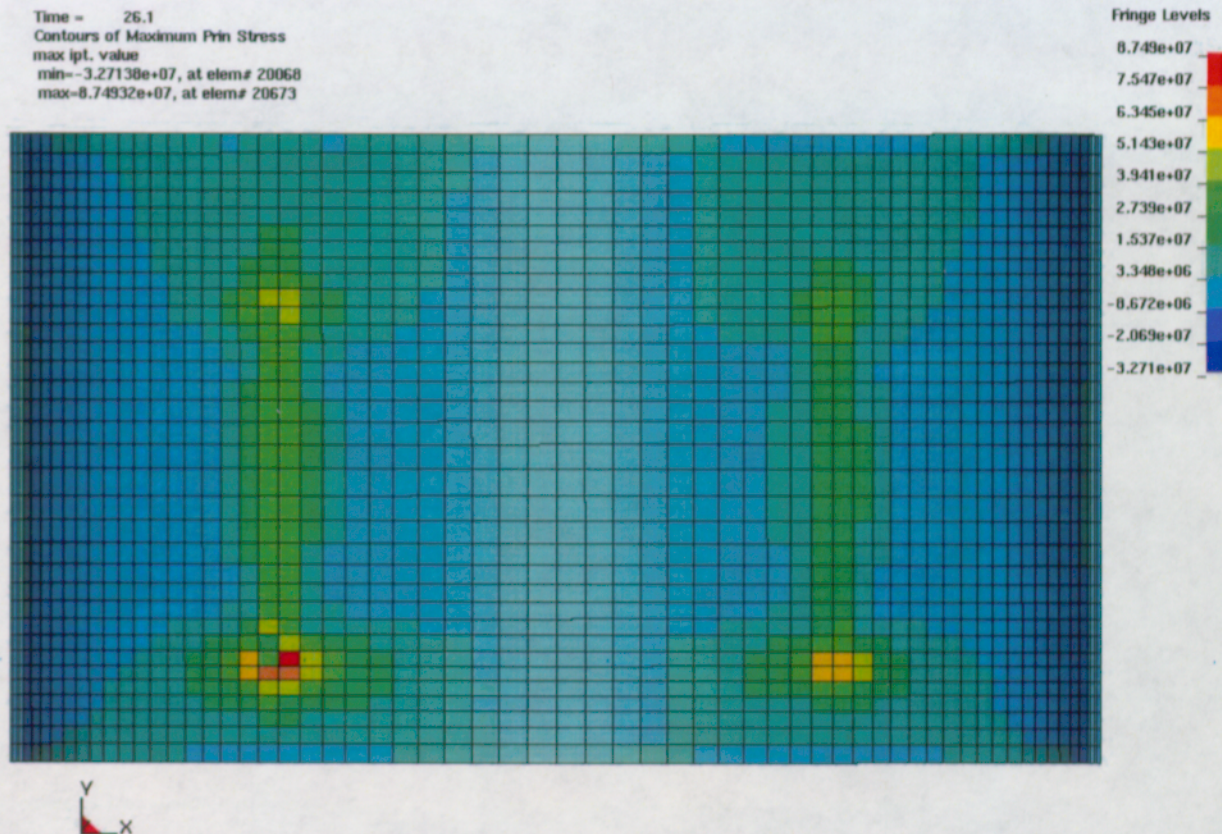


Source: BSC 2004 [DIRS 167083], Figure 22

Figure 19. Relative Vertical (Z) Velocity (Raw and Filtered) of Waste Package with Respect to Emplacement Pallet for Annual Frequency of Occurrence 1×10^{-4} 1/yr

Finally, according to Figure 20, the maximum residual 1st principal stress (87 MPa) is below the stress limit (80%-90% of yield strength) by a large margin. (Note that the stress unit in Figure 20 is Pascal.) It should be noted that since the deformation of the waste package outer barrier is elastic throughout the ground motion, the residual stresses due to that motion should be theoretically zero, and the actual residual stresses approach the static emplacement solution.

Therefore, the waste package outer barrier remains undamaged throughout the 1×10^{-4} 1/yr event (i.e., the outer barrier area exceeding established stress limits is zero).



Source: BSC 2004 [DIRS 167083], Figure 23

Figure 20. Residual 1st Principal Stress Plot in Outer Barrier (Top View) for Annual Frequency of Occurrence $1 \cdot 10^{-4}$ 1/yr.

7.1.2.3 Sources of Uncertainty and Variability

In the past interactions with the NRC (Kelmenson 2000 [DIRS 154350]) sources of uncertainty and variability affecting structural analyses were discussed. This particularly dealt with finite element analysis representations and the failure criterion for waste package structural analyses. Six other areas considered were:

1. Residual and differential thermal expansion stresses
2. Strain-rate effects
3. Dimensional and material variability
4. Seismic effect on ground motion
5. Initial tip-over velocities
6. Sliding and inertial effect of waste package contents.

At this time, additional uncertainties have not been identified. As the design progresses, any additional uncertainties that are identified will be addressed as part of the design process. These

identified uncertainties will be documented within the documents supporting the license application.

Finite Element Analysis Discretization and Failure Criterion—With regard to the adequacy of finite element analysis representations, a process has been developed to ensure that the mesh density is computationally adequate, and this process is followed for all structural calculations. The failure criterion is an application of the Tresca (strength of materials) failure criterion based on the implementation of ASME B&PV Code design-by-analysis primary stress intensity limits. A tiered evaluation approach is implemented that used increasingly less simplified, and increasing less conservative screening criterion whose satisfaction will assure meeting the ASME B&PV Code primary stress intensity limits.

For the six specific areas of uncertainty concern, the responses may be summarized as:

Residual and Differential Thermal Expansion Stresses—Differential thermal expansion is accommodated by providing adequate gaps between the two shells that comprise the waste package to ensure that there is no mutual loading due to thermal expansion. For residual stresses purposefully imposed on the outer corrosion barrier, the effects on structural analysis results are found to be negligible.

Strain-rate Effects—While material-specific strain-rate dependent properties are not currently available for Alloy 22 (UNS N06022) and stainless steel type 316, parametric studies of such effects based on stainless steel type 304 strain-rate dependent properties have shown that the use of static properties has negligible effect on the safety assessment.

Dimensional and Material Variability—Dimensional variability is addressed by assuming minimum dimensions for those parameters that are important to component performance. Material variability is accommodated by the use of ASME B&PV code—and other codes as necessary—structural properties, which provide for minimum structural performance margins.

Seismic Effect on Ground Motion—In the surface facility, in the transporter, and on the emplacement gantry, it is assumed that the fixturing is provided to restrain the waste package during evolutions in that facility, and these devices are sufficient to provide restraint during vibratory ground motion. For vibratory ground motion in the underground, results are provided for a seismic evaluation for an annual frequency of exceedance of $5 \cdot 10^{-4}$ per year. These results show that although the waste package experiences movement, a large margin to breach remains.

Initial Tip-over Velocities—A study has been performed to demonstrate that the increase in tip-over velocity due to credible vibratory ground motion causes a negligible increase in impact velocity.

Sliding and Inertial Effect of Waste Package Contents—The waste form contents are represented in dynamic structural analyses for which such motion is anticipated to be important. Examples of the loads and boundary conditions used in calculations and analyses can be found in the supporting calculations as referenced in Section 7 (BSC 2001 [DIRS 152655], BSC 2003

[DIRS 161691], BSC 2004 [DIRS 167083], BSC 2004 [DIRS 169705], and BSC 2003 [DIRS 165497]). In addition, the technical bases and or rationale for the loads and boundary conditions used in calculations supporting the license application will be based on the preclosure safety analysis and derivative design constraints.

7.1.2.3.1 Response to General Issue of Adequacy

7.1.2.3.1.1 Mesh Discretization

The main concern is the adequacy of the finite element analysis mesh discretization and the failure criterion.

A set process is followed in the development of the mesh for finite element analysis that provides confidence that the results are stationary in a numerical sense (Mecham 2004 [DIRS 169790], Section 6.2.3).

The purpose of mesh refinement is to ensure the mesh objectivity of the finite element analyses, i.e., that the results obtained are not mesh-sensitive. The basis for the validity of this process of successive refinement is that it has been found to produce convergent stress fields in a systematic manner. The acceptable variations in the stress fields are well within the benchmarking basis for the LS-DYNA code. A mesh-refinement study consists of the development of an optimum mesh that yields mesh-objective (mesh-insensitive) results. That mesh is then refined again, and computational results for the two mesh sizes are compared. The finite element representation is considered mesh-objective if the relative difference in results between the two meshes is approximately an order of magnitude smaller than the relative difference in mesh size in the region of interest; otherwise further mesh refinement is needed. The mesh size, as used throughout this section, refers to the volume or the area of the representative element (three-dimensional or two-dimensional, respectively) in the region of interest (for example, the element characterized by the highest stresses or strains).

The optimum mesh is created by the following sequence of steps:

- The initial mesh is created by following the customary engineering practices: the element type is appropriately chosen; the mesh is refined in the regions of interest (the highest stress/strain regions, initial impact regions, stress concentration regions, etc.); the mesh is mapped whenever possible; and the aspect ratio of elements is kept reasonable.
- The initial mesh is—in the region of interest—refined in one direction while the element size in the other two directions is kept unchanged (for example, the mesh is refined across the thickness while kept unchanged in the hoop and axial directions). The mesh-refinement procedure is repeated in this manner until the relative difference in results between the two successive meshes is acceptable (i.e., approximately an order of magnitude smaller than the relative difference in the mesh size). The mesh

dimension in this direction is then fixed at the largest value that satisfied the previously mentioned criterion.

- The intention of this one-direction-at-a-time mesh refinement is to create, in a consistent and systematic manner, a mesh that is objective.
- The same procedure is consecutively repeated in the remaining two directions.
- Whether the created mesh meets the requirement is verified by the final step: the simultaneous mesh refinement in all three directions. The level of this mesh refinement should be similar in all three directions. In this final step, the same mesh-acceptance criterion is invoked: the mesh is considered objective if the relative difference in stress results between the two meshes is approximately an order of magnitude smaller than the relative difference in mesh size in the region of interest.

The mesh objectivity is verified by the final step regardless of whether the final mesh is arrived at by the described one-direction-at-a-time mesh refinement or not. The one-direction-at-a-time mesh refinement is optional since its only purpose is to develop an optimum mesh (that satisfies the mesh-objectivity requirement) in a systematic way.

An example of the implementation of this mesh discretization approach may be found in the calculation entitled *44-BWR Waste Package Tip-Over from an Elevated Surface* (BSC 2004 [DIRS 169705], Section 6). While all calculations perform such discretization studies, this calculation is selected because it is the vehicle cited in the balance of this section to assess the importance of strain rates (Section 7.1.2.3.2.2) and initial tip-over velocities (Section 7.1.2.3.2.5).

7.1.2.3.1.2 Selection of the Failure Criterion

For structural analyses of preliminary designs that consider material nonlinear behavior, the maximum-shear-stress or Tresca (strength of materials) criterion is used in determining stress limits. In general terms, this criterion assumes that the design is safe as long as stress intensity (defined as the difference between the maximum and minimum principal stress) remains below a certain limit. In particular, the failure criterion chosen is the acceptance criteria for plastic analysis outlined in Appendix F, F-1341.2 of the ASME B&PV Code (ASME 2001 [DIRS 158115], Section III, Division 1). This is an acceptable vessel designer choice of ASME B&PV Code acceptance criteria for service loadings with Level D Service Limits for vessel designs in accordance with NC-3200 (Safety Class 2 Vessels) when a complete stress analysis is performed. (See ASME 2001 [DIRS 158115], NC-3211.1(c), Appendix XIII and Note (4) to Table NC-3217-1).

The ASME B&PV Code (ASME 2001 [DIRS 158115], Section III, Division 1, Appendix F, F-1341.2) suggests the following primary stress intensity limits for plastic analyses:

- The general primary membrane stress intensity shall not exceed $0.7 S_u$ for ferritic steel materials included in Section II, Part D, Subpart 1, Table 2A and the greater of $0.7 S_u$ and $S_y + \frac{1}{3} (S_u - S_y)$ for austenitic steel, high-nickel alloy, and copper-nickel alloy materials included in Section II, Part D, Subpart 1, Table 2A, where S_u and S_y are tensile strength and yield strength, respectively.
- The maximum primary stress intensity at any location shall not exceed $0.9 S_u$.
- The average primary shear across a section loaded in pure shear shall not exceed $0.42 S_u$.

The Pressure Vessel Research Council (PVRC) of the Welding Research Council (WRC) provides recommended guidelines (Hechmer and Hollinger 1998 [DIRS 166147]) to the ASME B&PV Code rule committees for assessing stress results from 3-D finite element analysis in terms of ASME B&PV Code stress limits in the design-by-analysis rules of ASME 2001 [DIRS 158115], Section III, Class 1, NB and Section VIII, Division 2. These guidelines were developed for linear analyses and PVRC recommends that future research work should be conducted to generate state-of-the-art guidelines for applying inelastic, large-deformation analyses. Therefore, a cautious use of the PVRC recommendations is made in developing methodologies for post-processing LS-DYNA nonlinear plastic simulations to assure conservative representations of the general primary membrane stress intensity and maximum primary stress intensity.

The PVRC recommendations also refer to an earlier PVRC (Phase 1) report, Hechmer and Hollinger 1998 [DIRS 166147], which recommended that the ASME B&PV Code Appendix F “should be revised to provide a limit on effective plastic strain which is more appropriate for events that are energy controlled, rather than load controlled, which is all that was considered when ASME B&PV Code Appendix F was written”. The Yucca Mountain Project recognizes that strain-based or deformation-based criterion may be more appropriate than stress-based limits for evaluation of the credible pre-closure sequence events, (see Mecham 2004 [DIRS 169790], Section 4.1.4.1). However, the project is also committed to applying the ASME B&PV Code for structural analyses, and until the ASME B&PV Code rule committees prepare rules in ASME B&PV Code Appendix F for using strain limits, primary stress intensity limits will be used.

The ASME B&PV Code design-by-analysis guidance recognizes the differences in importance of different types of stresses and provides guidance on their correct assignment to the different categories of stress intensity used to evaluate different types of failure modes. The three types of stresses are membrane, bending and peak stresses. The three categories of stress intensity are primary (P_m , P_L and P_b [general primary membrane, local primary membrane, and primary bending, respectively]), secondary (Q), and peak (F).

A primary stress is defined in ASME B&PV Code (ASME 2001 [DIRS 158115], Section III, Division 1, Appendix XIII) XIII-1123(h): “Primary stress is a normal stress developed by the imposed loading which is necessary to satisfy the laws of equilibrium of external and internal forces and moments. The basic characteristic of a primary stress is that it is not self-limiting.

Primary stresses which considerably exceed the yield strength will result in failure or, at least, in gross distortion.”

A secondary stress is defined in ASME B&PV Code (ASME 2001 [DIRS 158115], Section III, Division 1, Appendix XIII) XIII-1123(i): “Secondary stress is a normal or a shear stress developed by the constraint of adjacent parts or by self-constraint of the structure. The basic characteristic of a secondary stress is that it is self-limiting. Local yielding and minor distortions can satisfy the conditions which cause the stress to occur and failure from one application of the stress is not expected.” A cited example of a secondary stress is “bending stress at a gross structural discontinuity.” A gross structural discontinuity is defined in ASME B&PV Code (ASME 2001 [DIRS 158115], Section III, Division 1, Appendix XIII) XIII-1123(b): “Gross structural discontinuity is a source of stress or strain intensification which affects a relatively large portion of a structure and has a significant effect on the overall stress or strain pattern or on the structure as a whole.” Cited examples of gross structural discontinuities are head-to-shell junctions and junctions between shells of different thickness.

A local primary membrane stress is also defined in ASME B&PV Code (ASME 2001 [DIRS 158115], Section III, Division 1, Appendix XIII) XIII-1123(j): “Cases arise in which a membrane stress produced by pressure or other mechanical loading and associated with a discontinuity would, if not limited, produce excessive distortion in the transfer of load to other portions of the structure. Conservatism requires that such a stress be classified as a local primary-membrane stress even though it has some characteristics of a secondary stress.” The other differentiating feature of a local primary membrane stress is that it is localized, and ASME B&PV Code guidance is provided for evaluating if membrane stress fields are adequately “local” to be assigned a P_L classification rather than a more restrictive P_m classification.

The failure mode being addressed by the general primary membrane stress intensity (P_m) limit is “collapse” in the sense that collapse includes tensile instability and ductile rupture under short term loading (Hechmer and Hollinger 1998 [DIRS 166147], Guideline 1). The principle failure mode being addressed by the maximum primary stress intensity ($P_L + P_b$) is excessive plastic deformation. However, it also relates to plastic instability due to the nature of P_b .

The sequence events considered in this report are not repetitive where fatigue cracking or incremental collapse might be an issue. It follows that evaluation of secondary stress intensities (Q) or maximum total stress intensities ($P_L + P_b + Q + F$) are not appropriate. Brittle fracture is also precluded by the high ductility of the outer boundary material, Alloy 22 (UNS N06022), at the temperatures experienced after waste form loading. Although the high-stress areas are comprised of primary, secondary and peak stresses, only the primary stress intensities (P_m , P_L and P_b) contribute to plastic instability (tensile tearing) or excessive plastic deformation, and therefore, only the primary stress intensities are evaluated for the sequence events.

The ASME B&PV Code is used to determine which stress fields should be classified as primary and which should be classified as secondary when evaluating the sequence events (ASME 2001 [DIRS 158115], Section III, Division 1, Appendix XIII, Table XIII-1130-1). All membrane

stress fields are conservatively classified as primary. Classification of the bending stresses is more involved.

Review of representative analyses for the sequence events indicated that the most important wall-bending stresses occur near (within $(Rt)^{1/2}$, R = outer barrier mid-radius, t = outer barrier thickness) gross structural discontinuities. Some of these gross structural discontinuities are integral to the outer boundary and some are introduced by the constraint of adjacent parts or impact surfaces.

The integral gross discontinuities in the outer barrier are similar to ASME Code vessel details such as shell-to-lid junctures and step-changes in wall thickness. The bending stresses are being created by self-constraint, and (ASME 2001 [DIRS 158115], Section III, Division 1, Appendix XIII) Table XIII-1130-1 classifies these bending stresses as secondary. The only exception is at the shell-lid junction where concern about the predictability of the central stresses of the lid leads the Code to caution the designer to consider classifying the bending stresses as P_b (ASME 2001 [DIRS 158115], Section III, Division 1, Appendix XIII, Table XIII-1130-1, Note (4)). However, this is not appropriate guidance for inelastic analyses because the increased flexibility of the juncture caused by inelastic behavior is correctly captured and the central stresses of the lid will be accurately predicted.

The bending stresses created by the constraint of adjacent parts or impact surfaces (which can be considered [temporary] "adjacent parts") were reviewed on individual cases with attention to the amount and type of constraint introduced. In the design analyses to date, the constraint of the adjacent part (e.g., trunnion sleeve) or impact surface (e.g. emplacement pallet, crane hook or rock) created local yielding and minor local distortions in the outer barrier. The outer barrier distorted shape reduced the outer barrier bending stresses while increasing the outer barrier membrane stresses. The bending stresses in these locally yielded regions are therefore self-limiting and satisfy the basic characteristic of a secondary stress.

The structural criterion developed for the outer boundary for the sequence events is meant to directly address the dominant failure mode, tensile instability, and limit the membrane stresses to acceptable limits. The use of inelastic analyses ensures that local thinning or shape changes that could increase membrane stresses will be properly accounted for.

Inelastic analyses are conducted using true stress (σ_u) and true strain based constitutive relationships for Alloy 22 (UNS N06022):

The limit on P_m is $0.7\sigma_u$, and

the limit on P_L is $0.9\sigma_u$, where $P_b = 0$, and

σ_u is the true tensile strength at temperature (ASME 2001 [DIRS 158115], Section III, Division 1, Appendix F, F-1322.3(b) and F-1341.2).

As stated earlier P_L must be "local" to not be classified as a more restrictive general primary membrane stress intensity, P_m (ASME B&PV Code (ASME 2001 [DIRS 158115], Section III, Division 1, Appendix XIII, XIII-1123(j)). Interpretation of this guidance with respect to the ASME B&PV Code Appendix F limits results in requiring P_L values exceeding $0.77\sigma_u$ to not extend for greater than $\sqrt{R \cdot t}$ in any direction (not just the meridional direction), where R is the midsurface radius and t is the thickness of the outer barrier.

Rigorously performed, calculation of the primary membrane stress intensities involves:

- Identifying the governing wall location (stress classification plane normal to the mid-plane of the shell or lid thickness) which may not necessarily contain the maximum stressed point (Hechmer and Hollinger 1998 [DIRS 166147], Guidelines 3 and 4)
- Identifying stress component ($\sigma_x, \sigma_y, \sigma_z, \tau_{xy}, \tau_{yz}, \tau_{zx}$) fields across the wall of the outer barrier
- Averaging the stress component fields to create wall-averaged stress components
- Translating the wall-averaged stresses to principle stress directions by solving a cubic equation
- Calculating the difference between the maximum (σ_1) and minimum (σ_3) principle stress direction values

To simplify the calculation, the wall-average of the element total stress intensity (twice the maximum shear stress) values through the outer corrosion barrier is used to define the primary membrane stress intensities. This is a conservative representation because it ignores the possibly changing principle stress planes through the wall, and it includes the secondary and peak stress contributions.

The third Appendix F (ASME 2001 [DIRS 158115], Section III, Division 1) limit on average section shear is imposed whenever a location is governed by the $0.9\sigma_u P_L$ limit. When the wall-average of the total stress intensity exceeds $0.84\sigma_u$, an additional check is imposed that each of the three wall-averaged shear stresses is less than $0.42\sigma_u$.

7.1.2.3.2 Responses to Specific Issues

The following sections address the specific issues enumerated in Section 7.1.2.3

7.1.2.3.2.1 Residual and Differential Thermal Expansion Stresses

Differential thermal expansion is accommodated by providing adequate gaps between the two shells that comprise the waste package to ensure that there is no mutual loading due to thermal expansion. The required radial gap between the inner vessel and the outer corrosion barrier of the waste package is documented in a calculation entitled *Waste Package Outer Barrier Stress*

Due to Thermal Expansion with Various Barrier Gap Sizes (BSC 2001 [DIRS 152655]). This calculation resulted in a minimum gap spacing between the inner vessel and outer corrosion barrier to accommodate radial expansion to be set at 1 mm (0.04 in.) (BSC 2001 [DIRS 152655], Section 6.1, Table 4). The axial gap between the inner vessel and outer corrosion barrier and the lids of each is documented in a calculation entitled *Waste Package Axial Thermal Expansion Calculation* (BSC 2003 [DIRS 161691]). This calculation established a minimum axial gap of 10 mm (0.4 in.) between these two shells (BSC 2003 [DIRS 161691], Section 7, p. 13). A similar approach will be used to ensure clearance between the inner vessel of the waste package and the internals.

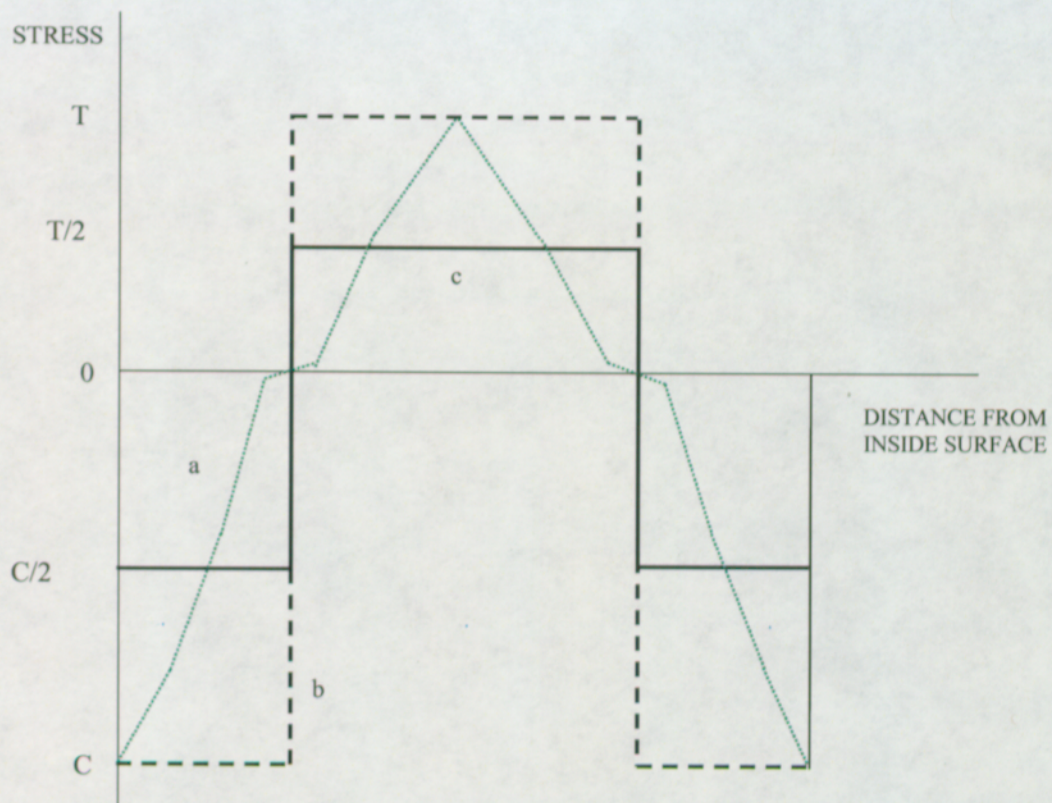
The waste package outer corrosion barrier is not in a stress-free condition at the beginning of service life due to residual stresses purposefully induced by solution annealing and quenching. The purpose of these residual stress fields is to create compressive residual stresses at the outside surface, and perhaps the inside surface (depending on the quenching techniques) of the outer corrosion barrier as well to help mitigate corrosion. The effect of this stress profile on the waste package during dynamic events is documented in a calculation entitled *Drop of Waste Package on Emplacement Pallet-A Mesh Study* (BSC 2003 [DIRS 165497], Section 6). While this calculation is prepared for a postclosure evaluation, it illustrates the basic physics of the phenomenon, and the conclusions are equally appropriate for preclosure evaluations of preclosure dynamic structural calculations.

The residual stresses due to the solution annealing and quenching are analyzed for a mockup waste package outer corrosion barrier in *Residual Stress Analyses on the 21 PWR Mockup Waste Package Outer Shell Due to Quenching and General corrosion Using a Side-wall Thickness of 20mm* (Herrera et al. 2002 [DIRS 166799]). The residual stress analyses are performed in (Herrera et al. 2002 [DIRS 166799], Section 6) for two different quenching techniques: (1) the outside quench (on the outside surface only) and (2) the double-sided quench (on both the inside and outside surfaces). The results reported herein correspond only to the residual stress distribution due to the double-sided quenching.

It must be recognized that the accuracy of this study is limited by the through-wall discretization of the outer corrosion barrier. Since only four layers of solid (brick) elements are used for the finite element analysis representation of the outer corrosion barrier in this calculation, the residual stress distribution is necessarily rather coarse. Furthermore, the one-point-integration solid elements used in this calculation are not best suited for the representation of the initial stress distribution. Nonetheless, no change has been made in the finite element analysis representation for the residual stress calculations since it is important to make a comparison between the results obtained by using the same representation, which is defined by the objective of the source calculation (BSC 2003 [DIRS 165497], Section 1).

Two different magnitudes of the initial stress distribution are used in this study to explore a sensitivity of results to the details of the stress distribution. (Note the schematic representation of the residual stress distribution—generic for both hoop and axial direction—presented as the dotted green line [a] in Figure 21). In the first approximation, the initial stress (i.e., the residual stress caused by the annealing and quenching) in each layer of elements is defined by using the

maximum stress value reached anywhere within the element layer (the dashed line [b] in Figure 21; see also row "Full" in Table 50). In the second approximation, the initial stress in each layer of elements is obtained by averaging the actual stress distribution (the green dotted line [a] in Figure 21) over the element layer. Keeping in mind the actual residual stress distribution, the averaging is performed by assigning to the approximated initial stress distribution one half of the maximum stress value reached anywhere within each element layer (solid line [c] in Figure 21; see also row "Half" in Table 50). The approximated initial stress distributions are presented in Figure 21. The actual stress values are obtained from (Herrera et al. 2002 [DIRS 166799], Figures 48 and 52). For the axial stress distribution the maximum compressive stress at both the inside and outside surface is $C = -300$ MPa; the maximum tensile stress at the middle surface is $T = 150$ MPa. For the hoop stress profile the maximum compressive stress at both inside and outside surface is $C = -260$ MPa; the maximum tensile stress at the middle surface is $T = 190$ MPa.

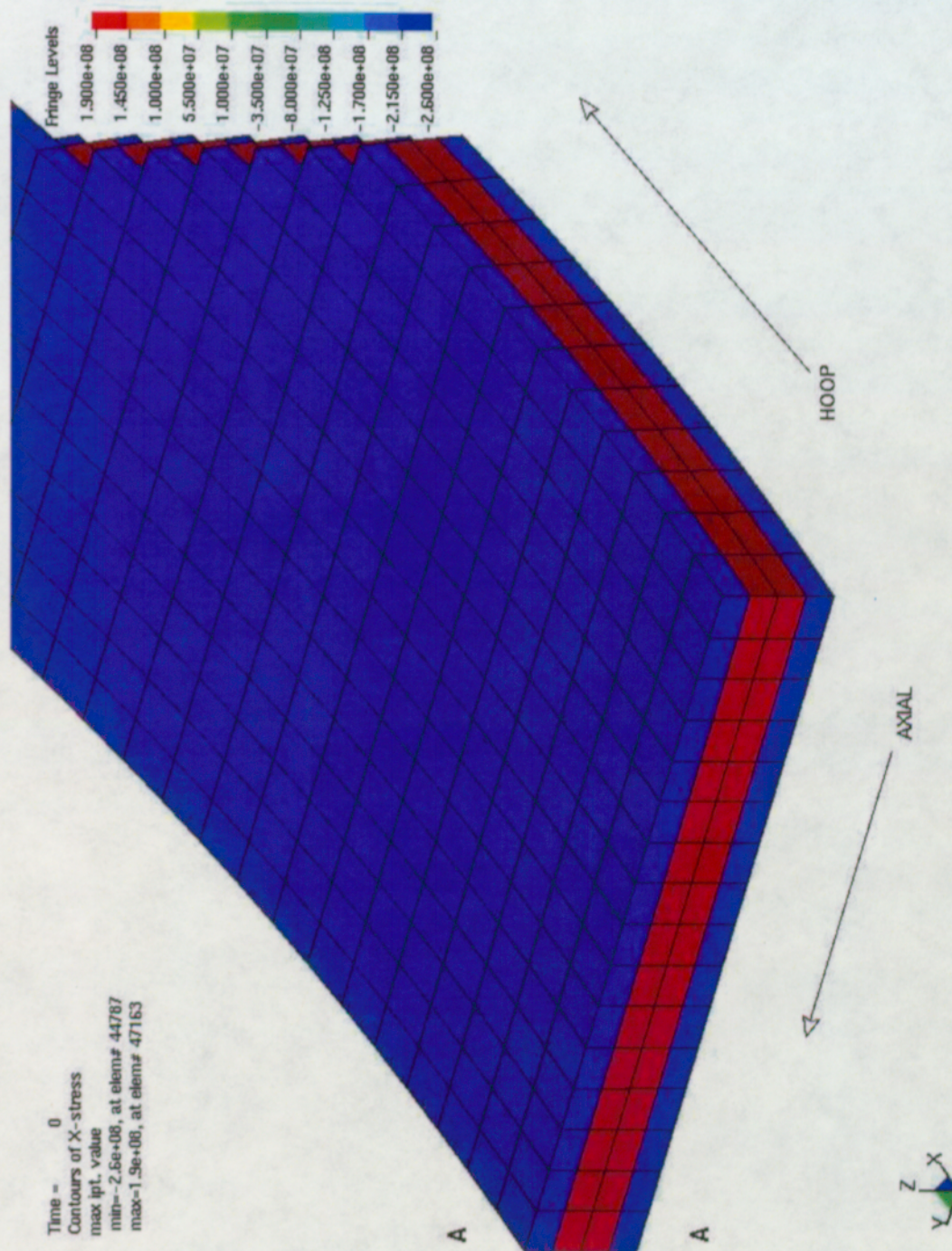


NOTES: (a) Schematic representation of axial and hoop stress distribution from Herrera et al. 2002 [DIRS 166799], Figures 48 and 52 (green dotted line), (b) first ("full") approximation (dashed line), and (c) second ("half") approximation (solid line).

Source: BSC 2003 [DIRS 165497], Figure VII-1

Figure 21. Initial Stress Distribution across the Outer Corrosion Barrier Wall

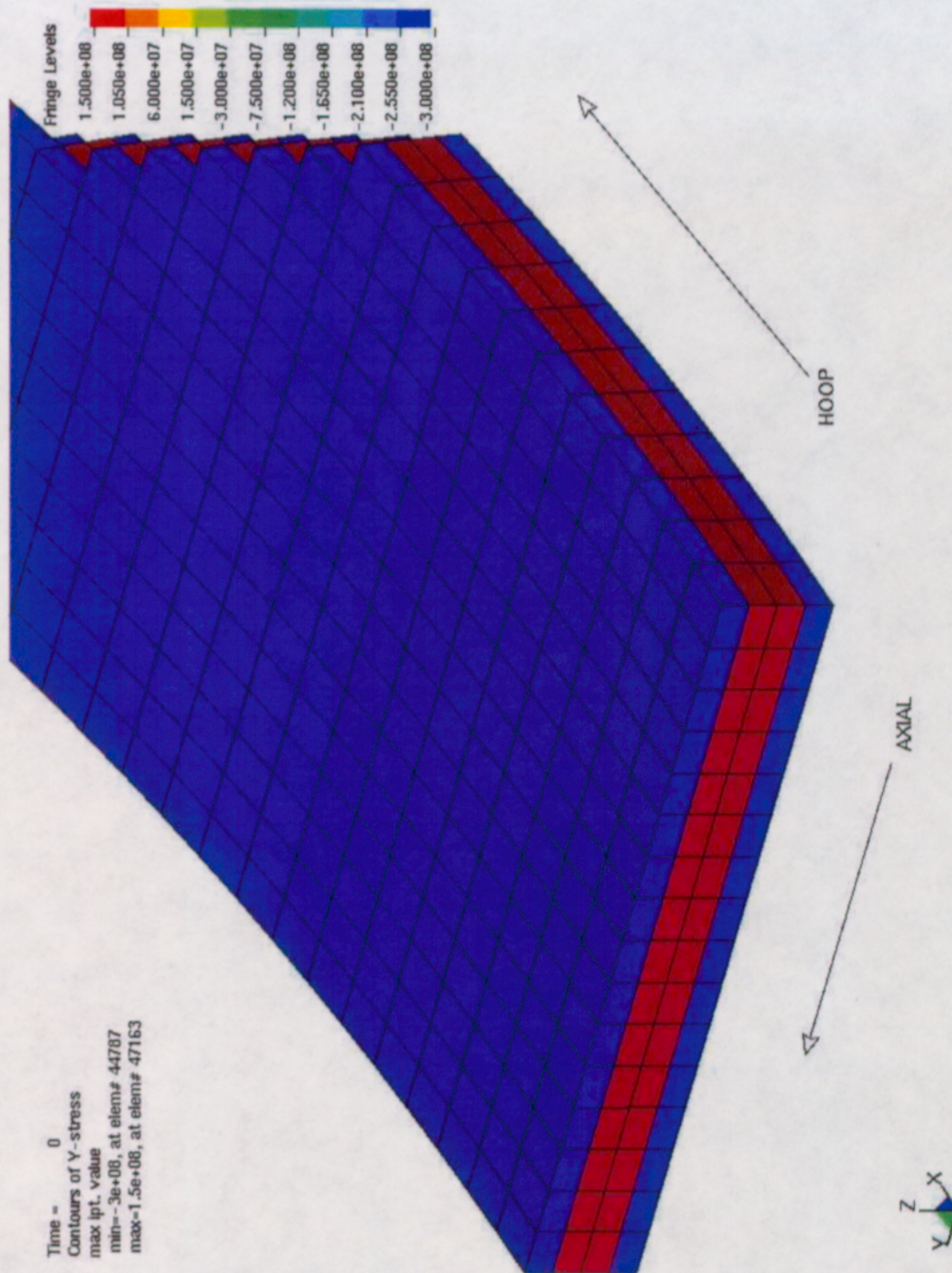
The resulting initial stress distributions in hoop and axial directions are, for the first approximation ("Full"), presented in Figure 22 and Figure 23, respectively. The results shown are in Pascals. (Note that LS-DYNA finite element analysis code requires the initial stresses to be specified in the global Cartesian coordinate system. Thus, the initial stress distribution in the x direction, presented in Figure 22, corresponds to the hoop stress distribution only at the symmetry plane.) The initial effective plastic strain, used for both approximations, is zero.



NOTE: Normal stress in the x-direction is identical to hoop stress at symmetry plane designated as A-A section.

Source: BSC 2003 [DIRS 165497], Figure VII-2

Figure 22. Initial Stress (Pa) Distribution in X Direction in Outer Corrosion Barrier Caused by Annealing and Double-Sided Quenching



Source: BSC 2003 [DIRS 165497], Figure VII-3

Figure 23. Initial Axial (Y-) Stress (Pa) Distribution in Outer Corrosion Barrier Caused by Annealing and Double-Sided Quenching

The results are presented in Table 50. The row designated with "No" represents the initially stress-free case (i.e., without the initial stress). The results obtained by using the first and second initial stress approximations are presented in rows "Full" and "Half," respectively.

Table 50. Results for Three Different Initial Stress Approximations

Magnitude of Residual Stress	Maximum Stress Intensity (MPa)	Maximum Effective Plastic Strain (%)	Damaged Area (80% criterion/90% criterion) ($\times 10^{-3} \text{ m}^2$) ^a
No	630	30.3	7.47 / 2.46
Half	632	30.4	6.41 / 2.29
Full	631	30.7	5.82 / 2.21

NOTE: ^aThis is the percentage of yield stress and is used in postclosure seismic analyses as a measure of susceptibility to accelerated corrosion.

Source: BSC 2003 [DIRS 165497], Table VII-1

According to results presented, the maximum stress intensity and the maximum effective plastic strain are not significantly affected by presence of the initial stress (i.e., the residual stress caused by the solution annealing and double-sided quenching). The damaged area is moderately sensitive to the initial stresses. The damaged area is used in postclosure analyses to assess the susceptibility to accelerated corrosion, which is not important for preclosure safety.

7.1.2.3.2.2 Strain-Rate Effects

The plastic behavior of materials is sensitive to strain rate, which is known as material strain-rate sensitivity. The strain-rate data for Alloy 22 (UNS N06022) and stainless steel type 316 (the stress-strain curves for different strain rates or the change of a characteristic stress with strain rate) are not available in literature at present. Thus, the effect of strain rate on the mechanical strengths of Alloy 22 (UNS N06022) and stainless steel type 316 is studied parametrically by using as a guidance the strain-rate data for stainless steel type 304 (Nicholas 1980, Figures 10 and 27) for both materials. Stainless steel type 304 is used as an analogue for stainless steel type 316 and Alloy 22 (UNS N06022) insofar as strain rate effects are concerned. The tangent (hardening) moduli for Alloy 22 (UNS N06022) and stainless steel type 316 are assumed to be unaffected by the rate of loading. The rationale is that according to the document, *Dynamic Tensile Testing of Structural Materials Using A Split Hopkinson Bar Apparatus* (Nicholas 1980 [DIRS 154072], Figure 10), the tangent modulus for stainless steel type 304 is not significantly affected by the strain rate. This evaluation is documented in a calculation entitled *44-BWR Waste Package Tip-Over from an Elevated Surface* (BSC 2004 [DIRS 169705], Attachment V).

Strain rate is accounted for in this study by using Cowper and Symonds approach that scales the yield strength with the factor:

$$\beta = 1 + \left(\frac{\dot{\epsilon}}{C} \right)^{1/p} \quad (\text{Eq. 1})$$

Here $\dot{\epsilon}$ is the strain rate, and C and p are input parameters obtained by fitting the experimental data (Hallquist 1998 [DIRS 155373], p. 16.37).

The test results provided for 304 stainless steel are used to establish reasonable limits for strain-rate factor β . The results obtained at strain rates of 20 s^{-1} and 900 s^{-1} are selected (Nicholas 1980 [DIRS 154072], Figures 10 and 27) for fitting of the strain-rate parameters, since those two values adequately span the strain-rate range relevant for this calculation. From that data (Nicholas 1980 [DIRS 154072], Figure 27, curve 304, $\epsilon = 0.10$)

$$\beta(\dot{\epsilon} = 20 \text{ s}^{-1}) = 1.135 \quad (\text{Eq. 2})$$

$$\beta(\dot{\epsilon} = 900 \text{ s}^{-1}) = 1.37 \quad (\text{Eq. 3})$$

To establish the upper bound for strain-rate effects, the change of stress of 13.5% at strain rate of 20 s^{-1} (compared to the static test) is increased to 20% (corresponding to relative increase of 50%). Thus, for the upper bound, $\beta(\dot{\epsilon} = 20 \text{ s}^{-1}) = 1.20$. Similarly, the change of stress of 37% at strain rate of 900 s^{-1} (compared to the static test) is increased to 55% (corresponding to relative increase of 50%); this value is then rounded to 60%. Thus, for the upper bound, $\beta(\dot{\epsilon} = 900 \text{ s}^{-1}) = 1.60$.

Results for 304 stainless steel from two additional sources are also presented in the source document for this data (Nicholas 1980 [DIRS 154072], Figure 27). All three test results from this source document are used to establish the lower bound for the strain-rate factor β , $\beta(\dot{\epsilon} = 20 \text{ s}^{-1}) = 1.05$ and $\beta(\dot{\epsilon} = 900 \text{ s}^{-1}) = 1.15$. The purpose of this lower bound is to explore sensitivity of results with regards to the amount of the strain-rate strengthening of material.

In summary, the scale factor β corresponding to strain rate of 20 s^{-1} is 1.05 and 1.20 for the lower and upper bounds, respectively (see Table 51). The scale factor β corresponding to strain rate of 900 s^{-1} is 1.15 and 1.60 for the lower and upper bounds, respectively (Table 51). Note that at both strain rates the increase of stress (expressed as percent increase compared to the static value) from the lower to the upper bound is four times. Also, for both the upper and lower bound the increase of stress (expressed as percent increase compared to the static value) from 20 s^{-1} to 900 s^{-1} is three times.

Table 51. Strain-Rate Parameters

	Lower Bound	Upper Bound
$\beta(20 \text{ s}^{-1})$	1.05	1.20
$\beta(900 \text{ s}^{-1})$	1.15	1.60
p	3.465	3.465
C	644,300	5,284

Source: BSC 2004 [DIRS 169705], Table V-1

These values can be used as boundary conditions for determination of strain-rate parameters in Table 51. For example for the lower bound, the expression,

$$1.05 = 1 + \left(\frac{20}{C}\right)^{1/p} \Rightarrow C = \frac{20}{0.05^p} \quad (\text{Eq. 4})$$

is obtained by substituting the first boundary condition ($\beta(\dot{\epsilon} = 20 \text{ s}^{-1}) = 1.05$) in Equation 1. Similarly, by substituting ($\beta(\dot{\epsilon} = 900 \text{ s}^{-1}) = 1.15$) in Equation 1,

$$1.15 = 1 + \left(\frac{900}{C}\right)^{1/p} \quad (\text{Eq. 5})$$

and adding Equation 4, the parameter p can be readily calculated:

$$0.15 = \left(\frac{900}{20/0.05^p}\right)^{1/p} \Rightarrow p = \frac{\ln(45)}{\ln(0.15) - \ln(0.05)} = 3.465 \quad (\text{Eq. 6})$$

From Equation 4 it follows directly that $C = 644,300 \text{ s}^{-1}$.

By repeating the same calculation for the upper-bound values of β the following parameters can be readily obtained, $p = 3.465$ and $C = 5,284 \text{ s}^{-1}$ (see Table 51).

Three calculations are performed to explore the strain-rate sensitivity of results presented in this calculation (see Table 52 and Table 54). The first calculation is performed with static material properties without strain-rate effects accounted for (row "No" in Table 52 and Table 54). The second calculation corresponds to the lower-bound strain-rate sensitivity (row "Low" in Table 52 and Table 54). Finally, the third calculation is performed with highly rate-sensitive material strengths (row "High" in Table 52 and Table 54, corresponding to the upper-bound strain-rate parameters in Table 53).

Table 52. Maximum Stress Intensity in Outer Corrosion Barrier and Inner Vessel for Three Different Levels of Strain-Rate Sensitivity

Strain-rate Sensitivity	Maximum Stress Intensity (MPa)	
	Inner Vessel	Outer Corrosion Barrier
No	518	902
Low	528	942
High	601	1,037

Source: BSC 2004 [DIRS 169705], Table V-2

Maximum stress intensity, as expected, increases with increased strain-rate sensitivity of the material strengths. The strain-rate strengthening of material implies increase of the true tensile strength, which must be quantified in order to make a meaningful assessment of the material condition upon deformation.

The strain rates encountered in the inner vessel and outer corrosion barrier, at the time when the maximum stress intensities occur, are determined from Figure 24 and presented in Table 53. Note that the effective-strain time histories presented in Figure 24 correspond to elements characterized by the maximum stress intensity (presented in Table 52), i.e., elements 27077 and 27078 (inner vessel) and element 10174 (outer corrosion barrier). Strain-rate factor β is then calculated using Equation 1 for the strain-rate parameters (presented in Table 51) and the strain rate (presented in Table 53). Finally, the true tensile strengths of Alloy 22 (UNS N06022) and stainless steel type 316 are scaled by the factor β .

Table 53. Parameters Defining Strain-Rate Sensitivity for Inner Vessel and Outer Corrosion Barrier at the Time Characterized by Maximum Stress Intensity

Strain-rate Sensitivity	Strain Rate (1/s)	Strain-Rate Factor β (-)	True Tensile Strength (MPa)
No	N/A	1	703
Low	11	1.042	733
High	11	1.168	821
Outer Corrosion Barrier			
No	N/A	1	971
Low	8	1.038	1,008
High	8	1.154	1,121

Source: BSC 2004 [DIRS 169705], Table V-3

The ratio of the maximum stress intensity and true tensile strength is calculated for the inner vessel and outer corrosion barrier for all three strain-rate sensitivity cases. In other words, the maximum stress intensity (Table 52) is divided by the strain-rate-scaled true tensile strength (Table 53). The calculation results are presented in Table 54.

Table 54. Ratio of Maximum Stress Intensity and True Tensile Strength in Outer Corrosion Barrier and Inner Vessel for Three Different Levels of Strain-Rate Sensitivity

Strain-rate Sensitivity	σ_{int} / σ_u	
	Inner Vessel	Outer Corrosion Barrier
No	0.74	0.93
Low	0.72	0.94
High	0.73	0.93

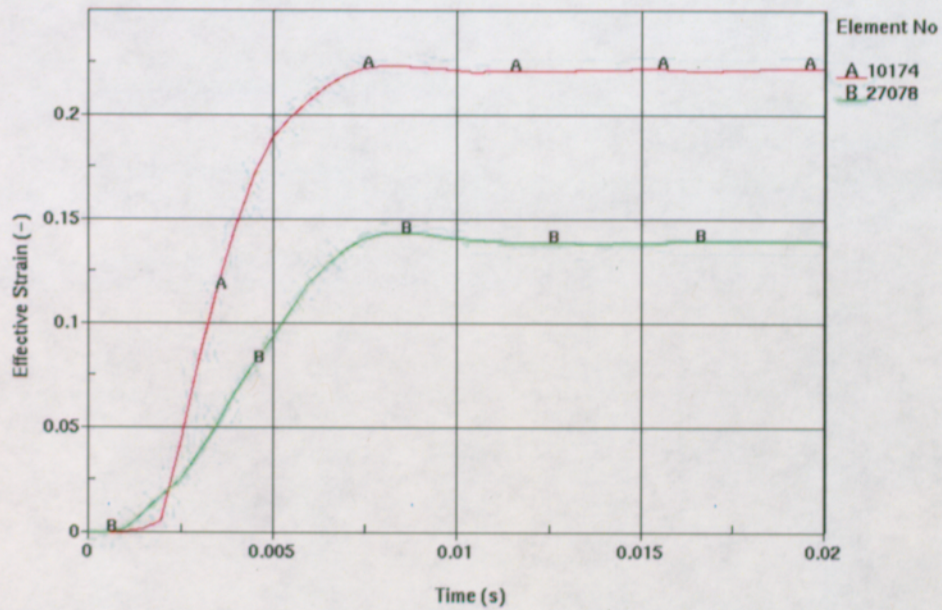
Source: BSC 2004 [DIRS 169705], Table V-4

Based on the results presented in Table 54, it can be concluded that:

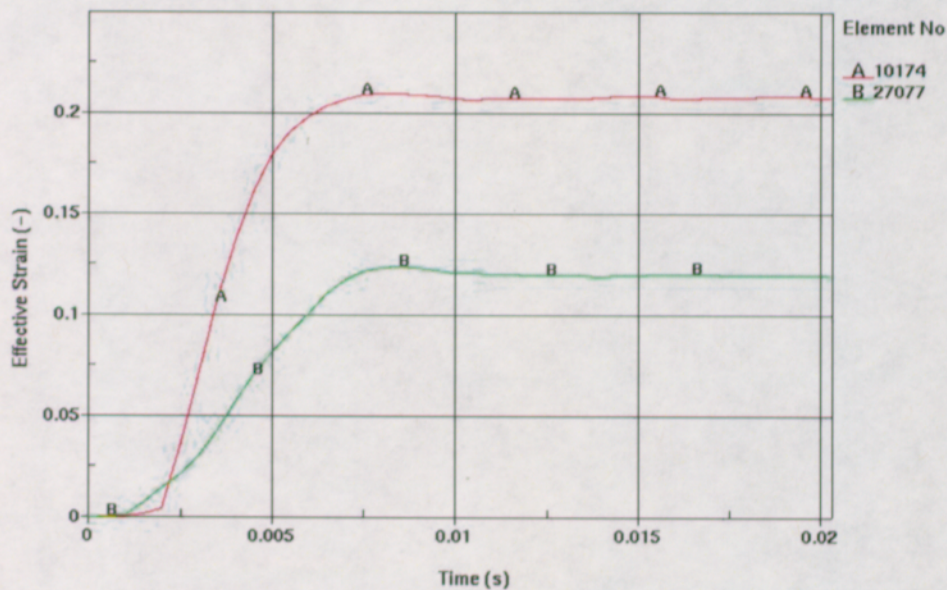
1. The level of strain-rate sensitivity (i.e., "Low" vs. "High") does not have a significant effect on the ratio of the maximum stress intensity and true tensile strength.
2. The use of the static material properties for the tip-over calculation does not have a significant effect on the ratio of the maximum stress intensity and true tensile strength.

Finally, it is important to note that the strain rates reported in Table 53 are the strain rates corresponding to times when the maximum stress intensities are recorded (as an example, for the outer corrosion barrier it is 0.007 s). At that time, the strain rate in the outer corrosion barrier is in rapid decline. Specifically, for the element characterized by the maximum stress intensity it is reduced from 70 s^{-1} to 8 s^{-1} . This raises fundamental questions. If a material is strengthened by elevated-strain-rate loading and then the rate of loading is reduced, is material strength going to reduce as well? If that is so, what is the characteristic time related to that strength reduction? Can it possibly happen "instantaneously"? These important questions are not addressed in available literature at present. Answering these, and similar, questions would require a detailed insight into mechanical and metallurgical aspects of the strain-rate strengthening of material. However, this is not necessary because the effect of strain-rate strengthening of the material is conservatively accounted for in this calculation by scaling the true tensile strength with the strain-rate factor β corresponding to the instantaneous strain rate at the time when the maximum stress intensity occurs. (As an example, if the strain rate of 70 s^{-1} could be used instead of 8 s^{-1} to scale the true tensile strength for the "High" outer corrosion barrier bound, the increase of the true tensile strength would be from $\sigma_u(\dot{\epsilon} = 8 \text{ s}^{-1}) = 1,121 \text{ MPa}$ to $\sigma_u(\dot{\epsilon} = 70 \text{ s}^{-1}) = 1,121 \text{ MPa}$, which would imply the reduction of the stress ratio from 0.93 to 0.90).

Therefore, based on the parametric study for strain-rate effects using stainless steel type 304 strain-rate dependent properties, it has been demonstrated that the use of static properties for stainless steel type 316 and Alloy 22 (UNS N06022) in lieu of material specific strain-rate effects is appropriate.



(a)



(b)

NOTE: (a) Low Strain-Rate Sensitivity and (b) High Strain-Rate Sensitivity
 Source: BSC 2004 [DIRS 169705], Figure V-1

Figure 24. Effective-Strain Time History for Elements Characterized by the Peak Maximum Stress Intensity in the Inner Vessel (Elements 27077 and 27078) and Outer Corrosion Barrier (Element 10174)

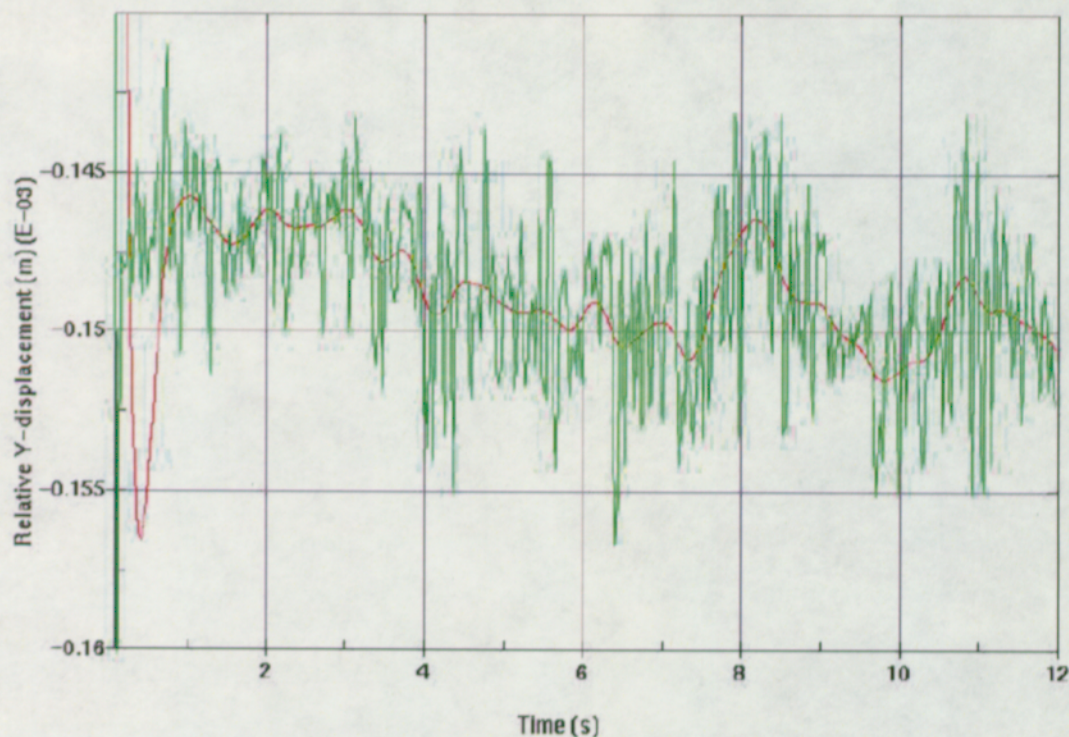
7.1.2.3.2.3 Dimensional and Material Variability

All structural calculations assume the thicknesses for the inner vessel and outer corrosion barrier are the minimum material thicknesses. Future drawings will indicate tolerances that show these dimensions as minimum values. This assures structural design requirements will be achieved.

Maintaining conservative answers due to material variability is managed by using the minimum material-property strengths available (e.g., from the ASME B&PV Code and other codes). When available, material properties that are temperature dependent are used for variable-temperature environment calculations. In general, when a range of values is given for material properties, the values that ensure conservative results are used.

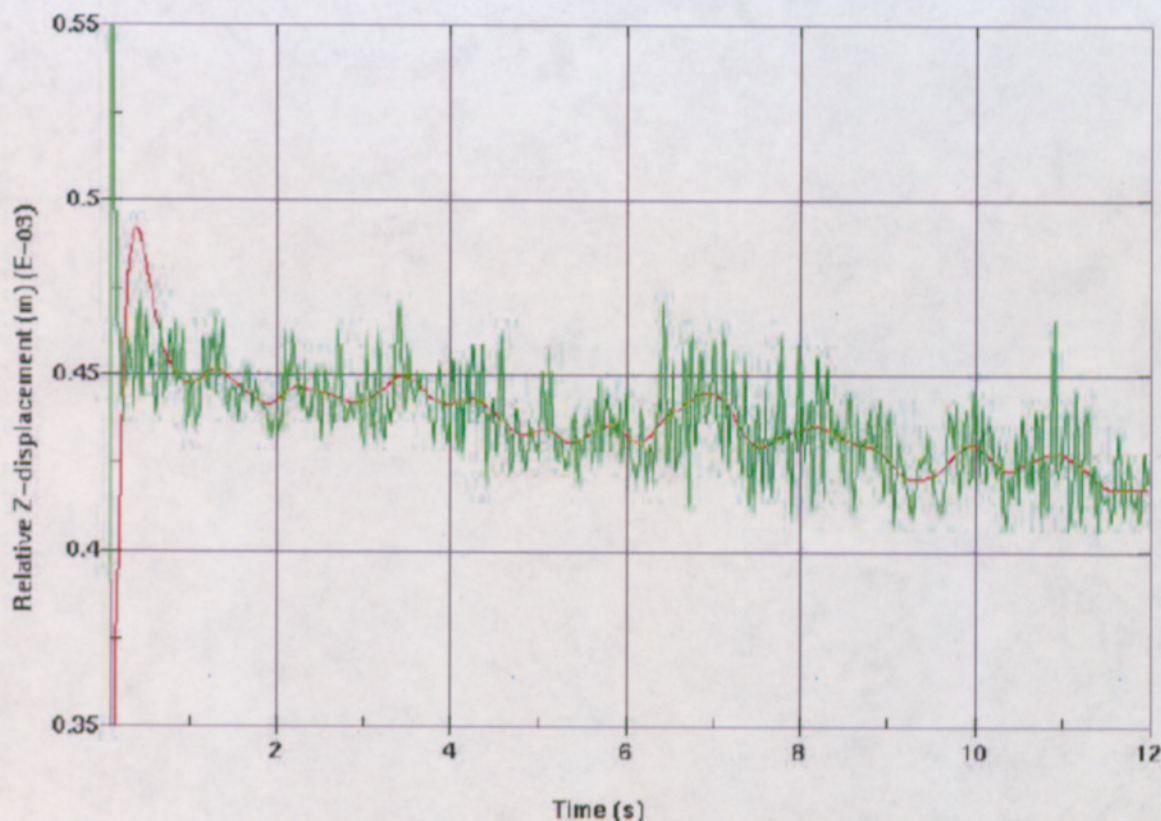
7.1.2.3.2.4 Seismic Effect on Ground Motion

In the surface facility, it is anticipated that fixtures are provided to restrain the waste package during evolutions in that facility, and these devices are sufficient to provide restraint during vibratory ground motion. For vibratory ground motion in the underground, margin to the breach of the waste package has been calculated for vibratory ground motion with an annual exceedance frequency (annual frequency of occurrence) of 5×10^{-4} per year. For this calculation, the motion of the waste package is very small, on the order of fractions of millimeters as illustrated in Figure 25 and Figure 26 (BSC 2004 [DIRS 167083], Section 6.3, pp. 64 to 65).



Source: BSC 2004 [DIRS 167083], Figure 10

Figure 25. Relative Longitudinal (Y) Displacement (Raw – green and Filtered – red) of Waste Package with Respect to Emplacement Pallet for Annual Frequency of Occurrence 5×10^{-4} per year.



Source: BSC 2004 [DIRS 167083], Figure 11

Figure 26. Relative Vertical (Z) Displacement (Raw – green and Filtered – red) of Waste Package with Respect to Emplacement Pallet for Annual Frequency of Occurrence 5×10^{-4} per year.

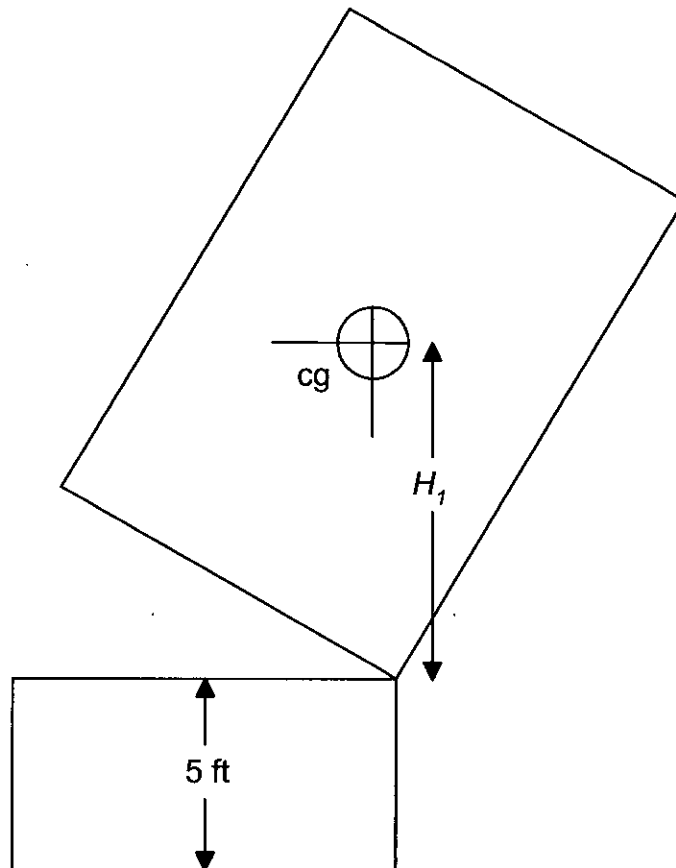
7.1.2.3.2.5 Initial Tip-Over Velocities

A sensitivity study is performed where a range of tip-over velocities were considered and bound those expected in the surface facilities. This evaluation is documented in a calculation entitled *44-BWR Waste Package Tip-Over from an Elevated Surface* (BSC 2004 [DIRS 169705], Attachment IV). The point of incipient toppling is illustrated in Figure 27.

Using the energy method, the rotational velocity of the waste package is calculated at the point just before impact. Table 55 shows a possible range of initial velocities. The peak ground velocity (PGV) is multiplied by values of 0, 1, 5, and 10, to span the parameter space.

$$mg\Delta h = \frac{1}{2} I\Delta(\omega^2) \quad (\text{Eq. 7})$$

Here, “ m ” is the mass of the waste package, “ g ” is the gravitational acceleration constant, “ Δh ” is the change in the height of the center of gravity of the waste package from the moment of toppling to impact, “ I ” is the moment of inertia of the waste package, and “ ω ” is the angular velocity.



Source: BSC 2004 [DIRS 169705], Figure 5-1

Figure 27. Waste Package Position at Maximum Potential Energy

Evaluating this expression,

$$(43,400 \text{ kg})(9.81 \text{ m/s}^2)(2.587 \text{ m}) = \frac{1}{2}(0.427 \text{e}^6 \text{ kg}\cdot\text{m}^2)(\omega^2 - \omega_0^2)$$

Here, " ω_0 " is the initial angular velocity.

The PGV has a value of 0.4378 m/s (DTN: MO0306SDSAVDTH.000 [DIRS 164033]) on the repository horizon, yielding:

$$\text{PGV } (10^{-4} \text{ event}) = 0.4378 \text{ m/s} = V_0$$

(The only ground motions available at this writing for this frequency of exceedance were for the repository horizon. Subsequent to the performance of this work, the PGV for an annual frequency of exceedance of $1 \cdot 10^{-4}$ per year at the surface became available (DTN: MO0312WHBDE104.001 [DIRS 167126]). This PGV is 1.17 m/s, which is about three

times the velocity at the repository horizon. The corresponding PGVs at the surface are higher and are covered by the sensitivity study range.)

Finally,

$$\omega_0 = V_0/H_1 \quad (\text{Eq. 8})$$

In this equation, " H_1 " is the distance from the center of gravity of the waste package to the bottom edge of the waste package at the point of toppling (see Figure 27).

Note that predicted PGV—albeit at the repository horizon—results in a negligible change in the rotational velocity at impact.

Table 55. Resultant Impact Velocities by Parameter

Parameter	V_0 (m/s)	ω_0 (rad/s)	ω (rad/s)
PGV*0	0	0	2.27
PGV*1	0.438	0.161	2.27
PGV*5	2.19	0.812	2.41
PGV*10	4.38	1.62	2.79

Source: BSC 2004 [DIRS 169705], Table IV-1

The resulting maximum stress intensities for this sensitivity study are shown in Table 56. While substantial increases in initial tip-over velocity result in higher stress levels, the effect is modest and is clearly a second-order effect. Further, for the PGV to be a significant contributor to the angular velocity at impact, the fixturing must fail; the waste package must reach the imminent-toppling configuration at the time of PGV; and the PGV must be applied in the proper direction. These considerations support the conclusion that the current treatment of initial velocity for tip-over calculations is appropriate.

Table 56. Resultant Maximum Stress Intensity by Parameter

	Part	σ_{int} (MPa)	σ_{int} / σ_u
PGV*0	Outer Corrosion Barrier	902	0.93
	Inner Vessel	518	0.74
	Inner Lid	426	0.61
	Spread Ring	286	0.41
PGV*5	Outer Corrosion Barrier	944	0.97
	Inner Vessel	558	0.79
	Inner Lid	442	0.63
	Spread Ring	292	0.42
PGV*10	Outer Corrosion Barrier	1079	1.1
	Inner Vessel	644	0.92
	Inner Lid	478	0.68
	Spread Ring	302	0.43

Source: BSC 2004 [DIRS 169705], Table IV-2

7.1.2.3.2.6 Sliding and Inertial Effect of Waste Package Contents

Inertial effects of waste package contents are an intrinsic part of dynamic structural calculations performed explicitly by finite element analysis codes. Sliding effects of waste package contents during impacts are evaluated in calculations where the movement of such contents is reasonably anticipated to affect the kinematics and the resulting stress fields. Coefficients of friction are used based on the materials and situation. An example of the treatment of the waste package contents is the calculation entitled *44-BWR Waste Package Tip-Over from an Elevated Surface* (BSC 2004 [DIRS 169705]). In this calculation, the internals of the waste package and the commercial SNF assemblies are explicitly represented (BSC 2004 [DIRS 169705], Section 5.3, p. 17).

When the waste package contents are not considered as important to the resulting measures of waste package performance, those contents are often simplified so that the mass and inertial effects are maintained but geometry is simplified.

7.2 POSTCLOSURE

7.2.1 Normal Operations

7.2.1.1 Thermal

The thermal calculations for normal operations are performed continuously through preclosure and postclosure times. The highest temperatures occur during the postclosure period, a few

decades after closure. Cladding temperatures remain below the 350 °C requirement. Details are given in Section 7.1.1.1.

7.2.1.2 Structural

The same criteria, statically, must be met as in the preclosure time period. Since the calculations were performed using degraded waste packages, the criteria is met (see Section 7.1.1.2).

For seismic concerns, refer to Appendix A.

8. OPERATIONAL CONSIDERATIONS

8.1 INTERFACE REQUIREMENTS

Interface requirements are discussed in this section. Functional requirements are taken from BSC 2004 [DIRS 167273].

Functional Requirement Number: 3.1.3.1

Functional Requirement Title: Waste Package Handling Limits

Functional Requirement Text: Waste package handling shall not introduce any surface defect in the corrosion barrier exceeding those identified by performance assessment and on interface exchange drawings. Surface defects include, but are not limited to, scratches, nicks, dents, and permanent changes to the surface stress condition (Table 57).

Table 57. Waste Package Handling Limits Performance Requirements

Performance Requirement Number	Performance Requirement Text	Applicability
1	This issue is under investigation and will be resolved prior to construction authorization. A closure weld defect is the area of most concern and shall be limited to 1.6 mm (1/16 inch) (BSC 2004 [DIRS 164475], p. 59-60).	Yes

Functional Requirement Number: 3.1.3.2

Functional Requirement Title: Waste Package Closure

Functional Requirement Text: Sealing operations shall be performed on the waste package (Table 58).

Table 58. Waste Package Closure Performance Requirements

Performance Requirement Number	Performance Requirement Text	Applicability
1	Waste package sealing operations shall meet the requirements for the waste package as specified in the SDD for the waste package closure system.	Yes

8.2 INTERFACE WITH OTHER SYSTEMS

The loaded waste package has its final closure performed by the waste package closure system in accordance with Section 3.1.3.2 of BSC 2004 [DIRS 167273], at which time it assumes its preclosure and postclosure functions.

During receiving, loading, sealing, and emplacement the waste package is handled by or interfaces with non-nuclear handling system, SNF/HLW transfer system, emplacement and retrieval system, remediation system, and emplacement drift system in addition to the waste package closure system. These systems must comply with Section 3.1.3.1 of BSC 2004 [DIRS 167273]. The waste package passes through the Warehouse and Non-Nuclear Receipt, Dry Transfer, Canister Handling, Remediation, and Subsurface Facilities.

The waste package is handled initially by the trunnions on the trunnion collars. The trunnion collars are installed upon receipt and removed after the waste package is returned to the horizontal position on the emplacement pallet. The waste package is loaded and under goes closure in the vertical position. After the waste package is placed on an emplacement pallet it is transported to the designated drift for emplacement and the trunnion collar is returned for reuse.

9. SUMMARY

This report describes the physical configuration of the commercial waste packages, describes the waste forms that they accommodate, and demonstrates how they respond to event sequences and prevent release of radionuclides. Also included are summaries of the assessments of ionizing does rates from the enclosed waste forms and postclosure performance assessments that provide information to Performance Assessment. Source of uncertainty in the sources analyses are described and the effect on the results discussed.

The design requirements and the supporting calculations are provided as justification for meeting each criterion in Section 7.1.2. An assessment of applicable design requirements for the 21-PWR and 44-BWR waste packages is summarized in Table 59 and taken from BSC 2004 [DIRS 167273]. The results are suitable for the intended use and the results are reasonable compared to the inputs.

Table 59. Summary of Design Performance Requirements

Functional Requirement Number	Performance Requirement Number	Performance Requirement	Comment
3.1.1.1	1	The sealed waste package shall not breach during normal operations or during credible preclosure event sequences.	Compliance demonstrated.
3.1.1.1	2	The waste package shall be designed and constructed to the codes and standards specified in Doraswamy 2004, [DIRS 169548], Section 5.1.1.	Compliance demonstrated.
3.1.1.1	3	Normal operations and credible event sequence load combinations are defined in Mecham 2004 [DIRS 169790], Section 6.2.2. Note: The normal operations and credible event sequence load combinations are in Mecham 2004 [DIRS 169790], Section 6.2.2 and are not present in Doraswamy 2004 [DIRS 169548].	Compliance demonstrated.
3.1.1.1	4	The waste package shall be designed to permit retrieval during the preclosure period until the completion of a performance confirmation program and NRC review of the information obtained from such a program.	Compliance demonstrated.
3.1.1.1	5	The waste package shall be designed to permit retrieval during the preclosure period so that any or all of the emplaced waste could be retrieved on a reasonable schedule starting at any time up to 50 years after waste emplacement operations are initiated, unless a different time period is approved or specified by the NRC.	Compliance demonstrated.
3.1.1.1	6	The waste package shall be designed to meet the full range of preclosure operating conditions for up to 300 years after the final waste emplacement.	Compliance demonstrated.
3.1.1.2	1	In conjunction with natural barriers and other engineered barriers, the sealed waste package shall limit transport of radionuclides in a manner sufficient to meet long-term repository performance requirements.	Compliance demonstrated.
3.1.1.2	2	The waste package shall be designed and constructed to the codes and standards specified in Doraswamy 2004 [DIRS 169548], Section 5.1.1.	Compliance demonstrated.
3.1.1.2	3	Normal operations and event load combinations are defined in Mecham 2004 [DIRS 169790], Section 6.2.2. Note: The normal operations and credible event sequence load combinations are in Mecham 2004 [DIRS 169790], Section 6.2.2 and are not present in Doraswamy 2004 [DIRS 169548].	Compliance demonstrated.
3.1.1.3	1	The methodology defined in the <i>Disposal Criticality Analysis Methodology Topical Report</i> (YMP 2003 [DIRS 165505]) shall be used to demonstrate acceptable criticality control for waste packages.	Compliance demonstrated.
3.1.1.3	2	The waste package shall meet criteria 4.9.2.2.2 from the Doraswamy 2004 [DIRS 169548], Section 4.9.2.	Compliance demonstrated.
3.1.1.4	1	The sealed waste package environment shall provide conditions that maintain waste form characteristics that restrict transport of radionuclides.	Compliance demonstrated.

Functional Requirement Number	Performance Requirement Number	Performance Requirement	Comment
3.1.1.4	2	The waste package shall maintain all commercial SNF waste forms containing zirconium-based cladding or stainless steel cladding during preclosure and postclosure periods at temperatures that will not accelerate the degradation of the cladding to the point that it affects the performance of the system.	Compliance demonstrated.
3.1.1.4	3	The waste package shall meet the temperature criteria in the Doraswamy 2004 [DIRS 169548], Section 5.1.3.2, for all Zirconium clad commercial fuel.	Compliance demonstrated.
3.1.1.4	4	The waste form region of the sealed waste package shall have an inert atmosphere with limited oxidizing agents.	Compliance demonstrated.
3.1.1.5	1	The maximum waste package power at emplacement is 11.8 kW.	Compliance demonstrated.
3.1.2.2	1	Table 7 and Table 8 identify parameters (size, weight, and inventory) that may be used for design.	Compliance demonstrated.
3.1.2.4	1	No qualified information is available at this time.	Pending
3.1.3.1	1	This issue is under investigation and will be resolved prior to construction authorization. A closure weld defect is the area of most concern and shall be limited to 1.6 mm (1/16 inch) (BSC 2004 [DIRS 164475], p. 59-60).	Under investigation
3.1.3.2	1	Sealing operations shall be performed on the waste package.	Compliance demonstrated.

10. REFERENCES

10.1 CITATIONS

[DIRS 166833]

Anderson, M.J. 2003. *Waste Package Design Technical Exchange, Waste Package Seismic Response*. Presented to U.S. Nuclear Regulatory Commission, June 5, 2003, Las Vegas, Nevada. Las Vegas, Nevada: Yucca Mountain Site Characterization Office. ACC: MOL.20030715.0011.

[DIRS 152655]

BSC (Bechtel SAIC Company) 2001. *Waste Package Outer Barrier Stress Due to Thermal Expansion with Various Barrier Gap Sizes*. CAL-EBS-ME-000011 REV 00. Las Vegas, Nevada: Bechtel SAIC Company. ACC: MOL.20011212.0222.

[DIRS 161537]

BSC (Bechtel SAIC Company) 2002. *Critical Distance Between Impact Locations for Multiple Rock Fall on Waste Package*. 000-00C-EBS0-00200-000-00A. Las Vegas, Nevada: Bechtel SAIC Company. ACC: MOL.20020916.0313.

[DIRS 165492]

BSC (Bechtel SAIC Company) 2002. *Static Waste Packages on Emplacement Pallet. ###-##C-EBS#-001##-###-0A#*. Las Vegas, Nevada: Bechtel SAIC Company. ACC: MOL.20020801.0132.

[DIRS 162692]

BSC (Bechtel SAIC Company) 2002. *Vertical Drop of 44-BWR Waste Package with Lifting Collars*. 000-00C-DSU0-00800-000-00A. Las Vegas, Nevada: Bechtel SAIC Company. ACC: MOL.20021015.0322.

[DIRS 167318]

BSC (Bechtel SAIC Company) 2003. *21 PWR Waste Package with Absorber Plates Fabrication Specification*. 000-3SS-DSU0-00100-000-00A. Las Vegas, Nevada: Bechtel SAIC Company. ACC: ENG.20031002.0005.

[DIRS 166610]

BSC (Bechtel SAIC Company) 2003. *21-PWR Waste Package with Absorber Plates Loading Curve Evaluation*. CAL-DSU-NU-000006 REV 00A. Las Vegas, Nevada: Bechtel SAIC Company. ACC: DOC.20031222.0007.

[DIRS 167319]

BSC (Bechtel SAIC Company) 2003. *44 BWR Waste Package Fabrication Specification*. 000-3SS-DSU0-00200-000-00A. Las Vegas, Nevada: Bechtel SAIC Company. ACC: ENG.20031002.0004.

[DIRS 166291]

BSC (Bechtel SAIC Company) 2003. *44-BWR Waste Package Swing Down*. 000-00C-DSU0-02100-000-00A. Las Vegas, Nevada: Bechtel SAIC Company. ACC: ENG.20031103.0002.

[DIRS 165058]

BSC (Bechtel SAIC Company) 2003. *BSC Position on the Use of the ASME Boiler and Pressure Vessel Code for the Yucca Mountain Waste Packages*. 000-30R-WIS0-00200-000-000. Las Vegas, Nevada: Bechtel SAIC Company. ACC: MOL.20030909.0054.

[DIRS 164364]

BSC (Bechtel SAIC Company) 2003. *BWR Source Term Generation and Evaluation*. 000-00C-MGR0-00200-000-00A. Las Vegas, Nevada: Bechtel SAIC Company. ACC: ENG.20030723.0001.

[DIRS 167031]

BSC (Bechtel SAIC Company) 2003. *Corner Drop of the 44-BWR Waste Package*. 000-00C-DSU0-01700-000-00A. Las Vegas, Nevada: Bechtel SAIC Company. ACC: ENG.20031215.0005.

[DIRS 166956]

BSC (Bechtel SAIC Company) 2003. *Design and Engineering Organization, 44-BWR Waste Package Configuration*. 000-MW0-DSU0-00502-000-00A. Las Vegas, Nevada: Bechtel SAIC Company. ACC: ENG.20031021.0004.

[DIRS 166596]

BSC (Bechtel SAIC Company) 2003. *Dose Rate Calculation for 44-BWR Waste Package*. 000-00C-DSU0-02300-000-00A. Las Vegas, Nevada: Bechtel SAIC Company. ACC: ENG.20030909.0003.

[DIRS 162711]

BSC (Bechtel SAIC Company) 2003. *Drift Degradation Analysis*. ANL-EBS-MD-000027 REV 02. Las Vegas, Nevada: Bechtel SAIC Company. ACC: DOC.20030709.0003.

[DIRS 165497]

BSC (Bechtel SAIC Company) 2003. *Drop of Waste Package on Emplacement Pallet - A Mesh Study*. 000-00C-DSU0-02200-000-00A. Las Vegas, Nevada: Bechtel SAIC Company. ACC: ENG.20030915.0001.

[DIRS 167167]

BSC (Bechtel SAIC Company) 2003. *Long-Term Strategy of Analyses and Component Design Subproject*. 000-30R-WIS0-00300-000-001. Las Vegas, Nevada: Bechtel SAIC Company. ACC: MOL.20030922.0169.

[DIRS 166943]

BSC (Bechtel SAIC Company) 2003. *Object Drop on 44-BWR and 21-PWR Waste Packages*. 000-00C-DSU0-02900-000-00A. Las Vegas, Nevada: Bechtel SAIC Company. ACC: ENG.20040105.0001.

[DIRS 164128]

BSC (Bechtel SAIC Company) 2003. *Preliminary Categorization of Event Sequences for License Application*. CAL-MGR-RL-000002 REV 00A. Las Vegas, Nevada: Bechtel SAIC Company. ACC: DOC.20030929.0010.

[DIRS 165179]

BSC (Bechtel SAIC Company) 2003. *Q-List*. TDR-MGR-RL-000005 REV 00. Las Vegas, Nevada: Bechtel SAIC Company. ACC: DOC.20030930.0002.

[DIRS 164975]

BSC (Bechtel SAIC Company) 2003. *Repository Design, 12-PWR Waste Package Configuration*. 000-MW0-DSU0-00301-000-00A. Las Vegas, Nevada: Bechtel SAIC Company. ACC: ENG.20030814.0004.

[DIRS 164976]

BSC (Bechtel SAIC Company) 2003. *Repository Design, 12-PWR Waste Package Configuration*. 000-MW0-DSU0-00302-000-00A. Las Vegas, Nevada: Bechtel SAIC Company. ACC: ENG.20030815.0006.

[DIRS 164977]

BSC (Bechtel SAIC Company) 2003. *Repository Design, 12-PWR Waste Package Configuration*. 000-MW0-DSU0-00303-000-00A. Las Vegas, Nevada: Bechtel SAIC Company. ACC: ENG.20030815.0007.

[DIRS 164726]

BSC (Bechtel SAIC Company) 2003. *Repository Twelve Waste Package Segment Thermal Calculation*. 800-00C-WIS0-00100-000-00A. Las Vegas, Nevada: Bechtel SAIC Company. ACC: ENG.20030915.0003.

[DIRS 163984]

BSC (Bechtel SAIC Company) 2003. *Sizing of Uncanistered Fuel Waste Package Cavity*. 000-00C-DSU0-02000-000-00A. Las Vegas, Nevada: Bechtel SAIC Company. ACC: ENG.20030624.0001.

[DIRS 166899]

BSC (Bechtel SAIC Company) 2003. *Thermal Evaluation and Loading Study of 44-BWR Waste Package*. 000-00C-WIS0-01300-000-00A. Las Vegas, Nevada: Bechtel SAIC Company. ACC: ENG.20031208.0005.

[DIRS 164075]

BSC (Bechtel SAIC Company) 2003. *Thermal Evaluation of a 21 PWR Waste Package in the Shielded Surface Facility Transporter*. 000-00C-DSU0-01300-000-00A. Las Vegas, Nevada: Bechtel SAIC Company. ACC: ENG.20030515.0001.

[DIRS 165968]

BSC (Bechtel SAIC Company) 2003. *Thermal Response of the 21-PWR to a Fire Accident*. 000-00C-DSU0-01600-000-00A. Las Vegas, Nevada: Bechtel SAIC Company. ACC: ENG.20030701.0002.

[DIRS 162007]

BSC (Bechtel SAIC Company) 2003. *Thermal Response of the 44-BWR Waste Package to Hypothetical Fire Accident*. 000-00C-DSU0-00600-000-00A. Las Vegas, Nevada: Bechtel SAIC Company. ACC: ENG.20030205.0011.

[DIRS 165093]

BSC (Bechtel SAIC Company) 2003. *Two-Dimensional Repository Thermal Design Calculations*. 000-00C-WIS0-00300-000-00B. Las Vegas, Nevada: Bechtel SAIC Company. ACC: ENG.20030630.0004.

[DIRS 163185]

BSC (Bechtel SAIC Company) 2003. *Value Study Report—Waste Package Reevaluation*. 000-3TS-EBS0-00100-000-000. Las Vegas, Nevada: Bechtel SAIC Company. ACC: MOL.20030327.0073.

[DIRS 166184]

BSC (Bechtel SAIC Company) 2003. *Vertical Drop of 5-DHLW/DOE SNF Short Waste Package with Trunnion Collars Design Calculation*. 000-00C-DSH0-00500-000-00A. Las Vegas, Nevada: Bechtel SAIC Company. ACC: ENG.20031002.0006.

[DIRS 166827]

BSC (Bechtel SAIC Company) 2003. *Vertical Lift of the Naval SNF Long Waste Package*. 000-00C-DNF0-00300-000-00A. Las Vegas, Nevada: Bechtel SAIC Company. ACC: ENG.20031121.0001.

[DIRS 161691]

BSC (Bechtel SAIC Company) 2003. *Waste Package Axial Thermal Expansion Calculation*. 000-00C-EBS0-00500-000-00A. Las Vegas, Nevada: Bechtel SAIC Company. ACC: ENG.20030416.0001.

[DIRS 164475]

BSC (Bechtel SAIC Company) 2003. *Analysis of Mechanisms for Early Waste Package/Drip Shield Failure*. CAL-EBS-MD-000030 REV 00B. Las Vegas, Nevada: Bechtel SAIC Company. ACC: DOC.20031001.0012.

[DIRS 167005]

BSC (Bechtel SAIC Company) 2003. *Waste Package Outer Shell Stresses Due to Internal Pressure at Elevated Temperatures*. 000-00C-EBS0-00600-000-00A. Las Vegas, Nevada: Bechtel SAIC Company. ACC: ENG.20030430.0003.

[DIRS 167024]

BSC (Bechtel SAIC Company) 2004. *21-PWR Tip Over from Elevated Surface*. 000-00C-DSU0-02700-000-00A. Las Vegas, Nevada: Bechtel SAIC Company. ACC: ENG.20040123.0176.

[DIRS 167032]

BSC (Bechtel SAIC Company) 2004. *21-PWR Waste Package 10-Degree Oblique Drop with Slap Down*. 000-00C-DSU0-03200-000-00A. Las Vegas, Nevada: Bechtel SAIC Company. ACC: ENG.20040209.0001.

[DIRS 167030]

BSC (Bechtel SAIC Company) 2004. *21-PWR Waste Package Drop with Emplacement Pallet*. 000-00C-DSU0-02400-000-00A. Las Vegas, Nevada: Bechtel SAIC Company. ACC: ENG.20040205.0004.

[DIRS 167393]

BSC (Bechtel SAIC Company) 2004. *Design and Engineering, 21-PWR Waste Package Configuration*. 000-MW0-DSU0-00401-000-00C. Las Vegas, Nevada: Bechtel SAIC Company. ACC: ENG.20040202.0023.

[DIRS 166953]

BSC (Bechtel SAIC Company) 2004. *Design and Engineering, 21-PWR Waste Package Configuration*. 000-MW0-DSU0-00402-000-00B. Las Vegas, Nevada: Bechtel SAIC Company. ACC: ENG.20040119.0004.

[DIRS 167394]

BSC (Bechtel SAIC Company) 2004. *Design and Engineering, 21-PWR Waste Package Configuration*. 000-MW0-DSU0-00403-000-00C. Las Vegas, Nevada: Bechtel SAIC Company. ACC: ENG.20040202.0024.

[DIRS 166929]

BSC (Bechtel SAIC Company) 2004. *Design and Engineering, 24-BWR Waste Package Configuration*. 000-MW0-DSU0-00601-000-00A. Las Vegas, Nevada: Bechtel SAIC Company. ACC: ENG.20040119.0006.

[DIRS 166958]

BSC (Bechtel SAIC Company) 2004. *Design and Engineering, 24-BWR Waste Package Configuration*. 000-MW0-DSU0-00602-000-00A. Las Vegas, Nevada: Bechtel SAIC Company. ACC: ENG.20040119.0007.

[DIRS 166959]

BSC (Bechtel SAIC Company) 2004. *Design and Engineering, 24-BWR Waste Package Configuration*. 000-MW0-DSU0-00603-000-00A. Las Vegas, Nevada: Bechtel SAIC Company. ACC: ENG.20040119.0008.

[DIRS 167550]

BSC (Bechtel SAIC Company) 2004. *Design and Engineering, 44-BWR Waste Package Configuration*. 000-MW0-DSU0-00501-000-00B. Las Vegas, Nevada: Bechtel SAIC Company. ACC: ENG.20040213.0005.

[DIRS 167555]

BSC (Bechtel SAIC Company) 2004. *Design and Engineering, 44-BWR Waste Package Configuration*. 000-MW0-DSU0-00503-000-00B. Las Vegas, Nevada: Bechtel SAIC Company. ACC: ENG.20040213.0006.

[DIRS 167780]

BSC (Bechtel SAIC Company) 2004. *Errata for Seismic Consequence Abstraction*. MDL-WIS-PA-000003 REV 0 ERRATA 1. Las Vegas, Nevada: Bechtel SAIC Company. ACC: DOC.20030818.0006; DOC.20040218.0002.

[DIRS 167718]

BSC (Bechtel SAIC Company) 2004. *Horizontal Drop of the 21-PWR Waste Package Supplemental Calculation*. 000-00C-DSU0-00500-000-00A. Las Vegas, Nevada: Bechtel SAIC Company. ACC: ENG.20040301.0003.

[DIRS 167372]

BSC (Bechtel SAIC Company) 2004. *Horizontal Drop of the 44-BWR Waste Package with Emplacement Pallet*. 000-00C-DSU0-03100-000-00A. Las Vegas, Nevada: Bechtel SAIC Company. ACC: ENG.20040225.0021.

[DIRS 167182]

BSC (Bechtel SAIC Company) 2004. *Rock Fall on Waste Packages*. 000-00C-MGR0-01400-000-00A. Las Vegas, Nevada: Bechtel SAIC Company. ACC: ENG.20040225.0012.

[DIRS 167083]

BSC (Bechtel SAIC Company) 2004. *Structural Calculations of Waste Package Exposed to Vibratory Ground Motion*. 000-00C-WIS0-01400-000-00A. Las Vegas, Nevada: Bechtel SAIC Company. ACC: ENG.20040217.0008.

[DIRS 167392]

BSC (Bechtel SAIC Company) 2004. *Swing Down Drop of the 21-PWR Waste Package*. 000-00C-DSU0-03000-000-00A. Las Vegas, Nevada: Bechtel SAIC Company. ACC: ENG.20040303.0004.

[DIRS 166695]

BSC (Bechtel SAIC Company) 2004. *Thermal Evaluation and Loading Study of 21-PWR Waste Package*. 000-00C-DSU0-02600-000-00B. Las Vegas, Nevada: Bechtel SAIC Company. ACC: ENG.20040120.0003.

[DIRS 169593]

BSC (Bechtel SAIC Company) 2004. *Dose Rate Calculation for 21-PWR Waste Package*. 000-00C-DSU0-01800-000-00B. Las Vegas, Nevada: Bechtel SAIC Company. ACC: ENG.20040607.0001.

[DIRS 169647]

BSC (Bechtel SAIC Company) 2004. *Vertical Drop of 21-PWR Waste Package with Lifting Collars*. 000-00C-DSU0-03400-000-00A. Las Vegas, Nevada: Bechtel SAIC Company. ACC: ENG.20040607.0006.

[DIRS 169705]

BSC (Bechtel SAIC Company) 2004. *44-BWR Waste Package Tip-Over from an Elevated Surface*. 000-00C-DSU0-01500-000-00B. Las Vegas, Nevada: Bechtel SAIC Company. ACC: ENG.20040316.0009.

[DIRS 169706]

BSC (Bechtel SAIC Company) 2004. *44-BWR Waste Package 10-Degree Oblique Drop with Slap Down*. 000-00C-DSU0-01900-000-00A. Las Vegas, Nevada: Bechtel SAIC Company. ACC: ENG.20040504.0008.

[DIRS 169707]

BSC (Bechtel SAIC Company) 2004. *Horizontal Drop of the 44-BWR Waste Package*. 000-00C-DSU0-01400-000-00B. Las Vegas, Nevada: Bechtel SAIC Company. ACC: ENG.20040524.0008.

[DIRS 167273]

BSC (Bechtel SAIC Company) 2004. *DOE and Commercial Waste Package System Description Document*. 000-3YD-DS00-00100-000-003. Las Vegas, Nevada: Bechtel SAIC Company. ACC: ENG.20040322.0008.

[DIRS 167278]

BSC (Bechtel SAIC Company) 2004. *Waste Package Closure System Description Document*. 100-3YD-HW00-00100-000-001. Las Vegas, Nevada: Bechtel SAIC Company. ACC: ENG.20040310.0021.

[DIRS 169059]

BSC (Bechtel SAIC Company) 2004. *Errata for Sampling of Stochastic Input Parameters for Rockfall and Structural Response Calculations Under Vibratory Ground Motion*. ANL-EBS-PA-000009 REV 00 Errata 1. Las Vegas, Nevada: Bechtel SAIC Company. ACC: DOC.20030707.0003; DOC.20040312.0003.

[DIRS 169959]

BSC (Bechtel SAIC Company) 2004. *Assessment of Proposed Change in Neutron Absorber Material for CSNF Waste Packages* 000-30R-DS00-00100-000 Revision 00. Las Vegas, Nevada: Bechtel SAIC Company. ACC: ENG.20040615.0015.

[DIRS 170059]

BSC (Bechtel SAIC Company) 2004. *Corner Drop of the 21-PWR Waste Package*. 000-00C-DSU0-03300-000-00A. Las Vegas, Nevada: Bechtel SAIC Company. ACC: ENG.20040624.0034.

[DIRS 169062]

BSC (Bechtel SAIC Company) 2004. *Waste Package Envelope Dimensions for Facilities & Handling*. 000-B20-MGR0-00101-000-00A. Las Vegas, Nevada: Bechtel SAIC Company. ACC: ENG.20040423.0004.

[DIRS 166941]

BSC (Bechtel SAIC Company) 2004. *Waste Form, Heat Output, and Waste Package Spacing for an Idealized Drift Segment*. 000-00C-WIS0-00500-000-00A. Las Vegas, Nevada: Bechtel SAIC Company. ACC: ENG.20040121.0007.

[DIRS 166275]

Canori, G.F. and Leitner, M.M. 2003. *Project Requirements Document*. TER-MGR-MD-000001 REV 02. Las Vegas, Nevada: Bechtel SAIC Company. ACC: DOC.20031222.0006.

[DIRS 159153]

Chen, W.F. 1982. *Plasticity in Reinforced Concrete*. New York, New York: McGraw-Hill. TIC: 240453.

[DIRS 100224]

CRWMS M&O 1997. *Determination of Waste Package Design Configurations*. BBAA00000-01717-0200-00017 REV 00. Las Vegas, Nevada: CRWMS M&O. ACC: MOL.19970805.0310.

[DIRS 100259]

CRWMS M&O 1997. *Waste Package Materials Selection Analysis*. BBA000000-01717-0200-00020 REV 01. Las Vegas, Nevada: CRWMS M&O. ACC: MOL.19980324.0242.

[DIRS 145022]

CRWMS M&O 1999. *1999 Design Basis Waste Input Report for Commercial Spent Nuclear Fuel*. B00000000-01717-5700-00041 REV 01. Washington, D.C.: CRWMS M&O. ACC: MOV.19991217.0001.

[DIRS 157822]

CRWMS M&O 2000. *Corner Drop of 21-PWR Waste Package*. CAL-UDC-ME-000008 REV 00. Las Vegas, Nevada: CRWMS M&O. ACC: MOL.20001113.0306.

[DIRS 149351]

CRWMS M&O 2000. *Pressurized System Missile Impact on Waste Packages*. CAL-EBS-ME-000006 REV 00. Las Vegas, Nevada: CRWMS M&O. ACC: MOL.20000420.0397.

[DIRS 138173]

CRWMS M&O 2000. *Waste Package Containment Barrier Materials and Drip Shield Selection Report*. B00000000-01717-2200-00225 REV 00. Las Vegas, Nevada: CRWMS M&O. ACC: MOL.20000209.0300.

[DIRS 138189]

CRWMS M&O 2000. *Waste Package Internal Materials Selection Report*. B00000000-01717-2200-00226 REV 00. Las Vegas, Nevada: CRWMS M&O. ACC: MOL.20000209.0299.

[DIRS 138192]

CRWMS M&O 2000. *Waste Package Neutron Absorber, Thermal Shunt, and Fill Gas Selection Report*. B00000000-01717-2200-00227 REV 00. Las Vegas, Nevada: CRWMS M&O. ACC: MOL.20000209.0301.

[DIRS 105164]

DOE (U.S. Department of Energy) 1999. *Site Characterization Progress Report Yucca Mountain, Nevada*. DOE/RW-0512. Number 19. Washington, D.C.: U.S. Department of Energy, Office of Civilian Radioactive Waste Management. ACC: HQO.19990813.0018.

[DIRS 155970]

DOE (U.S. Department of Energy) 2002. *Final Environmental Impact Statement for a Geologic Repository for the Disposal of Spent Nuclear Fuel and High-Level Radioactive Waste at Yucca Mountain, Nye County, Nevada*. DOE/EIS-0250. Washington, D.C.: U.S. Department of Energy, Office of Civilian Radioactive Waste Management. ACC: MOL.20020524.0314; through; MOL.20020524.0320.

[DIRS 158398]

DOE (U.S. Department of Energy) 2002. *U.S. Department of Energy Spent Nuclear Fuel and High-Level Radioactive Waste to the Monitored Geologic Repository. Volume 1 of Integrated Interface Control Document*. DOE/RW-0511 Rev. 01. Las Vegas, Nevada: U.S. Department of Energy. ACC: MOL.20020614.0342.

[DIRS 168669]

DOE (U.S. Department of Energy) 2004. *Quality Assurance Requirements and Description*. DOE/RW-0333P, Rev. 14. Washington, D.C.: U.S. Department of Energy, Office of Civilian Radioactive Waste Management. ACC: DOC.20040331.0004.

[DIRS 169548]

Doraswamy, N. 2004. "Preliminary Draft Input Version of Project Design Criteria Document." Interoffice memorandum from N. Doraswamy (BSC) to Distribution, May 26, 2004, 0526041747, with attachment. ACC: MOL.20040526.0027. TBV-5850

[DIRS 155373]

Hallquist, J.O. 1998. *LS-DYNA, Theoretical Manual*. Livermore, California: Livermore Software Technology Corporation. TIC: 238997.

[DIRS 166147]

Hechmer, J.L. and Hollinger, G.L. 1998. *3D Stress Criteria Guidelines for Application*. WRC Bulletin 429. New York, New York: Welding Research Council. TIC: 254432.

[DIRS 166799]

Herrera, M.; Ku, F.; and Tang, S. 2002. *Calculation Package, Residual Stress Analyses on the 21 PWR Mockup Waste Package Outer Shell Due to Quenching and General Corrosion Using a Side-Wall Thickness of 20mm*. File No. TRW-06Q-319. [San Jose, California]: Structural Integrity Associates. ACC: MOL.20020925.0127.

[DIRS 106219]

Jaeger, J.C. and Cook, N.G.W. 1979. *Fundamentals of Rock Mechanics*. 3rd Edition. New York, New York: Chapman and Hall. TIC: 218325.

[DIRS 137700]

Jones, N. 1994. "Low Velocity Perforation of Metal Plates." Chapter 3 of *Shock and Impact on Structures*. Brebbia, C.A. and Sanchez-Galvez, V., eds. Billerica, Massachusetts: Computational Mechanics Publications. TIC: 247052.

[DIRS 154350]

Kelmenson, R. 2000. "Meeting Summary, NRC/DOE Technical Exchange Meeting on Container Life and Source Term (CLST), September 12-13, 2000." E-mail from R. Kelmenson to C. Hanlon (DOE/YMSCO), T. Gunter (DOE/YMSCO), A. Gil (DOE/YMP), P. Russell (DOE/YMSCO), September 27, 2000, with attachment. ACC: MOL.20001127.0049.

[DIRS 169790]

Mechem, D.C. 2004. *Waste Package Component Design Methodology Report*. 000-30R-WIS0-00100-000-001. Las Vegas, Nevada: Bechtel SAIC Company. ACC: ENG.20040617.0012.

[DIRS 154072]

Nicholas, T. 1980. *Dynamic Tensile Testing of Structural Materials Using A Split Hopkinson Bar Apparatus*. AFWAL-TR-80-4053. Wright-Patterson Air Force Base, Ohio: Air Force Wright Aeronautical Laboratories. TIC: 249469.

[DIRS 156800]

Plinski, M.J. 2001. *Waste Package Operations Fabrication Process Report*. TDR-EBS-ND-000003 REV 02. Las Vegas, Nevada: Bechtel SAIC Company. ACC: MOL.20011003.0025.

[DIRS 170052]

Thomas, D.A. 2004. "Preliminary 44 BWR Waste Package Criticality Loading Curve." Interoffice memorandum from D.A. Thomas (BSC) to M.J. Anderson, June 17, 2004, 0617041993. ACC: MOL.20040618.0081. TBV-5889

[DIRS 165505]

YMP (Yucca Mountain Site Characterization Project) 2003. *Disposal Criticality Analysis Methodology Topical Report*. YMP/TR-004Q, Rev. 02. Las Vegas, Nevada: Yucca Mountain Site Characterization Office. ACC: DOC.20031110.0005.

10.2 CODES, STANDARDS, REGULATIONS, AND PROCEDURES

[DIRS 158535]

10 CFR 63. 2002. Energy: Disposal of High-Level Radioactive Wastes in a Geologic Repository at Yucca Mountain, Nevada. Readily available.

[DIRS 118049]

10 CFR 961. Energy: Standard Contract for Disposal of Spent Nuclear Fuel and/or High-Level Radioactive Waste. Readily available.

[DIRS 102016]

ANSI N14.6-1993. *American National Standard for Radioactive Materials - Special Lifting Devices for Shipping Containers Weighing 10000 Pounds (4500 kg) or More*. New York, New York: American National Standards Institute. TIC: 236261.

[DIRS 168413]

AP-3.12Q, Rev. 2, ICN 2. *Design Calculations and Analyses*. Washington, D.C.: U.S. Department of Energy, Office of Civilian Radioactive Waste Management. ACC: DOC.20040318.0002.

[DIRS 104317]

ASM (American Society for Metals) 1980. *Properties and Selection: Stainless Steels, Tool Materials and Special-Purpose Metals*. Volume 3 of *Metals Handbook*. 9th Edition. Benjamin, D., ed. Metals Park, Ohio: American Society for Metals. TIC: 209801.

[DIRS 158115]

ASME (American Society of Mechanical Engineers) 2001. *2001 ASME Boiler and Pressure Vessel Code (includes 2002 addenda)*. New York, New York: American Society of Mechanical Engineers. TIC: 251425.

[DIRS 168403]

ASTM B 932-04. 2004. *Standard Specification for Low-Carbon Nickel-Chromium-Molybdenum-Gadolinium Alloy Plate, Sheet, and Strip*. West Conshohocken, Pennsylvania: American Society for Testing and Materials. TIC: 255846.

[DIRS 163274]

NRC (U.S. Nuclear Regulatory Commission) 2003. *Yucca Mountain Review Plan, Final Report*. NUREG-1804, Rev. 2. Washington, D.C.: U.S. Nuclear Regulatory Commission, Office of Nuclear Material Safety and Safeguards. TIC: 254568.

[DIRS 101681]

Nuclear Waste Policy Act of 1982. 42 U.S.C. 10101 et seq. Readily available.

[DIRS 103936]

Resource Conservation and Recovery Act of 1976. 42 U.S.C. 6901 et seq. Readily available.

10.3 SOURCE DATA

[DIRS 164033]

MO0306SDSAVDTH.000. Seismic Design Spectra and Acceleration, Velocity, and Displacement Time Histories for the Emplacement Level at 10-4 Annual Exceedance Frequency. Submittal date: 06/26/2003.

[DIRS 167126]

MO0312WHBDE104.001. Seismic Design Spectra and Time Histories for the Surface Facilities Area (Point D/E) at 10-4 Annual Exceedance Frequency. Submittal date: 12/12/2003.

APPENDIX A

A.1 POSTCLOSURE WASTE PACKAGE RESPONSE TO VIBRATORY GROUND MOTION DUE TO SEISMICITY

The information in this appendix fulfills two functions. First, it demonstrates the compliance of the waste package to System Description Document requirements. Second, it provided information to respond to parts of Key Technical Agreements CLST 2.08 and CLST 2.09 (Anderson 2003 [DIRS 166833], page 2) applicable to the waste packages.

A.1.1 Preclosure Rock Fall on Waste Package

The results for point-loading rock falls are presented. For credible preclosure rock falls, it is shown that the waste package does not breach. It is further shown that the drip shield provides protection for the waste package, such that the waste package is not contacted by the inner surface of the drip shield due to deformation of the drip shield. The use of the postclosure point-loading rockfall evaluations to generate areas susceptible to accelerated corrosion is also described.

A.1.2 Embrittlement Due to Thermal Aging

When CLST 2.08 and CLST 2.09 Agreements were made, the final closure weld of the waste package was to be remediated by induction annealing. With further investigation and study, the remediation method for this weld has changed to either laser peening or low-plasticity burnishing. Since neither of these treatment methods involve elevated temperatures, the potential of embrittlement of the final closure weld region due to thermal aging no longer exists; therefore, this potential source of material structural performance degradation no longer exists.

A.1.3 Waste Package Response to Vibratory Ground Motion

The analyses supporting postclosure assessment of damage to the waste packages and drip shields due to seismically induced vibratory ground motion are described and shown to be inputs to the seismic model abstraction used within the TSPA-LA framework. Thus, the analyses are demonstrated to be fully compliant with those used to address Structural Deformation and Seismicity KTI issues.

The information in this report is responsive to agreements made between DOE and NRC. The report contains the information that DOE considers necessary for the NRC to review for closure of this agreement.

A.2 TECHNICAL BASIS

A.2.1 Preclosure Rock Fall On Waste Package

Rock falls may occur both in the preclosure and postclosure periods. For the preclosure period, the drip shields have not yet been emplaced, so rocks may fall onto the emplaced waste packages. For the postclosure period, the drip shields intercept the falling rock blocks and protect the waste packages. The point-loading rock falls occur only the non-lithophysal regions

of the repository, since only that region can generate large and structurally challenging rock blocks.

A.2.1.1 Preclosure Rock Falls

This is described in section 7.1.2.2.1, with the rest of the preclosure event sequences. Please refer to section 7.1.2.2.1 for information on this scenario.

A.2.2 Effects of Multiple Rock Falls

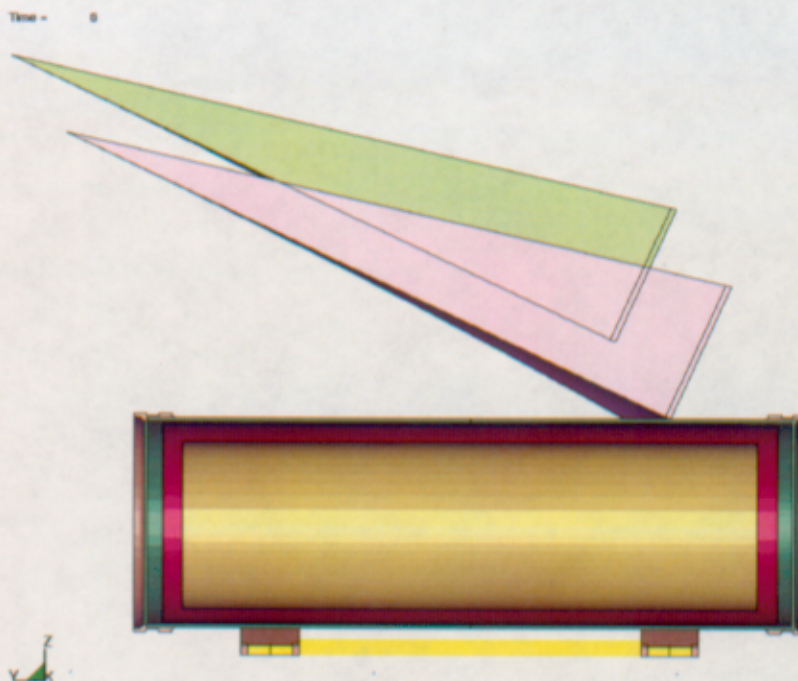
A.2.2.1 Multiple Rock Falls

One of the first questions that arises when the effect of the fall of more than one rock block is investigated is how close must a second rock impact relative to the first fallen rock be in order to influence the stress field generated by the first rock. This question has been addressed for rock falls on the waste package in *Critical Distance Between Impact Locations for Multiple Rock Fall on Waste Package* (BSC 2002 [DIRS 161537]).

A.2.2.1.1 Critical Distance between Rock Impacts for Waste Package

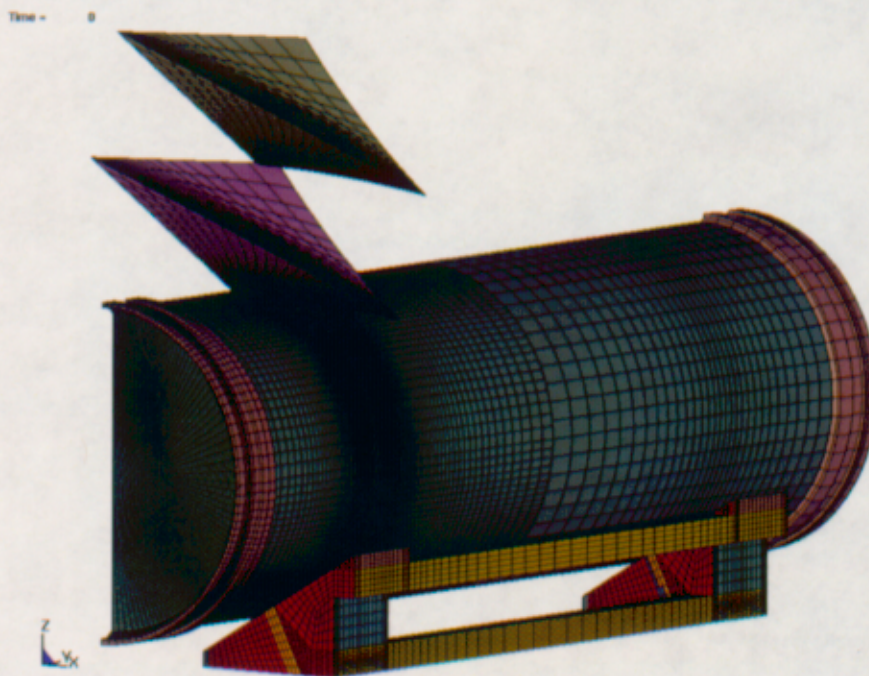
For multiple rock fall on waste packages, the calculation was performed with the following goals: (1) reporting the results in terms of chosen set of stress and strain components, (2) the relative change in these components as a function of the impact distance; and (3) identification of the critical distance. The critical distance is defined as the one for which the maximum effective plastic strain in the first (primary) impact region of the waste package outer corrosion barrier is negligibly affected by the second rock fall. The waste package used for calculation was the Naval SNF Long waste package.

The rock geometries used in this evaluation are depicted schematically in Figure A-1. A typical finite element analysis mesh used in this evaluation is shown in Figure A-2.



Source: BSC 2002 [DIRS 161537], Figure 2.

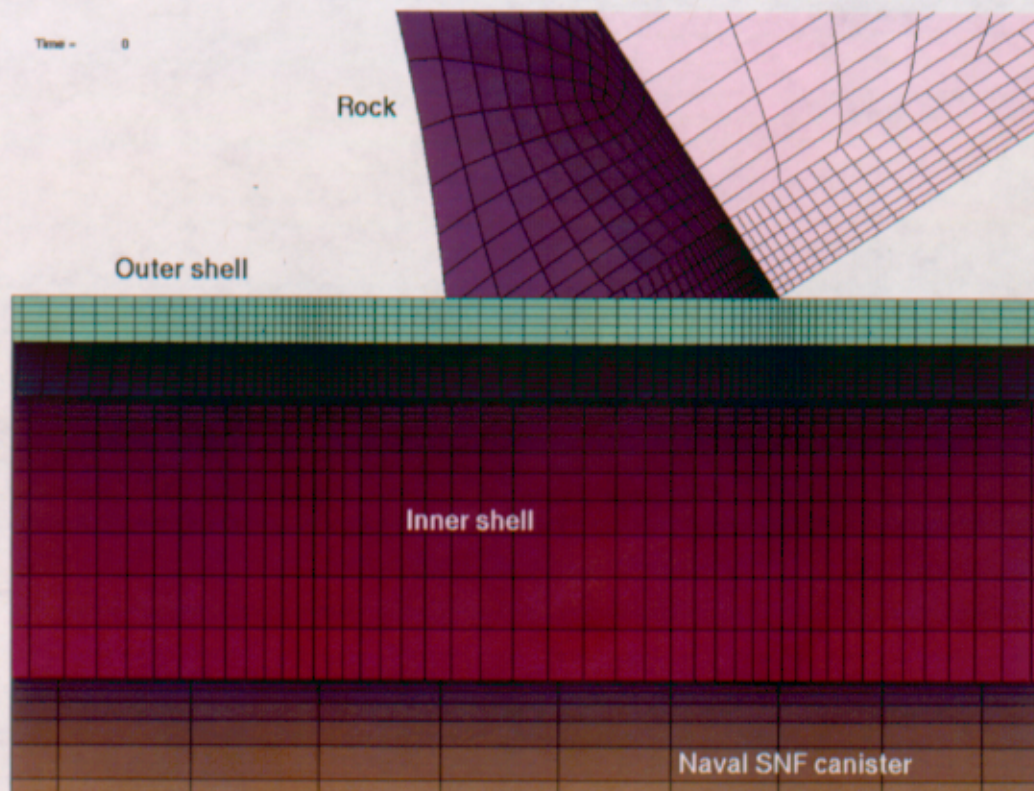
Figure A-1. Simulation Setup for 6-MT Rock Fall with 50 cm Distance Between Impact Locations



Source: BSC 2002 [DIRS 161537], Figure 3.

Figure A-2. Finite Element Representation for 1-MT Rock Fall with 25 cm Distance Between Impact Locations

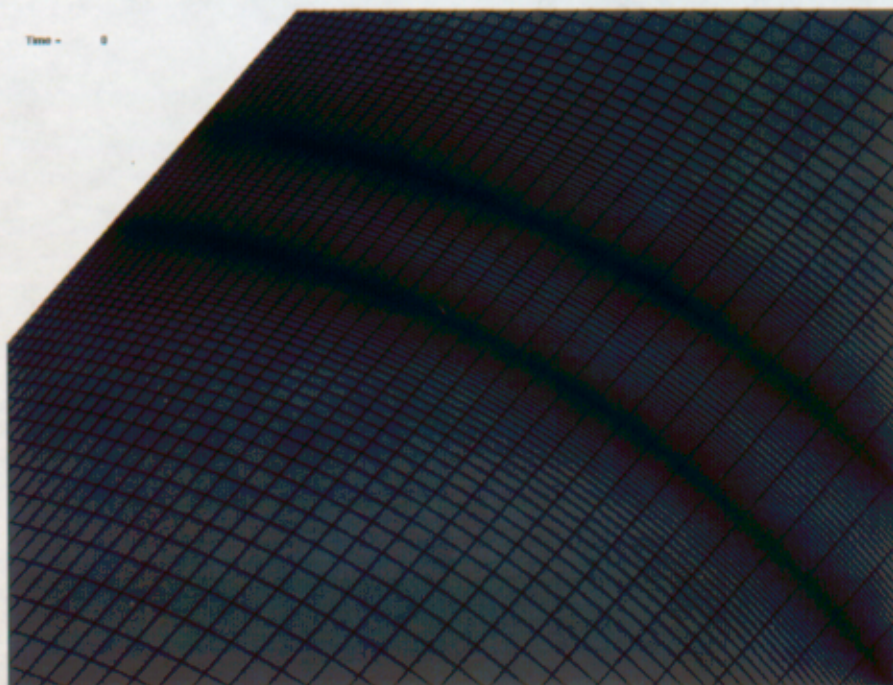
The waste package outer corrosion barrier, trunnion collar sleeve, and the waste package outer corrosion barrier lid are represented by solid (brick) elements. The outer corrosion barrier is the most important waste package component in this calculation. Therefore all stresses and strains are reported exclusively for that part. The finite element representation of the outer corrosion barrier consists of finely-meshed half where rock impacts take place, and the other – coarsely-meshed half. The finite element representation of the outer corrosion barrier in the former has five layers of brick elements across the thickness, while only two layers of brick elements span the thickness of the latter. Furthermore, the finite element mesh is refined in the impact regions in both axial and hoop directions (see Figures A-2 and A-4).



Source: BSC 2002 [DIRS 161537], Figure 4.

Figure A-3. Detail of Finite Element Representation Close to Impact Locations

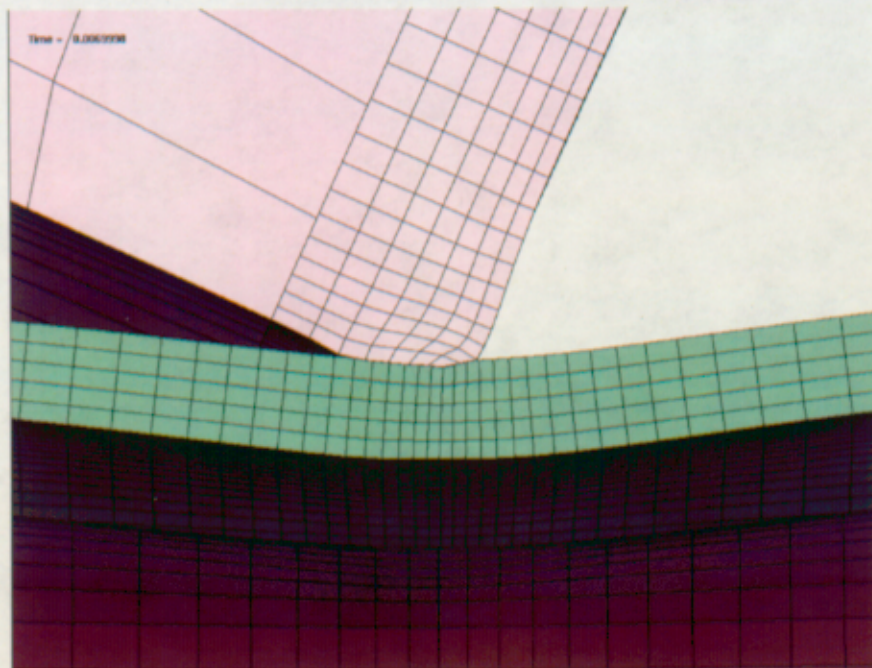
The finite element representation of the waste package uses a loose-fit gap between the outer corrosion barrier and inner vessel with a size of 4.0 mm (0.16 in.) (Plinski 2001 [DIRS 156800], p. 17). Observing the importance of preserving the nominal dimensions of the outer corrosion barrier, the thickness of the inner vessel is reduced from 50 mm to 46 mm (2.0 in. to 1.8 in.). Consequently, the inner vessel is free to move within the outer corrosion barrier, as well as the Naval SNF canister within the inner vessel.



Source: BSC 2002 [DIRS 161537], Figure 5.

Figure A-4. Detail of Finite Element Representation of Outer Corrosion Barrier

The finite element representation of rocks is also divided in two regions: small finely-meshed impact region and large coarsely-meshed remaining part of the rock (see Figure A-2). The continuity of deformation between two rock parts is ensured by tied interface contact. The fine mesh in the impact region is essential for the rock deformation. The fine mesh, coupled with elastic-ideally-plastic constitutive representation ensures more realistic rock deformation in the impact zone compared to the elastic rock, i.e. simulates the localized crushing of the rock and the consequent load distribution over the larger outer corrosion barrier area (see Figure A-5). The rock shapes are based on the rock geometry and dimensions obtained from an older version of the *Drift Degradation Analysis* (BSC 2003 [DIRS 162711], Table IX-2, and pages IX-4 through IX-15); however, this should have a negligible effect on the determination of the critical distance.

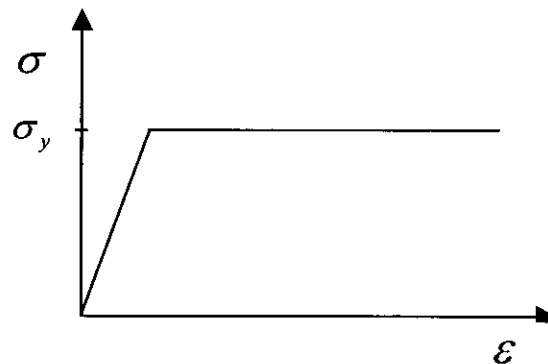


Source: BSC 2002 [DIRS 161537], Figure 6.

Figure A-5. Waste Package and Rock Deformation in Impact Region

In general, the constitutive representation of rock behavior (i.e., stress-strain relation) should address various complexities of rock deformation. In contrast to the elastic-ideally-brittle behavior of rock under tension, the stress-strain behavior of rock under compression can take numerous forms depending on the loading conditions (lateral confinement is a notable example), geometry (i.e., the slenderness ratio of the test specimen), and size. The brittle materials in general, when subjected to compression, exhibit the wide range of nonlinear stress-strain behaviors due to the nucleation, propagation, and coalescence of microcracks under different boundary conditions (Jaeger and Cook 1979 [DIRS 106219], Sections 4.2 through 4.5). Moreover, the compressive strength of brittle materials (including rock) is significantly higher than their tensile strength. Finally, unlike engineering metals, the rocks may exhibit nonlinear behavior even under moderate hydrostatic compression, and significant effect of size on strength (Jaeger and Cook 1979 [DIRS 106219], Sections 4, 6, and 7, for detailed discussion). The variety of constitutive representations is developed to address the most prominent features of behavior of brittle materials (Chen 1982 [DIRS 159153], pp. 362 and 363). These complex constitutive representations require many input parameters. Some of them are not available at present, while the others are not intrinsic properties of material but rather fitting parameters whose estimation requires unavailable data. Thus, a reasonable simplification of rock constitutive behavior is deemed necessary. Fortunately, the stress state in rocks is of no interest in this analysis—the rock deformation is important only as much as it affects the stresses and strains in the waste package outer corrosion barrier, which is the objective of this work. Thus, as a first approximation, the constitutive representation of rock behavior should appropriately capture local crushing of the rock at the point of impact, resulting in distribution of impact energy over the larger contact area. It is, therefore, considered appropriate to conservatively represent the rock behavior as elastic-ideally-plastic—see Figure A-6 (Jaeger and Cook, 1979 [DIRS 106219], Section 9). This representation of nonlinear behavior offers advantages

compared to the elastic representation while remaining conservative under the given loading conditions. The unconfined compressive strength of rock, used as the yield strength in the constitutive representation (see Figure A-6), is one of the parameters in this study that affects the results. A conservative value of the unconfined compressive strength is therefore used to provide a bounding set of results. Noting that the loading conditions of the rock are predominantly compressive, 290 MPa is to be an appropriate upper bound of the rock strength.



Source: BSC 2002 [DIRS 161537], Figure 7.

Figure A-6. Elastic-Ideally-Plastic Constitutive Representation

Table A-1 presents results for the 0.1-MT rock fall for three different impact distances: 50 mm (2.0 in.), 0.25 m (9.8 in.), and 0.50 m (20 in.). The value in parenthesis represents the maximum value of the parameter attained after the first impact in the waste package outer corrosion barrier in the course of drop simulation. The value outside the parenthesis represents a relative value of the corresponding parameter after the second impact. For example, the 0.1-MT rock fall results in the maximum stress intensity after the first impact of 328 MPa for an element at the impact location. The maximum stress intensity at the same element following the second impact is 226 MPa. Therefore, the relative value of maximum stress intensity after the second impact is 0.69 of the maximum stress intensity after the first impact; both values refer to the same location characterized by the maximum value after the first impact. The second impact is characterized by its own maximum value, reached at different location (in the second-impact region). The objective of this calculation is to observe the change at the primary impact location following the secondary impact.

Table A-1. Relative Change of Stresses and Effective Plastic Strain for 0.1-MT Rock Fall for Three Different Impact Distances

Distance of Second Impact (m)	Stress Intensity	Residual Stress Intensity	Residual First Principal Stress	Effective Plastic Strain
0.05	0.69 (328. MPa)	0.86 (164. MPa)	0.88 (167. MPa)	1.19 (5.05%)
0.25	0.61 (327. MPa)	0.97 (161. MPa)	0.95 (163. MPa)	1.03 (5.02%)
0.50	0.57 (328. MPa)	0.93 (175. MPa)	0.95 (166. MPa)	1.00 (5.01%)

Source: BSC 2002 [DIRS 161537], Table 6-2.

The first observation from Table A-1 is that—as expected—the maximum stress intensity at the primary impact region after the second impact does not come near the value reached after the first impact. The maximum stress intensity after the second impact is naturally a function of the distance between impacts, but even for a relatively small distance between two impact locations (such as 0.05 m [2 in]) the maximum stress intensity at the first location is below 70 percent of the one reached after the first impact. This has a consequence on immediate breach of the outer corrosion barrier: if the outer corrosion barrier does not breach after the first rock fall it is highly unlikely it will breach in the primary impact region following the second rock fall. In other words, it is unlikely that maximum stress intensity in the waste package outer corrosion barrier will be pushed over the limit as a consequence of the second rock fall, unless the second rock hits exactly the same location.

As far as the residual stresses are concerned, the trend is similar for both stress intensity and first principal stress. The most notable observation is that the maximum residual stresses in the primary impact region are not amplified (i.e., ratio does not exceed 1.0) by the second rock fall, regardless of the distance between impacts (within the given range). This, of course, does not imply that the second rock fall does not increase the residual stresses anywhere in the primary impact region of the outer corrosion barrier, but it does not do so in the region characterized by the maximum residual stresses. This can be explained by a careful examination of the outer corrosion barrier deformation. After the primary impact, a dent is created in the outer corrosion barrier. The surfaces of this dent are characterized by maximum residual stresses, reflecting the plastic deformation caused by the rock. After the second impact, though, the curvature of this primary dent is flattened since the second rock fall creates, in the primary impact region, bending moments of opposite sign from the one created previously by the first rock fall. Nonetheless, with increase of the impact distance the residual stresses are - as expected - increasingly unaffected by the second impact (the ratio approaches to 1.0).

The most helpful parameter to observe the critical distance between impact locations is the effective plastic strain. This is not surprising since the effective plastic strain is a cumulative strain measure that takes into account whole deformation history. It is a hardening parameter that, similarly to plastic work, provides an excellent measure of the plastic distortion. It can be seen from Table A-1 that the effective plastic strain in the primary impact region increases for 19 percent, following the secondary impact, when the impact distance is 0.05 m (2 in). This increase of the effective plastic strain is much smaller when the impact distance is increased to 0.25 m (9.8 in), and completely disappears at 0.50 m (20 in).

All qualitative observations from 0.1-MT rock fall related to the maximum stress intensity, maximum residual stresses, and maximum effective plastic strain remain valid for the 1-MT rock fall (Table A-2). The absolute values of stresses and strain are, of course, higher for the 1-MT rock fall reflecting the larger impact energy. The most important quantitative observation is that for the distance between impact locations of 0.25 m (9.8 in), the relative increase of the effective plastic strain is still relatively pronounced (7 percent).

Table A-2. Relative Change of Stresses and Effective Plastic Strain for 1-MT Rock Fall for Three Different Impact Distances

Distance of Second Impact (m)	Stress Intensity	Residual Stress Intensity	Residual First Principal Stress	Effective plastic strain
0.05	0.45 (488. MPa)	0.95 (245. MPa)	0.85 (334. MPa)	1.15 (15.4%)
0.25	0.36 (487. MPa)	0.98 (227. MPa)	1.00 (320. MPa)	1.07 (15.6%)
0.50	0.31 (496. MPa)	0.96 (229. MPa)	0.96 (325. MPa)	1.01 (15.4%)

Source: BSC 2002 [DIRS 161537], Table 6-3.

The results provided in Table A-3 indicate that this increase is much less pronounced in the case of 6-MT rock fall. A plausible explanation is that in the case of 0.1-MT rock fall the rock is so small that it really does not affect stress/strain state some distance away. On the other hand, in the case of 6-MT rock fall, the absolute strains are twice as high, which results in a smaller relative change for the similar absolute change in strain. Furthermore, for the 6-MT rock fall case, a smaller part of impact (kinetic) energy is actually transformed into the deformation energy since the center of gravity of the rock is not right above the impact location, than in the two other cases.

Table A-3. Relative Change of Stresses and Effective Plastic Strain for 6-MT Rock Fall for Three Different Impact Distances

Distance of Second Impact (m)	Stress Intensity	Residual Stress Intensity	Residual First Principal Stress	Effective plastic strain
0.05	0.46 (550. MPa)	0.94 (236. MPa)	0.47 (318. MPa)	1.08 (35.7%)
0.25	0.33 (546. MPa)	0.92 (239. MPa)	0.80 (311. MPa)	1.01 (35.1%)
0.50	0.36 (545. MPa)	0.87 (235. MPa)	0.86 (324. MPa)	1.00 (35.8%)

Source: BSC 2002 [DIRS 161537], Table 6-4.

According to the results presented in Tables A-1 through A-3, it is conservative to define the critical distance between impact locations for multiple rock fall on the waste package to be 0.50 m (20 in). The results suggest that for this impact distance the effective plastic strain in the primary impact region is practically unaffected by the second rock fall (the limit being 1 percent of relative change of the effective plastic strain). Additionally, although the residual stresses appear to be slightly affected in the case of 6-MT rock fall, the nature of the change is such that the maximum residual stresses are actually reduced by the second rock fall.

A.2.3 Waste Package Response to Vibratory Ground Motion

Structural response calculations have been performed to determine the damage from impacts between the waste package and emplacement pallet and from impacts between adjacent waste packages under vibratory ground motions (BSC 2004 [DIRS 167083]). The potential for damage from impacts between the waste package and drip shield is included in the analysis, but produces negligible damage because the drip shield is unrestrained.

Damage to the waste package from vibratory ground motion is determined by structural response calculations using a commercially available version of the finite element program LS-DYNA. A set of 15 calculations for the dynamic waste package response was performed for a set of

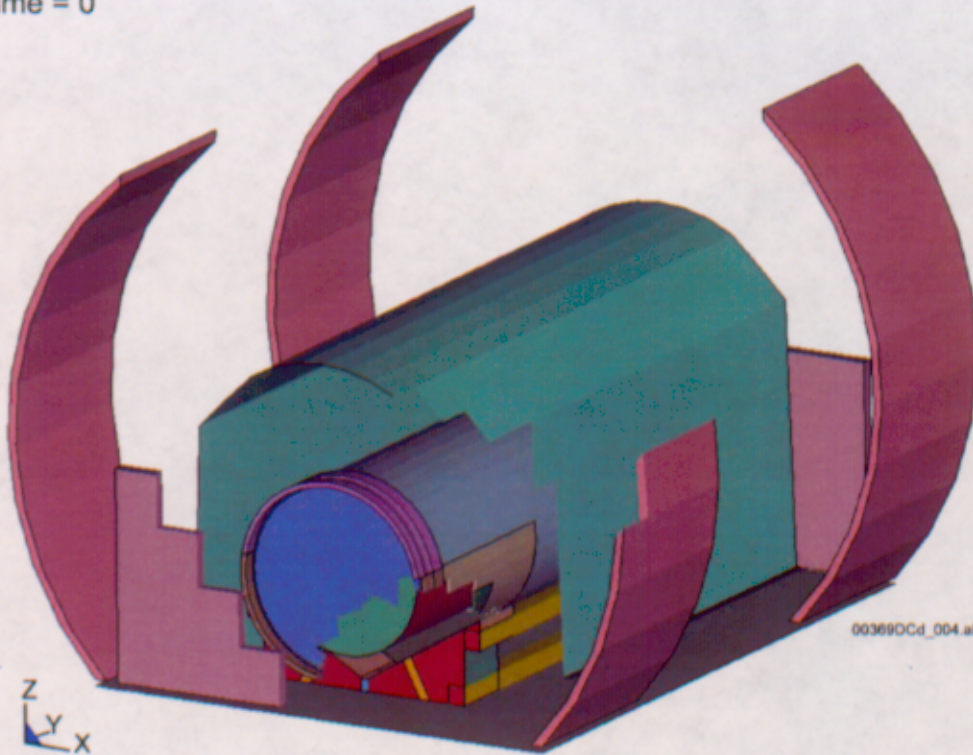
15 ground motions¹ with a peak ground velocity of 2.44 m/s. A similar set of calculations was also performed for a peak ground velocity of 5.35 m/s (BSC 2004 [DIRS 167083]). Figure A-7 shows the cutaway view of the setup for the waste package simulations. The adjacent waste package is conservatively represented in Figure A-7 as an essentially rigid wall anchored to the invert. The rigid wall is used for computational feasibility but results in an overestimate of the damage from end-to-end impacts. Figure A-8 shows the finite-element mesh on the outer corrosion barrier of the waste package. This mesh is fine in regions labeled "C" and "F" because most impacts occur in these regions for the 2.44 m/s peak ground velocity ground motions.

The stochastic (uncertain) input parameters for the 15 simulations are the 15 sets of three-component ground-motion time histories, the metal-to-metal friction coefficient, and the metal-to-rock friction coefficient. A Monte Carlo sampling scheme defines the appropriate combinations of ground-motion time histories and friction coefficients (BSC 2004 [DIRS 169059], Section 6.4) for each peak ground velocity level. The set of 15 ground-motion time histories for these analyses is identical with that for the analyses of rock fall induced by vibratory ground motion.

These calculations incorporate the potential for corrosion to degrade the waste package over the first 20,000 years after repository closure by reducing the thickness of the Alloy 22 (UNS N06022) outer barrier on the waste package by 2 mm (0.08 in.). These calculations evaluate mechanical properties at 150°C to represent the potential degradation in mechanical strength if a seismic hazard occurs during the initial thermal pulse after repository closure. The adequacy of the finite-element mesh and the effect of the use of rigid elements to reduce run times were considered through detailed studies that support the primary calculations (BSC 2004 [DIRS 167083], Attachments IX and VI).

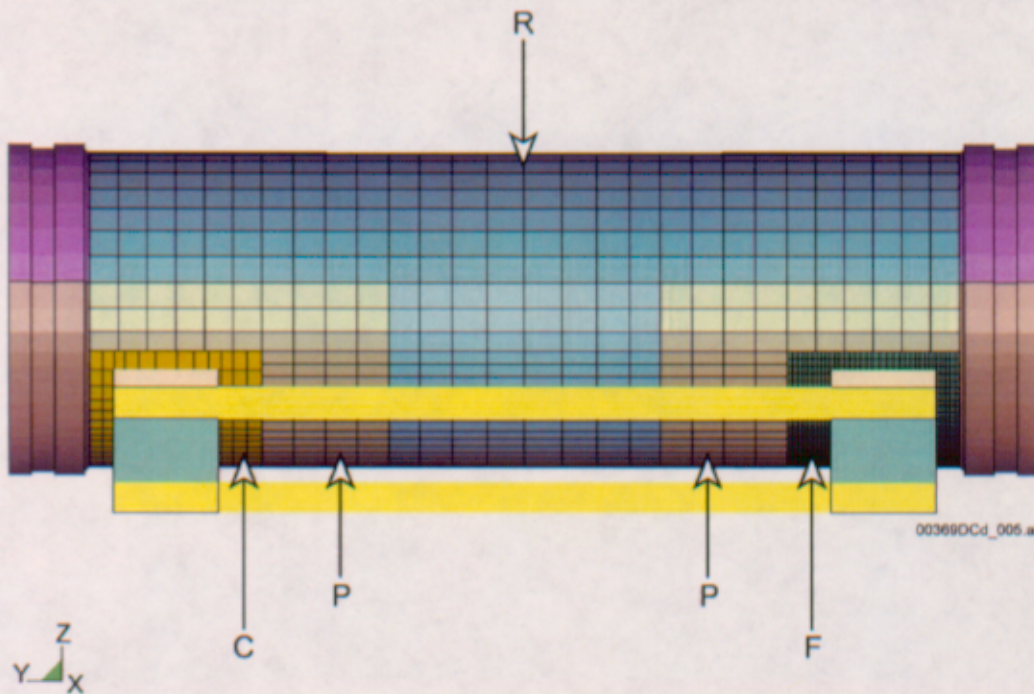
¹ A total of 17 sets of three component ground motions are generated for the emplacement drifts. Structural response calculations are performed with 15 sets of ground motions. The damage abstractions are often based on results from less than 15 calculations because of input errors or numerical difficulties.

Time = 0



Source: BSC 2004 [DIRS 167083], Figure 2.

Figure A-7. Cutaway View of Setup for Waste Package Vibratory Simulations



Source: BSC 2004 [DIRS 167083], Figure 4.

Figure A-8. Finite-Element Mesh for the Outer Corrosion Barrier of the Waste Package

The structural response calculations do not represent the dynamic response of the invert to the ground motion. The invert is represented as an elastic body whose surface responds instantaneously and uniformly with the three-component ground-motion time history. This is a reasonable approach for small-amplitude ground-motions because the invert is compacted under the weight of the waste package and drip shield and because any remaining steel framework in the invert will provide some integrity to the rock mass. For high-amplitude ground motions, the invert ballast is likely to be violently redistributed, allowing the heavy engineered barrier system components to settle on the bottom of the drift, directly in contact with the rock floor. Applying the ground motions in the rock directly to the surface of the invert is again a reasonable approach for this case.

The damage to the waste package is determined by comparing the residual first principal stress on the waste package outer corrosion barrier to the failure criterion for Alloy 22 (UNS N06022). Two residual stress thresholds are used to define the failed area on the outer corrosion barrier of the waste package. The two stress thresholds are 80 and 90 percent (BSC 2004 [DIRS 167083], Section 1) of the yield strength of Alloy 22 (UNS N06022).

The failed elements are then converted into a failed surface area. This conversion conservatively assumes that if a single element on the surface of the waste package fails, then all elements beneath this element also fail. This is a conservative approach because the elements inside the thickness of the waste package may be in a compressive state that will arrest crack propagation from a stress corrosion crack.

The failed areas for 14 realizations at a peak ground velocity of 2.44 m/s are summarized in Table A-4 (BSC 2004 [DIRS 167083], Table 6.1.4-2). The mean damage for the 80 percent residual stress threshold is approximately twice as large as the mean damage for the 90 percent residual stress threshold. The variability in damage (i.e., the ratio of the maximum damage to the minimum damage for a given peak ground velocity value ground motion level), is approximately a factor of 10 for each residual stress threshold. The uncertainty in damage is dominated by the uncertainty in ground motion rather than the uncertainty in the residual stress threshold. These observations are also true for the 14 calculations for a peak ground velocity of 5.35 m/s, corresponding to an exceedance frequency of $1 * 10^{-7}$ per year (BSC 2004 [DIRS 167780], Section 6.5.1).

Table A-4. Failed Area from Vibratory Ground Motion at a Peak Ground Velocity of 2.44 m/s

Realization Number ^a	Ground Motion Number	Failed Area on the Waste Package					
		Waste Package to Emplacement Pallet Interaction (m ² ; % of total outer corrosion barrier area)		Waste Package to Waste Package Interaction (m ² ; % of total outer corrosion barrier area)		Total (m ² ; % of total outer corrosion barrier area)	
		80% Yield Strength	90% Yield Strength	80% Yield Strength	90% Yield Strength	80% Yield Strength	90% Yield Strength
1	7	0.0029; 0.010	0.0014; 0.0050	0.023; 0.082	0.012; 0.043	0.026; 0.092	0.013; 0.046
2	16 ^b	0; 0	0; 0	0.017; 0.060	0.0089; 0.032	0.017; 0.060	0.0089; 0.032
3	4	0.0050; 0.018	0; 0	0.19; 0.67	0.083; 0.29	0.20; 0.71	0.083; 0.29
4	8	0.030; 0.11	0.0064; 0.023	0.12; 0.43	0.061; 0.22	0.15; 0.53	0.067; 0.24
5	11	0.0015; 0.0053	0; 0	0.15; 0.53	0.066; 0.23	0.15; 0.53	0.066; 0.23
6	1	0.025; 0.089	0.0028; 0.0099	0.15; 0.53	0.063; 0.22	0.18; 0.64	0.066; 0.23
7	2	0.017; 0.060	0; 0	0.11; 0.39	0.057; 0.20	0.13; 0.46	0.057; 0.20
9	10	0.0035; 0.012	0; 0	0.12; 0.43	0.062; 0.22	0.12; 0.43	0.062; 0.22
10	9	0; 0	0; 0	0.014; 0.050	0.0071; 0.025	0.014; 0.050	0.0071; 0.025
11	5	0.012; 0.043	0.0037; 0.013	0.074; 0.26	0.032; 0.11	0.086; 0.30	0.036; 0.13
12	6	0.0039; 0.014	0; 0	0.073; 0.26	0.036; 0.13	0.077; 0.27	0.036; 0.13
13	12	0; 0	0; 0	0.032; 0.11	0.016; 0.057	0.032; 0.11	0.016; 0.057
14	14	0.010; 0.035	0.0043; 0.015	0.0056; 0.020	0.0029; 0.010	0.016; 0.057	0.0072; 0.026
15	3	0.0078; 0.028	0.0015; 0.0053	0.020; 0.071	0.010; 0.035	0.028; 0.099	0.012; 0.043
				Mean Value ^c		0.310%	0.136%
				Standard Deviation ^c		0.237%	0.097%
				Minimum Value ^c		0.050%	0.025%
				Maximum Value ^c		0.710%	0.136%

NOTE: ^a Only 14 realizations are presented in this table. Results for realization 8 are not presented because of an error in the input file for this calculation.

^b Calculations are performed with 15 ground motions numbered 1, 2, 3, ..., 14, and 16. Time history 15 is not used because it has an anomalous response spectrum.

^c Mean, standard deviation, minimum and maximum failed areas are calculated in *Seismic Consequence Abstraction* (BSC 2004 [DIRS 167780], Attachment II)

Source: BSC 2004 [DIRS 167083], Table 6.1.4-2.

The results in Table A-4 also demonstrate that the total failed area is dominated by the contribution from end-to-end impacts of adjacent waste packages. The failed area from waste package-to-emplacement pallet impacts is much smaller than the damage due to the end-to-end impacts of adjacent waste packages, with the exception of realization number 14. The damage from end-to-end impacts is the dominant contribution because the adjacent waste package is conservatively represented as an essentially rigid wall anchored to the invert. The rigid wall is used for computational simplicity, but results in overestimating the damage from end-to-end impacts. This same observation is true for the failed areas from the 5.35 m/s peak ground velocity level.

The results for peak ground velocities of 2.44 m/s and 5.35 m/s have been supplemented with three additional simulations for a peak ground velocity value of 1.067 m/s, corresponding to the 1×10^{-5} per year annual exceedance frequency. Exact ground motions are not available for a peak ground velocity of 1.067 m/s, so approximate ground motions were created by scaling the three acceleration components for selected ground motions with a peak ground velocity of 2.44 m/s by the ratio of the peak ground velocity values, or by $(1.067/2.44 =) 0.4066$. This procedure is not exact, but it provides a reasonable approach to extend the peak ground velocity range of this damage abstraction. The three selected ground motions have the highest intensity (energy) among the set of 15 ground motions with 2.44 m/s peak ground velocity. The damage results for these three scaled ground motions are documented in *Structural Calculations of Waste Package Exposed to Vibratory Ground Motion* (BSC 2004 [DIRS 167083], Table XI-2).

Additional details on how these results are used in the seismic damage abstraction may be found in Technical Basis Document 14, Seismic Events (Anderson 2003 [DIRS 166833])

APPENDIX B

B.1 21-PWR Waste Package

B.1.1 Design Basis Source

Tables B-1 through B-5 present surface dose rates averaged over segments of the radial and axial surfaces of the 21-PWR waste package without any concrete structure surrounding it (see Figure B-1 for segment and surface locations). Tables B-6 through B-10 present surface dose rates averaged over segments of the radial and axial surfaces of the 21-PWR waste package with the 30.48-cm (12-in) thick concrete structure located 3 m (9.8 ft) away. The neutron intensity peaking factor is 2.24 for both sets of calculations. It can be seen that by including the concrete structure outside the waste package, the dose rates increase by approximately 3 to 10 percent on the waste package external surfaces, depending on location (the closer to the concrete wall, the higher the increase in dose rates). This increase in dose rates is due to scattering radiation from the concrete structure. The dose rates on the inner surface of the waste package are not affected by the concrete structure. Further, the tables show that the contributions from secondary gamma rays to the total dose rates are very small, as the primary gamma source is the predominant contributor for an unshielded waste package. Consequently, these will not be included in future sections of this report. However, secondary gamma contributions may become important in a shielded case (BSC 2004 [DIRS 169593]).

Table B-1. Dose Rates on Inner Surface of Inner Vessel: Design Basis PWR SNF (no Concrete)

Axial Location (Surface 111)	Gamma		Neutron		Sec. Gamma		Total	
	Dose Rate (rem/h)	Relative Error						
Segment 1	6.54E+03	0.0014	1.49E+01	0.0011	4.72E-02	0.0031	6.55E+03	0.0014
Segment 2	1.31E+04	0.0013	2.08E+01	0.0012	6.35E-02	0.0035	1.32E+04	0.0013
Segment 3	1.60E+04	0.0015	3.14E+01	0.0009	8.85E-02	0.0025	1.60E+04	0.0015
Segment 4	2.15E+04	0.0015	6.79E+01	0.0005	2.12E-01	0.0011	2.15E+04	0.0015
Segment 5	2.69E+04	0.0012	8.67E+01	0.0004	2.80E-01	0.0010	2.70E+04	0.0012
Segment 6	2.69E+04	0.0011	8.90E+01	0.0004	2.91E-01	0.0009	2.70E+04	0.0011
Segment 7	2.69E+04	0.0012	8.71E+01	0.0004	2.82E-01	0.0010	2.70E+04	0.0012
Segment 8	2.17E+04	0.0015	6.99E+01	0.0005	2.22E-01	0.0011	2.18E+04	0.0014
Segment 9	2.02E+04	0.0023	3.60E+01	0.0013	1.16E-01	0.0036	2.02E+04	0.0023

Source: BSC 2004 [DIRS 169593], Table 6.1-1.

Table B-2. Dose Rates on Waste Package Outer Radial Surface: Design Basis PWR SNF (no Concrete)

Axial Location (Surface 4)	Gamma		Neutron		Sec. Gamma		Total	
	Dose Rate (rem/h)	Relative Error						
Segment 1	2.20E+02	0.0016	3.07E+00	0.0012	1.21E-02	0.0038	2.23E+02	0.0016
Segment 2	4.64E+02	0.0017	4.46E+00	0.0013	1.59E-02	0.0045	4.68E+02	0.0017
Segment 3	5.14E+02	0.0023	6.76E+00	0.0010	2.23E-02	0.0031	5.21E+02	0.0023
Segment 4	4.58E+02	0.0033	1.45E+01	0.0005	4.70E-02	0.0014	4.72E+02	0.0032
Segment 5	5.65E+02	0.0028	1.84E+01	0.0004	6.33E-02	0.0012	5.83E+02	0.0027
Segment 6	5.66E+02	0.0028	1.89E+01	0.0004	6.62E-02	0.0012	5.85E+02	0.0027
Segment 7	5.66E+02	0.0028	1.85E+01	0.0004	6.38E-02	0.0012	5.85E+02	0.0027
Segment 8	4.69E+02	0.0034	1.49E+01	0.0005	4.94E-02	0.0014	4.84E+02	0.0033
Segment 9	5.91E+02	0.0039	7.68E+00	0.0014	2.63E-02	0.0048	5.99E+02	0.0038

Source: BSC 2004 [DIRS 169593], Table 6.1-2.

Table B-3. Dose Rates on Radial Surface 1 m from Waste Package: Design Basis PWR SNF (no Concrete)

Axial Location (Surface 50)	Gamma		Neutron		Sec. Gamma		Total	
	Dose Rate (rem/h)	Relative Error						
Segment 1	9.08E+01	0.0027	1.69E+00	0.0008	5.60E-03	0.0026	9.25E+01	0.0026
Segment 2	1.17E+02	0.0035	2.25E+00	0.0009	7.34E-03	0.0030	1.19E+02	0.0034
Segment 3	1.39E+02	0.0030	2.81E+00	0.0007	9.11E-03	0.0022	1.42E+02	0.0030
Segment 4	1.61E+02	0.0025	3.98E+00	0.0004	1.28E-02	0.0012	1.65E+02	0.0025
Segment 5	2.09E+02	0.0022	5.15E+00	0.0003	1.67E-02	0.0010	2.14E+02	0.0022
Segment 6	2.11E+02	0.0022	5.50E+00	0.0003	1.80E-02	0.0010	2.17E+02	0.0021
Segment 7	2.05E+02	0.0022	5.11E+00	0.0003	1.67E-02	0.0010	2.10E+02	0.0022
Segment 8	1.42E+02	0.0028	3.83E+00	0.0004	1.24E-02	0.0012	1.46E+02	0.0028
Segment 9	1.08E+02	0.0067	2.77E+00	0.0011	8.94E-03	0.0038	1.10E+02	0.0065

Source: BSC 2004 [DIRS 169593], Table 6.1-3.

Table B-4. Dose Rates on Radial Surface 2 m from Waste Package: Design Basis PWR SNF (no Concrete)

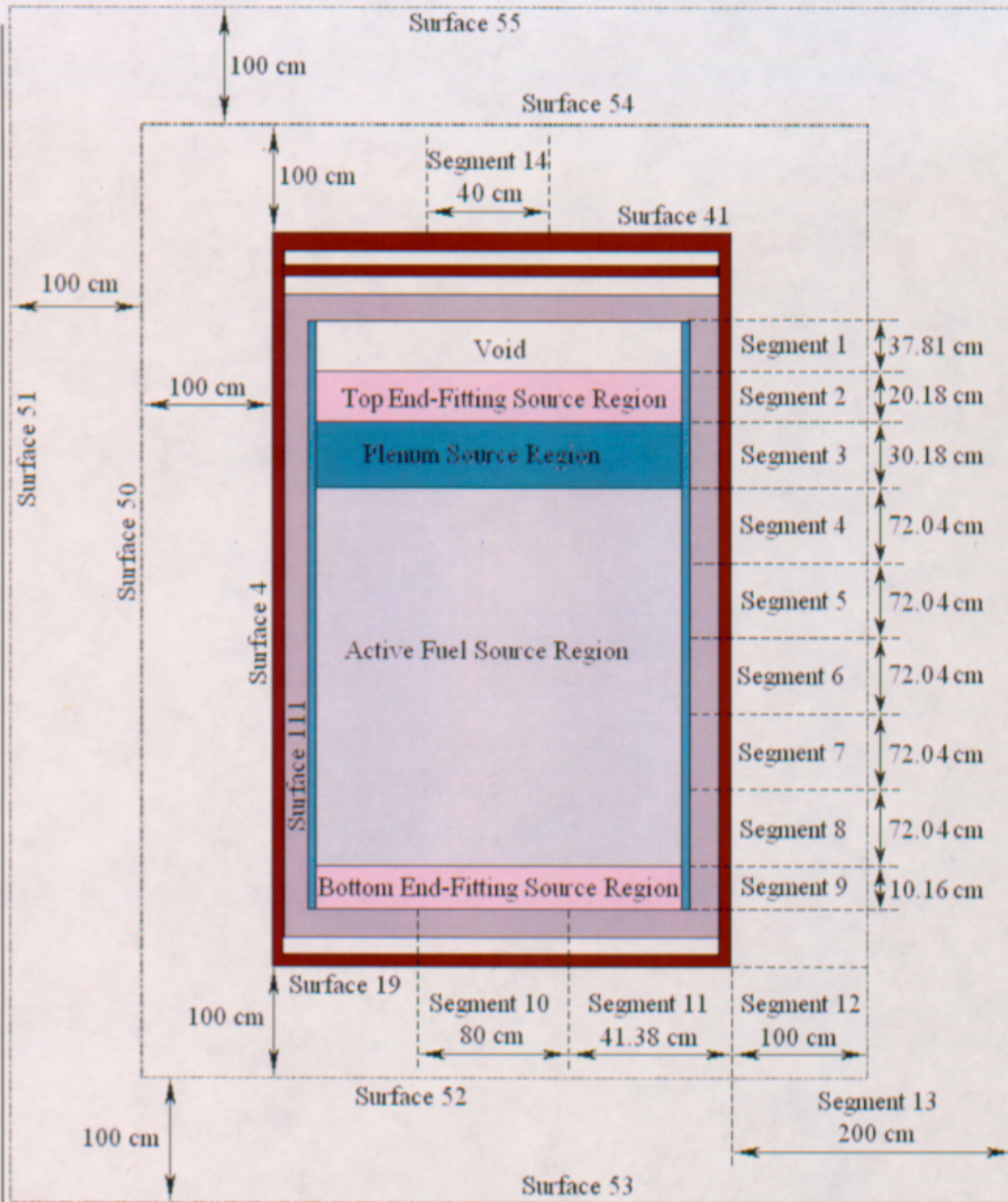
Axial Location (Surface 51)	Gamma		Neutron		Sec. Gamma		Total	
	Dose Rate (rem/h)	Relative Error						
Segment 1	5.56E+01	0.0033	1.27E+00	0.0007	4.11E-03	0.0023	5.68E+01	0.0032
Segment 2	6.54E+01	0.0043	1.50E+00	0.0008	4.82E-03	0.0028	6.69E+01	0.0042
Segment 3	7.39E+01	0.0035	1.71E+00	0.0006	5.52E-03	0.0022	7.57E+01	0.0034
Segment 4	8.74E+01	0.0054	2.12E+00	0.0004	6.83E-03	0.0013	8.95E+01	0.0053
Segment 5	1.19E+02	0.0021	2.57E+00	0.0003	8.24E-03	0.0011	1.22E+02	0.0021
Segment 6	1.22E+02	0.0021	2.72E+00	0.0003	8.75E-03	0.0011	1.24E+02	0.0020
Segment 7	1.14E+02	0.0022	2.53E+00	0.0004	8.14E-03	0.0012	1.16E+02	0.0021
Segment 8	7.57E+01	0.0029	2.04E+00	0.0004	6.58E-03	0.0013	7.78E+01	0.0028
Segment 9	6.11E+01	0.0072	1.69E+00	0.0011	5.46E-03	0.0037	6.28E+01	0.0070

Source: BSC 2004 [DIRS 169593], Table 6.1-4.

Table B-5. Dose Rates on Segments of Axial Surfaces: Design Basis PWR SNF (no Concrete)

Axial Location	Gamma		Neutron		Sec. Gamma		Total	
	Dose Rate (rem/h)	Relative Error						
Top of Waste Package (Surface 41)								
Segment 10	3.59E+02	0.0029	4.40E+00	0.0017	1.70E-02	0.0053	3.64E+02	0.0029
Segment 11	2.18E+02	0.0021	2.97E+00	0.0012	1.18E-02	0.0037	2.21E+02	0.0021
Segment 12	6.40E+01	0.0019	1.08E+00	0.0010	3.79E-03	0.0033	6.51E+01	0.0019
1 m from Waste Package top (Surface 54)								
Segment 11	9.83E+01	0.0022	8.60E-01	0.0014	3.04E-03	0.0045	9.92E+01	0.0022
Segment 12	3.27E+01	0.0019	5.09E-01	0.0010	1.84E-03	0.0030	3.32E+01	0.0019
2 m from Waste Package top (Surface 55)								
Segment 11	4.62E+01	0.0030	3.60E-01	0.0022	1.17E-03	0.0070	4.65E+01	0.0030
Segment 13	1.34E+01	0.0016	3.01E-01	0.0006	1.06E-03	0.0017	1.37E+01	0.0016
Bottom of Waste Package (Surface 19)								
Segment 14	1.21E+03	0.0067	1.49E+01	0.0024	4.99E-02	0.0079	1.23E+03	0.0067
Segment 10	1.20E+03	0.0038	1.37E+01	0.0015	4.63E-02	0.0048	1.21E+03	0.0038
Segment 11	8.15E+02	0.0023	8.41E+00	0.0010	2.92E-02	0.0030	8.24E+02	0.0022
Segment 12	1.04E+02	0.0037	2.57E+00	0.0007	8.35E-03	0.0023	1.06E+02	0.0036
1 m from Waste Package bottom (Surface 52)								
Segment 11	3.53E+02	0.0024	2.46E+00	0.0010	7.80E-03	0.0032	3.56E+02	0.0024
Segment 12	1.04E+02	0.0021	1.27E+00	0.0008	4.18E-03	0.0023	1.05E+02	0.0021
2 m from Waste Package bottom (Surface 53)								
Segment 11	1.57E+02	0.0033	9.80E-01	0.0014	2.96E-03	0.0049	1.58E+02	0.0033
Segment 13	3.52E+01	0.0018	5.67E-01	0.0005	1.89E-03	0.0014	3.58E+01	0.0018

Source: BSC 2004 [DIRS 169593], Table 6.1-5.



Source: BSC 2004 [DIRS 169593], Figure 5.2-2.

Figure B-1. Surface Segments Used for Dose Rate Calculations

Table B-6. Dose Rates on Inner Surface of Inner Vessel: Design Basis PWR SNF (Concrete)

Axial Location (Surface 111)	Gamma		Neutron		Sec. Gamma		Total	
	Dose Rate (rem/h)	Relative Error						
Segment 1	6.53E+03	0.0012	1.56E+01	0.0013	6.66E-02	0.0040	6.55E+03	0.0012
Segment 2	1.31E+04	0.0012	2.16E+01	0.0014	8.22E-02	0.0045	1.32E+04	0.0012
Segment 3	1.60E+04	0.0014	3.23E+01	0.0011	1.07E-01	0.0034	1.60E+04	0.0014
Segment 4	2.15E+04	0.0012	6.89E+01	0.0006	2.30E-01	0.0014	2.15E+04	0.0012
Segment 5	2.69E+04	0.0010	8.78E+01	0.0005	2.99E-01	0.0012	2.70E+04	0.0010
Segment 6	2.69E+04	0.0010	9.01E+01	0.0005	3.10E-01	0.0012	2.70E+04	0.0010
Segment 7	2.69E+04	0.0010	8.82E+01	0.0005	3.00E-01	0.0012	2.70E+04	0.0010
Segment 8	2.17E+04	0.0012	7.10E+01	0.0006	2.41E-01	0.0013	2.18E+04	0.0012
Segment 9	2.02E+04	0.0021	3.70E+01	0.0015	1.37E-01	0.0044	2.02E+04	0.0021

Source: BSC 2004 [DIRS 169593], Table 6.1-6.

Table B-7. Dose Rates on Waste Package Outer Radial Surface: Design Basis PWR SNF (Concrete)

Axial Location (Surface 4)	Gamma		Neutron		Sec. Gamma		Total	
	Dose Rate (rem/h)	Relative Error						
Segment 1	2.26E+02	0.0015	4.32E+00	0.0014	1.02E-01	0.0087	2.30E+02	0.0015
Segment 2	4.71E+02	0.0016	5.75E+00	0.0015	1.08E-01	0.0111	4.77E+02	0.0016
Segment 3	5.20E+02	0.0021	8.11E+00	0.0011	1.15E-01	0.0088	5.28E+02	0.0021
Segment 4	4.66E+02	0.0030	1.59E+01	0.0006	1.42E-01	0.0047	4.82E+02	0.0029
Segment 5	5.73E+02	0.0025	2.00E+01	0.0005	1.60E-01	0.0042	5.94E+02	0.0024
Segment 6	5.75E+02	0.0025	2.04E+01	0.0005	1.64E-01	0.0041	5.95E+02	0.0024
Segment 7	5.73E+02	0.0025	2.00E+01	0.0005	1.60E-01	0.0042	5.94E+02	0.0024
Segment 8	4.76E+02	0.0029	1.64E+01	0.0006	1.46E-01	0.0046	4.92E+02	0.0028
Segment 9	5.98E+02	0.0035	9.11E+00	0.0016	1.25E-01	0.0133	6.07E+02	0.0034

Source: BSC 2004 [DIRS 169593], Table 6.1-7.

Table B-8. Dose Rates on Radial Surface 1 m from Waste Package: Design Basis PWR SNF (Concrete)

Axial Location (Surface 50)	Gamma		Neutron		Sec. Gamma		Total	
	Dose Rate (rem/h)	Relative Error						
Segment 1	1.01E+02	0.0025	3.07E+00	0.0010	5.21E-02	0.0037	1.04E+02	0.0025
Segment 2	1.28E+02	0.0032	3.68E+00	0.0012	5.56E-02	0.0045	1.31E+02	0.0031
Segment 3	1.50E+02	0.0027	4.29E+00	0.0009	5.85E-02	0.0036	1.55E+02	0.0026
Segment 4	1.74E+02	0.0022	5.54E+00	0.0005	6.40E-02	0.0025	1.79E+02	0.0022
Segment 5	2.24E+02	0.0019	6.79E+00	0.0005	6.95E-02	0.0024	2.31E+02	0.0018
Segment 6	2.26E+02	0.0020	7.18E+00	0.0005	7.13E-02	0.0023	2.33E+02	0.0019
Segment 7	2.20E+02	0.0019	6.77E+00	0.0005	6.94E-02	0.0024	2.27E+02	0.0019
Segment 8	1.54E+02	0.0025	5.42E+00	0.0006	6.31E-02	0.0026	1.59E+02	0.0024
Segment 9	1.20E+02	0.0058	4.30E+00	0.0015	5.81E-02	0.0060	1.24E+02	0.0056

Source: BSC 2004 [DIRS 169593], Table 6.1-8.

Table B-9. Dose Rates on Radial Surface 2 m from Waste Package: Design Basis PWR SNF (Concrete)

Axial Location (Surface 51)	Gamma		Neutron		Sec. Gamma		Total	
	Dose Rate (rem/h)	Relative Error						
Segment 1	6.75E+01	0.0031	2.73E+00	0.0008	4.90E-02	0.0032	7.03E+01	0.0030
Segment 2	7.84E+01	0.0039	3.02E+00	0.0010	5.08E-02	0.0040	8.15E+01	0.0038
Segment 3	8.68E+01	0.0031	3.29E+00	0.0008	5.24E-02	0.0033	9.02E+01	0.0030
Segment 4	1.01E+02	0.0022	3.82E+00	0.0005	5.54E-02	0.0024	1.05E+02	0.0022
Segment 5	1.37E+02	0.0018	4.37E+00	0.0005	5.85E-02	0.0023	1.41E+02	0.0017
Segment 6	1.40E+02	0.0019	4.57E+00	0.0005	5.93E-02	0.0023	1.45E+02	0.0018
Segment 7	1.32E+02	0.0020	4.34E+00	0.0005	5.84E-02	0.0023	1.36E+02	0.0019
Segment 8	8.95E+01	0.0025	3.75E+00	0.0005	5.53E-02	0.0024	9.33E+01	0.0024
Segment 9	7.41E+01	0.0061	3.32E+00	0.0013	5.32E-02	0.0053	7.75E+01	0.0058

Source: BSC 2004 [DIRS 169593], Table 6.1-9.

Table B-10. Dose Rates on Segments of Axial Surfaces: Design Basis PWR SNF (Concrete)

Axial Location	Gamma		Neutron		Sec. Gamma		Total	
	Dose Rate (rem/h)	Relative Error						
Top of Waste Package (Surface 41)								
Segment 10	3.63E+02	0.0027	5.16E+00	0.0021	9.47E-02	0.0151	3.68E+02	0.0026
Segment 11	2.21E+02	0.0020	3.77E+00	0.0015	9.21E-02	0.0089	2.25E+02	0.0020
Segment 12	7.34E+01	0.0019	2.36E+00	0.0009	5.14E-02	0.0032	7.58E+01	0.0019
1 m from Waste Package top (Surface 54)								
Segment 11	1.07E+02	0.0023	1.97E+00	0.0017	4.41E-02	0.0052	1.09E+02	0.0022
Segment 12	4.15E+01	0.0023	1.65E+00	0.0011	4.31E-02	0.0030	4.32E+01	0.0022
2 m from Waste Package top (Surface 55)								
Segment 11	5.49E+01	0.0032	1.43E+00	0.0020	3.97E-02	0.0055	5.63E+01	0.0031
Segment 13	2.13E+01	0.0018	1.32E+00	0.0006	3.98E-02	0.0022	2.26E+01	0.0017
Bottom of Waste Package (Surface 19)								
Segment 14	1.22E+03	0.0060	1.59E+01	0.0028	1.34E-01	0.0268	1.23E+03	0.0059
Segment 10	1.20E+03	0.0034	1.48E+01	0.0017	1.34E-01	0.0153	1.22E+03	0.0034
Segment 11	8.20E+02	0.0020	9.48E+00	0.0012	1.21E-01	0.0087	8.30E+02	0.0020
Segment 12	1.15E+02	0.0031	4.03E+00	0.0008	5.93E-02	0.003	1.19E+02	0.0030
1 m from Waste Package bottom (Surface 52)								
Segment 11	3.65E+02	0.0022	3.83E+00	0.0012	5.31E-02	0.0047	3.69E+02	0.0022
Segment 12	1.16E+02	0.0019	2.63E+00	0.0008	4.96E-02	0.0029	1.18E+02	0.0019
2 m from Waste Package bottom (Surface 53)								
Segment 11	1.71E+02	0.0030	2.31E+00	0.0014	4.56E-02	0.0051	1.73E+02	0.0029
Segment 13	4.60E+01	0.0016	1.82E+00	0.0005	4.47E-02	0.0021	4.79E+01	0.0015

Source: BSC 2004 [DIRS 169593], Table 6.1-10.

B.1.2 Average Source

Tables B-11 through B-15 present surface dose rates averaged over segments of the radial and axial surfaces of the 21-PWR waste package with the 30.48-cm (12-in) thick concrete structure located 3 m (9.8 ft) away. The neutron intensity peaking factor used in the calculation is 2.38 (BSC 2004 [DIRS 169593], Section 5.2.1).

Table B-11. Dose Rates on Inner Surface of Inner Vessel: Average PWR SNF (Concrete)

Axial Location (Surface 111)	Gamma		Neutron		Total	
	Dose Rate (rem/h)	Relative Error	Dose Rate (rem/h)	Relative Error	Dose Rate (rem/h)	Relative Error
Segment 1	9.32E+02	0.0054	4.01E+00	0.0011	9.36E+02	0.0053
Segment 2	1.94E+03	0.0054	5.53E+00	0.0012	1.94E+03	0.0054
Segment 3	3.37E+03	0.0045	8.26E+00	0.0009	3.38E+03	0.0045
Segment 4	8.51E+03	0.0022	1.76E+01	0.0005	8.53E+03	0.0022
Segment 5	1.08E+04	0.0018	2.24E+01	0.0004	1.08E+04	0.0018
Segment 6	1.08E+04	0.0018	2.30E+01	0.0004	1.08E+04	0.0018
Segment 7	8.68E+03	0.0022	2.25E+01	0.0004	8.71E+03	0.0022
Segment 8	8.54E+03	0.0022	1.82E+01	0.0005	8.56E+03	0.0022
Segment 9	4.14E+03	0.0069	9.45E+00	0.0013	4.15E+03	0.0069

Source: BSC 2004 [DIRS 169593], Table 6.2-1.

Table B-12. Dose Rates on Waste Package Outer Radial Surface: Average PWR SNF (Concrete)

Axial Location (surface 4)	Gamma		Neutron		Total	
	Dose Rate (rem/h)	Relative Error	Dose Rate (rem/h)	Relative Error	Dose Rate (rem/h)	Relative Error
Segment 1	2.85E+01	0.0064	1.11E+00	0.0012	2.96E+01	0.0062
Segment 2	5.89E+01	0.0061	1.47E+00	0.0013	6.03E+01	0.0059
Segment 3	8.25E+01	0.0075	2.07E+00	0.0009	8.46E+01	0.0074
Segment 4	1.51E+02	0.0055	4.08E+00	0.0005	1.56E+02	0.0054
Segment 5	1.93E+02	0.0044	5.10E+00	0.0004	1.98E+02	0.0043
Segment 6	1.94E+02	0.0044	5.22E+00	0.0004	1.99E+02	0.0043
Segment 7	1.93E+02	0.0044	5.12E+00	0.0004	1.98E+02	0.0043
Segment 8	1.53E+02	0.0055	4.19E+00	0.0005	1.57E+02	0.0053
Segment 9	9.73E+01	0.0122	2.32E+00	0.0014	9.96E+01	0.0120

Source: BSC 2004 [DIRS 169593], Table 6.2-2.

Table B-13. Dose Rates on Radial Surface 1 m from Waste Package: Average PWR SNF (Concrete)

Axial Location (surface 50)	Gamma		Neutron		Total	
	Dose Rate (rem/h)	Relative Error	Dose Rate (rem/h)	Relative Error	Dose Rate (rem/h)	Relative Error
Segment 1	1.99E+01	0.0079	7.85E-01	0.0009	2.07E+01	0.0076
Segment 2	2.73E+01	0.0090	9.41E-01	0.0010	2.82E+01	0.0087
Segment 3	3.58E+01	0.0072	1.10E+00	0.0008	3.69E+01	0.0070
Segment 4	5.02E+01	0.0047	1.42E+00	0.0005	5.16E+01	0.0045
Segment 5	7.30E+01	0.0035	1.74E+00	0.0004	7.47E+01	0.0035
Segment 6	7.51E+01	0.0035	1.84E+00	0.0004	7.70E+01	0.0034
Segment 7	7.28E+01	0.0035	1.73E+00	0.0004	7.45E+01	0.0034
Segment 8	4.76E+01	0.0049	1.38E+00	0.0005	4.90E+01	0.0047
Segment 9	3.42E+01	0.0122	1.10E+00	0.0012	3.53E+01	0.0118

Source: BSC 2004 [DIRS 169593], Table 6.2-3.

Table B-14. Dose Rates on Radial Surface 2 m from Waste Package: Average PWR SNF (Concrete)

Axial Location (surface 51)	Gamma		Neutron		Total	
	Dose Rate (rem/h)	Relative Error	Dose Rate (rem/h)	Relative Error	Dose Rate (rem/h)	Relative Error
Segment 1	1.67E+01	0.0079	6.97E-01	0.0007	1.74E+01	0.0076
Segment 2	2.01E+01	0.0090	7.73E-01	0.0009	2.09E+01	0.0087
Segment 3	2.34E+01	0.0073	8.42E-01	0.0007	2.42E+01	0.0071
Segment 4	2.94E+01	0.0047	9.76E-01	0.0005	3.04E+01	0.0045
Segment 5	4.35E+01	0.0036	1.12E+00	0.0004	4.46E+01	0.0035
Segment 6	4.56E+01	0.0035	1.17E+00	0.0004	4.68E+01	0.0034
Segment 7	4.28E+01	0.0036	1.11E+00	0.0004	4.39E+01	0.0035
Segment 8	2.79E+01	0.0049	9.58E-01	0.0005	2.89E+01	0.0047
Segment 9	2.27E+01	0.0127	8.48E-01	0.0011	2.35E+01	0.0122

Source: BSC 2004 [DIRS 169593], Table 6.2-4.

Table B-15. Dose Rates on Segments of Axial Surfaces: Average PWR SNF (Concrete)

Axial Location	Gamma		Neutron		Total	
	Dose Rate (rem/h)	Relative Error	Dose Rate (rem/h)	Relative Error	Dose Rate (rem/h)	Relative Error
Top of Waste Package (Surface 41)						
Segment 10	5.10E+01	0.0104	1.32E+00	0.0018	5.23E+01	0.0101
Segment 11	3.09E+01	0.0079	9.66E-01	0.0012	3.19E+01	0.0076
Segment 12	1.22E+01	0.0069	6.02E-01	0.0008	1.28E+01	0.0065
1 m from Waste Package top (Surface 54)						
Segment 11	1.64E+01	0.0088	5.06E-01	0.0015	1.69E+01	0.0085
Segment 12	7.28E+00	0.0084	4.21E-01	0.0009	7.70E+00	0.0079
2 m from Waste Package top (Surface 55)						
Segment 11	9.00E+00	0.0121	3.65E-01	0.0017	9.37E+00	0.0116
Segment 13	4.42E+00	0.0054	3.37E-01	0.0005	4.76E+00	0.0051
Bottom of Waste Package (Surface 19)						
Segment 14	2.13E+02	0.0195	4.07E+00	0.0024	2.17E+02	0.0191
Segment 10	2.09E+02	0.0115	3.78E+00	0.0015	2.13E+02	0.0113
Segment 11	1.43E+02	0.0068	2.42E+00	0.0010	1.45E+02	0.0067
Segment 12	2.71E+01	0.0077	1.03E+00	0.0006	2.82E+01	0.0074
1 m from Waste Package bottom (Surface 52)						
Segment 11	6.70E+01	0.0070	9.76E-01	0.0010	6.70E+01	0.0069
Segment 12	2.25E+01	0.0061	6.73E-01	0.0007	2.25E+01	0.0059
2 m from Waste Package bottom (Surface 53)						
Segment 11	3.18E+01	0.0092	5.90E-01	0.0012	3.24E+01	0.0090
Segment 13	9.75E+00	0.0046	4.64E-01	0.0004	1.02E+01	0.0044

Source: BSC 2004 [DIRS 169593], Table 6.2-5.

B.1.3 Maximum Source

Tables B-16 through B-20 present surface dose rates averaged over segments of the radial and axial surfaces of the 21-PWR waste package with the 30.48-cm (12-in) thick concrete structure located 3 m (9.8 ft) away. The neutron intensity peaking factor used in the calculation is 2.47 (BSC 2004 [DIRS 169593], Section 5.2.1).

Table B-16. Dose Rates on Inner Surface of Inner Vessel: Maximum PWR SNF (Concrete)

Axial Location (Surface 111)	Gamma		Neutron		Total	
	Dose Rate (rem/h)	Relative Error	Dose Rate (rem/h)	Relative Error	Dose Rate (rem/h)	Relative Error
Segment 1	1.46E+04	0.0013	4.57E+01	0.0039	1.46E+04	0.0013
Segment 2	2.93E+04	0.0013	6.29E+01	0.0042	2.94E+04	0.0013
Segment 3	3.65E+04	0.0014	9.37E+01	0.0032	3.66E+04	0.0014
Segment 4	5.28E+04	0.0012	2.01E+02	0.0018	5.30E+04	0.0012
Segment 5	6.65E+04	0.0010	2.58E+02	0.0016	6.68E+04	0.0010
Segment 6	6.65E+04	0.0010	2.66E+02	0.0015	6.67E+04	0.0010
Segment 7	6.66E+04	0.0010	2.60E+02	0.0016	6.68E+04	0.0010
Segment 8	5.34E+04	0.0012	2.08E+02	0.0018	5.36E+04	0.0012
Segment 9	4.61E+04	0.0021	1.08E+02	0.0045	4.62E+04	0.0021

Source: BSC 2004 [DIRS 169593], Table 6.3-1.

Table B-17. Dose Rates on Waste Package Outer Radial Surface: Maximum PWR SNF (Concrete)

Axial Location (Surface 4)	Gamma		Neutron		Total	
	Dose Rate (rem/h)	Relative Error	Dose Rate (rem/h)	Relative Error	Dose Rate (rem/h)	Relative Error
Segment 1	5.00E+02	0.0016	1.26E+01	0.0042	5.13E+02	0.0016
Segment 2	1.04E+03	0.0017	1.68E+01	0.0045	1.06E+03	0.0016
Segment 3	1.18E+03	0.0022	2.36E+01	0.0034	1.20E+03	0.0022
Segment 4	1.18E+03	0.0022	4.66E+01	0.0018	1.22E+03	0.0028
Segment 5	1.46E+03	0.0023	5.87E+01	0.0016	1.52E+03	0.0022
Segment 6	1.46E+03	0.0023	6.04E+01	0.0015	1.52E+03	0.0022
Segment 7	1.46E+03	0.0023	5.91E+01	0.0016	1.51E+03	0.0022
Segment 8	1.20E+03	0.0028	4.81E+01	0.0018	1.24E+03	0.0027
Segment 9	1.36E+03	0.0037	2.64E+01	0.0049	1.39E+03	0.0036

Source: BSC 2004 [DIRS 169593], Table 6.3-2.

Table B-18. Dose Rates on Radial Surface 1 m from Waste Package: Maximum PWR SNF (Concrete)

Axial Location (Surface 50)	Gamma		Neutron		Total	
	Dose Rate (rem/h)	Relative Error	Dose Rate (rem/h)	Relative Error	Dose Rate (rem/h)	Relative Error
Segment 1	2.35E+02	0.0027	9.00E+00	0.0032	2.44E+02	0.0026
Segment 2	3.00E+02	0.0033	1.08E+01	0.0035	3.11E+02	0.0032
Segment 3	3.58E+02	0.0028	1.26E+01	0.0027	3.71E+02	0.0027
Segment 4	4.27E+02	0.0022	1.63E+01	0.0017	4.44E+02	0.0021
Segment 5	5.65E+02	0.0018	2.00E+01	0.0014	5.85E+02	0.0018
Segment 6	5.72E+02	0.0019	2.12E+01	0.0014	5.93E+02	0.0018
Segment 7	5.56E+02	0.0018	2.00E+01	0.0015	5.76E+02	0.0018
Segment 8	3.83E+02	0.0024	1.59E+01	0.0017	3.99E+02	0.0023
Segment 9	2.96E+02	0.0057	1.26E+01	0.0042	3.09E+02	0.0055

Source: BSC 2004 [DIRS 169593], Table 6.3-3.

Table B-19. Dose Rates on Radial Surface 2 m from Waste Package: Maximum PWR SNF (Concrete)

Axial Location (surface 51)	Gamma		Neutron		Total	
	Dose Rate (rem/h)	Relative Error	Dose Rate (rem/h)	Relative Error	Dose Rate (rem/h)	Relative Error
Segment 1	1.62E+02	0.0031	8.06E+00	0.0025	1.70E+02	0.0030
Segment 2	1.89E+02	0.0039	8.88E+00	0.0030	1.98E+02	0.0038
Segment 3	2.11E+02	0.0031	9.66E+00	0.0024	2.21E+02	0.0030
Segment 4	2.49E+02	0.0022	1.12E+01	0.0016	2.61E+02	0.0021
Segment 5	3.43E+02	0.0017	1.28E+01	0.0015	3.56E+02	0.0017
Segment 6	3.52E+02	0.0018	1.34E+01	0.0014	3.66E+02	0.0017
Segment 7	3.30E+02	0.0019	1.28E+01	0.0015	3.43E+02	0.0018
Segment 8	2.24E+02	0.0025	1.10E+01	0.0016	2.35E+02	0.0023
Segment 9	1.85E+02	0.0060	9.75E+00	0.0039	1.94E+02	0.0057

Source: BSC 2004 [DIRS 169593], Table 6.3-4.

Table B-20. Dose Rates on Segments of Axial Surfaces: Maximum PWR SNF (Concrete)

Axial Location	Gamma		Neutron		Total	
	Dose Rate (rem/h)	Relative Error	Dose Rate (rem/h)	Relative Error	Dose Rate (rem/h)	Relative Error
Top of Waste Package (Surface 41)						
Segment 10	8.13E+02	0.0028	1.52E+01	0.0062	8.28E+02	0.0028
Segment 11	4.95E+02	0.0021	1.10E+01	0.0044	5.06E+02	0.0020
Segment 12	1.67E+02	0.0020	6.87E+00	0.0028	1.73E+02	0.0019
1 m from Waste Package top (Surface 54)						
Segment 11	2.42E+02	0.0025	5.76E+00	0.0051	2.47E+02	0.0024
Segment 12	9.50E+01	0.0024	4.84E+00	0.0032	9.98E+01	0.0022
2 m from Waste Package top (Surface 55)						
Segment 11	1.25E+02	0.0034	4.19E+00	0.0060	1.29E+02	0.0033
Segment 13	4.96E+01	0.0019	3.87E+00	0.0019	5.35E+01	0.0017
Bottom of Waste Package (Surface 19)						
Segment 14	2.78E+03	0.0061	4.66E+01	0.0087	2.83E+03	0.0060
Segment 10	2.77E+03	0.0036	4.34E+01	0.0053	2.81E+03	0.0035
Segment 11	1.88E+03	0.0021	2.77E+01	0.0035	1.91E+03	0.0021
Segment 12	2.76E+02	0.0031	1.19E+01	0.0023	2.87E+02	0.0030
1 m from Waste Package bottom (Surface 52)						
Segment 11	8.41E+02	0.0023	1.12E+01	0.0035	8.52E+02	0.0022
Segment 12	2.67E+02	0.0020	7.74E+00	0.0024	2.75E+02	0.0020
2 m from Waste Package bottom (Surface 53)						
Segment 11	3.93E+02	0.0031	6.72E+00	0.0044	4.00E+02	0.0031
Segment 13	1.08E+02	0.0017	5.34E+00	0.0016	1.13E+02	0.0016

Source: BSC 2004 [DIRS 169593], Table 6.3-5.

B.2 44-BWR

B.2.1 Average Source

Tables B-21 through B-25 present surface dose rates averaged over segments of the radial and axial surfaces of the 44-BWR waste package without any concrete structure surrounding it (see Figures B-3 and B-4 for segment and surface locations). Tables B-26 through B-30 present surface dose rates averaged over segments of the radial and axial surfaces of the 44-BWR waste package with the 30.48-cm (12-in) thick concrete structure located 3 m (9.8 ft) away. The neutron intensity peaking factor is 2.62 for both sets of calculations. It can be seen that by including the concrete structure outside the waste package, the dose rates increase by approximately 3 to 10 percent on the waste package external surfaces, depending on location (the closer to the concrete wall, the higher the increase in dose rates). This increase in dose rates is due to scattering radiation from the concrete structure. The dose rates on the inner surface of the waste package are not affected by the concrete structure. Further, the tables show that the contributions from secondary gamma rays to the total dose rates are very small, as the primary gamma source is the predominant contributor for an unshielded waste package. Consequently, these will not be included in future sections of this report. However, secondary gamma contributions may become important in a shielded case (BSC 2003 [DIRS 166596]).

Table B-21. Dose Rates on Inner Surface of Inner Vessel: Average BWR SNF (no Concrete)

Axial Location (Surface 111)	Gamma		Neutron		Sec. Gamma		Total	
	Dose Rate (rem/h)	Relative Error						
Segment 1	9.20E+02	0.0029	1.69E+00	0.0044	5.19E-03	0.0116	9.21E+02	0.0029
Segment 2	1.69E+03	0.0022	2.19E+00	0.0039	6.31E-03	0.0110	1.70E+03	0.0022
Segment 3	3.23E+03	0.0022	3.47E+00	0.0029	9.24E-03	0.0078	3.23E+03	0.0022
Segment 4	7.39E+03	0.0013	7.80E+00	0.0014	2.33E-02	0.0032	7.40E+03	0.0013
Segment 5	7.45E+03	0.0013	9.76E+00	0.0012	2.98E-02	0.0029	7.46E+03	0.0013
Segment 6	7.47E+03	0.0013	1.00E+01	0.0012	3.09E-02	0.0028	7.48E+03	0.0013
Segment 7	7.50E+03	0.0013	9.79E+00	0.0012	2.99E-02	0.0028	7.51E+03	0.0013
Segment 8	5.87E+03	0.0016	7.88E+00	0.0014	2.36E-02	0.0032	5.88E+03	0.0016
Segment 9	2.00E+03	0.0050	3.92E+00	0.0032	1.18E-02	0.0084	2.00E+03	0.0050

Source: BSC 2003 [DIRS 166596], Table 6.1-1.

Table B-22. Dose Rates on Waste Package Outer Radial Surface: Average BWR SNF (no Concrete)

Axial Location (Surface 4)	Gamma		Neutron		Sec. Gamma		Total	
	Dose Rate (rem/h)	Relative Error						
Segment 1	2.77E+01	0.0028	3.46E-01	0.0046	1.38E-03	0.013	2.80E+01	0.0027
Segment 2	5.66E+01	0.0021	4.65E-01	0.0040	1.72E-03	0.0119	5.71E+01	0.0021
Segment 3	9.91E+01	0.0026	7.46E-01	0.0030	2.47E-03	0.0085	9.99E+01	0.0026
Segment 4	1.23E+02	0.0030	1.66E+00	0.0014	5.26E-03	0.0036	1.25E+02	0.0030
Segment 5	1.22E+02	0.0030	2.07E+00	0.0012	6.90E-03	0.0032	1.24E+02	0.0029
Segment 6	1.23E+02	0.0030	2.11E+00	0.0012	7.17E-03	0.0031	1.25E+02	0.0029
Segment 7	1.23E+02	0.0030	2.07E+00	0.0012	6.92E-03	0.0032	1.25E+02	0.0030
Segment 8	9.57E+01	0.0038	1.68E+00	0.0014	5.38E-03	0.0036	9.74E+01	0.0038
Segment 9	3.91E+01	0.0089	8.45E-01	0.0033	2.89E-03	0.0096	3.99E+01	0.0087

Source: BSC 2003 [DIRS 166596], Table 6.1-2.

Table B-23. Dose Rates on Radial Surface 1 m from Waste Package: Average BWR SNF (no Concrete)

Axial Location (Surface 50)	Gamma		Neutron		Sec. Gamma		Total	
	Dose Rate (rem/h)	Relative Error						
Segment 1	1.70E+01	0.0041	1.94E-01	0.0022	6.39E-04	0.0087	1.72E+01	0.0040
Segment 2	2.26E+01	0.0039	2.47E-01	0.0019	7.85E-04	0.0078	2.28E+01	0.0038
Segment 3	2.94E+01	0.0034	3.11E-01	0.0016	9.86E-04	0.0062	2.98E+01	0.0034
Segment 4	3.94E+01	0.0023	4.44E-01	0.001	1.40E-03	0.0033	3.98E+01	0.0023
Segment 5	4.43E+01	0.0023	5.76E-01	0.0008	1.82E-03	0.0028	4.49E+01	0.0023
Segment 6	4.53E+01	0.0023	6.15E-01	0.0008	1.95E-03	0.0027	4.59E+01	0.0023
Segment 7	4.34E+01	0.0024	5.73E-01	0.0008	1.81E-03	0.0029	4.40E+01	0.0024
Segment 8	3.46E+01	0.0026	4.33E-01	0.001	1.36E-03	0.0033	3.50E+01	0.0026
Segment 9	2.22E+01	0.0056	3.05E-01	0.0019	9.62E-04	0.0078	2.25E+01	0.0055

Source: BSC 2003 [DIRS 166596], Table 6.1-3.

Table B-24. Dose Rates on Radial Surface 2 m from Waste Package: Average BWR SNF (no Concrete)

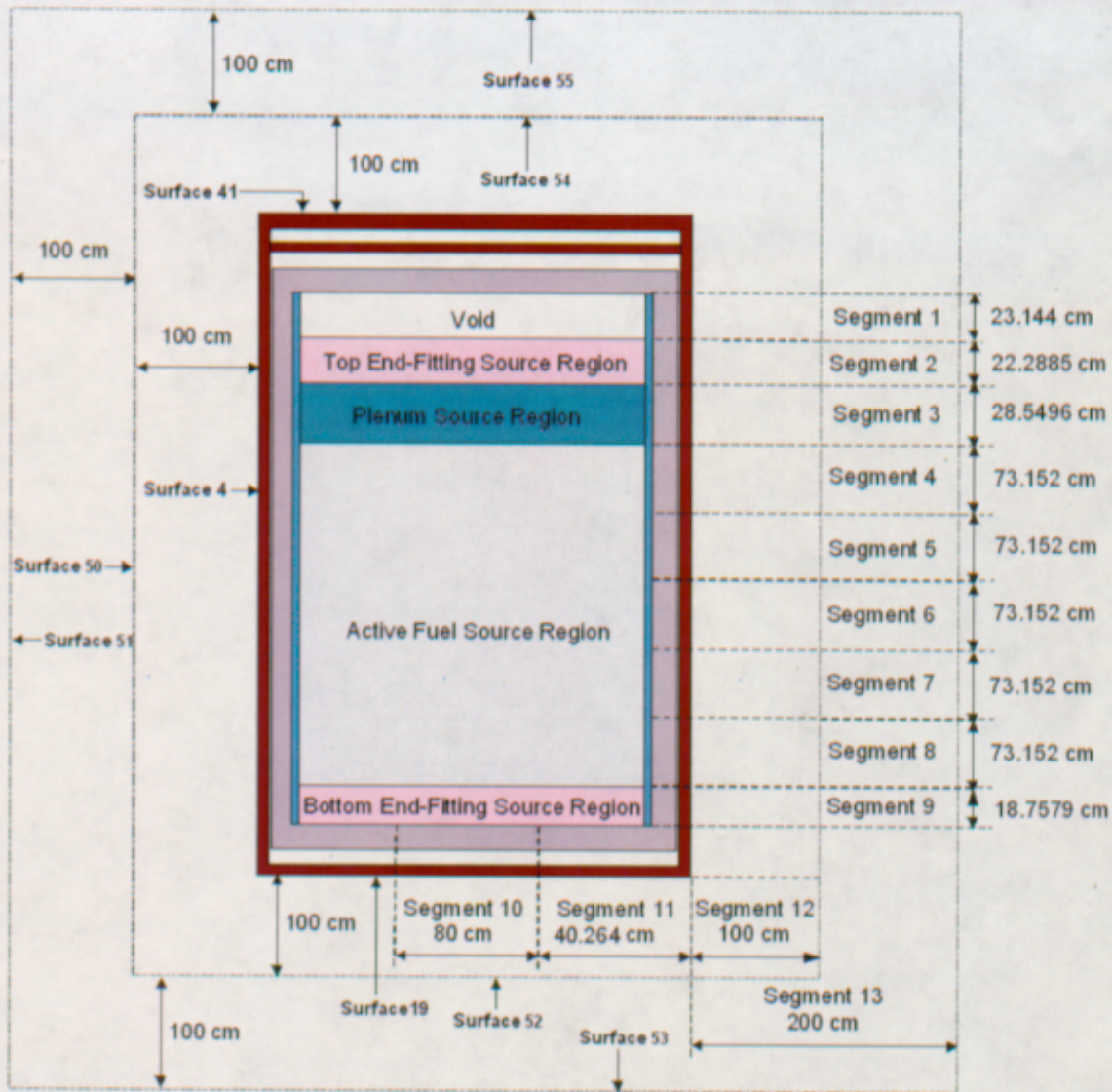
Axial Location (Surface 51)	Gamma		Neutron		Sec. Gamma		Total	
	Dose Rate (rem/h)	Relative Error						
Segment 1	1.21E+01	0.0045	1.45E-01	0.0018	4.59E-04	0.0078	1.23E+01	0.0044
Segment 2	1.42E+01	0.0044	1.66E-01	0.0018	5.26E-04	0.0075	1.44E+01	0.0043
Segment 3	1.67E+01	0.0037	1.90E-01	0.0015	6.02E-04	0.0062	1.69E+01	0.0036
Segment 4	2.11E+01	0.0023	2.36E-01	0.0009	7.39E-04	0.0034	2.13E+01	0.0023
Segment 5	2.48E+01	0.0023	2.87E-01	0.0008	8.97E-04	0.0031	2.51E+01	0.0022
Segment 6	2.58E+01	0.0022	3.06E-01	0.0008	9.48E-04	0.0030	2.61E+01	0.0022
Segment 7	2.38E+01	0.0024	2.85E-01	0.0008	8.85E-04	0.0031	2.41E+01	0.0023
Segment 8	1.87E+01	0.0026	2.31E-01	0.0009	7.21E-04	0.0035	1.89E+01	0.0026
Segment 9	1.39E+01	0.0054	1.86E-01	0.0018	5.84E-04	0.0075	1.41E+01	0.0053

Source: BSC 2003 [DIRS 166596], Table 6.1-4.

Table B-25. Dose Rates on Segments of Axial Surfaces: Average BWR SNF (no Concrete)

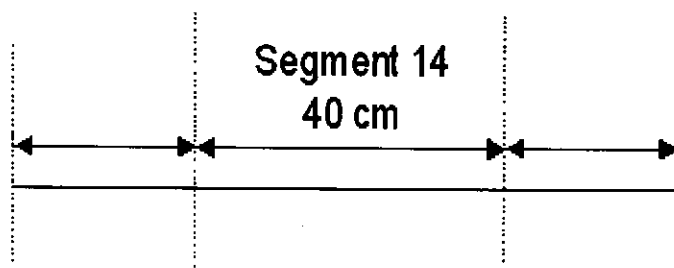
Axial Location	Gamma		Neutron		Sec. Gamma		Total	
	Dose Rate (rem/h)	Relative Error						
Top of Waste Package (Surface 41)								
Segment 10	5.71E+01	0.0037	5.28E-01	0.0049	1.97E-03	0.0146	5.77E+01	0.0036
Segment 11	3.35E+01	0.0027	3.43E-01	0.0037	1.38E-03	0.0101	3.38E+01	0.0026
Segment 12	1.02E+01	0.0025	1.33E-01	0.0022	4.59E-04	0.0084	1.03E+01	0.0024
1 m from Waste Package top (Surface 54)								
Area equal to Waste Package top surface	1.54E+01	0.0027	9.86E-02	0.0037	3.49E-04	0.0122	1.55E+01	0.0026
Segment 12	5.11E+00	0.0025	5.98E-02	0.0025	2.13E-04	0.0079	5.17E+00	0.0025
2 m from Waste Package top (Surface 55)								
Area equal to Waste Package top surface	7.18E+00	0.0037	4.09E-02	0.0049	1.32E-04	0.0194	7.22E+00	0.0036
Segment 13	2.22E+00	0.0023	3.52E-02	0.0014	1.22E-04	0.0045	2.26E+00	0.0022
Bottom of Waste Package (Surface 19)								
Segment 14	8.91E+01	0.0134	1.38E+00	0.0045	4.55E-03	0.0109	9.05E+01	0.0132
Segment 11	5.53E+01	0.0098	8.31E-01	0.0034	2.80E-03	0.008	5.61E+01	0.0097
Segment 12	1.16E+01	0.0069	2.63E-01	0.002	8.41E-04	0.0066	1.19E+01	0.0068
1 m from Waste Package bottom (Surface 52)								
Area equal to Waste Package bottom surface	2.55E+01	0.0098	2.40E-01	0.0035	7.24E-04	0.0096	2.57E+01	0.0097
Segment 12	7.48E+00	0.0081	1.26E-01	0.0025	4.08E-04	0.0066	7.61E+00	0.0080
2 m from Waste Package bottom (Surface 53)								
Area equal to Waste Package bottom surface	1.16E+01	0.0129	9.59E-02	0.0045	2.73E-04	0.0148	1.17E+01	0.0128
Segment 13	2.98E+00	0.0058	5.82E-02	0.0015	1.89E-04	0.0041	3.04E+00	0.0057

Source: BSC 2003 [DIRS 166596], Table 6.1-5.



Source: BSC 2003 [DIRS 166596], Figure 5.2-2.

Figure B-2. Surface Segments Used for Dose Rate Calculations



Source: BSC 2003 [DIRS 166596], Figure 5.2-3.

Figure B-3. Segment of Bottom Surface of Outer Lid Used in Dose Rate Calculations

Table B-26. Dose Rates on Inner Surface of Inner Vessel: Average BWR SNF (Concrete)

Axial Location (Surface 111)	Gamm		Neutron		Sec. Gamma		Total	
	Dose Rate (rem/h)	Relative Error						
Segment 1	9.20E+02	0.0030	1.78E+00	0.0050	7.33E-03	0.0149	9.22E+02	0.0030
Segment 2	1.70E+03	0.0023	2.28E+00	0.0045	8.32E-03	0.0138	1.70E+03	0.0022
Segment 3	3.22E+03	0.0023	3.56E+00	0.0034	1.13E-02	0.0099	3.23E+03	0.0023
Segment 4	7.39E+03	0.0014	7.90E+00	0.0017	2.54E-02	0.0040	7.40E+03	0.0014
Segment 5	7.45E+03	0.0014	9.88E+00	0.0015	3.19E-02	0.0036	7.46E+03	0.0014
Segment 6	7.47E+03	0.0014	1.01E+01	0.0014	3.29E-02	0.0034	7.48E+03	0.0014
Segment 7	7.50E+03	0.0014	9.89E+00	0.0015	3.19E-02	0.0035	7.51E+03	0.0014
Segment 8	5.87E+03	0.0017	7.99E+00	0.0016	2.55E-02	0.0039	5.87E+03	0.0017
Segment 9	1.99E+03	0.0053	4.03E+00	0.0037	1.37E-02	0.0101	2.00E+03	0.0053

Source: BSC 2003 [DIRS 166596], Table 6.1-6.

Table B-27. Dose Rates on Waste Package Outer Radial Surface: Average BWR SNF (Concrete)

Axial Location (Surface 4)	Gamma		Neutron		Sec. Gamma		Total	
	Dose Rate (rem/h)	Relative Error						
Segment 1	2.94E+01	0.0035	4.83E-01	0.0047	1.15E-02	0.0256	2.99E+01	0.0035
Segment 2	5.88E+01	0.0025	6.10E-01	0.0043	1.17E-02	0.0238	5.94E+01	0.0024
Segment 3	1.01E+02	0.0027	8.95E-01	0.0032	1.29E-02	0.0204	1.02E+02	0.0027
Segment 4	1.25E+02	0.0031	1.82E+00	0.0016	1.56E-02	0.0104	1.27E+02	0.0030
Segment 5	1.24E+02	0.0032	2.24E+00	0.0014	1.76E-02	0.0098	1.26E+02	0.0031
Segment 6	1.25E+02	0.0031	2.28E+00	0.0014	1.81E-02	0.0096	1.28E+02	0.0030
Segment 7	1.25E+02	0.0031	2.24E+00	0.0014	1.79E-02	0.0096	1.27E+02	0.0030
Segment 8	1.21E+02	0.0032	1.84E+00	0.0016	1.60E-02	0.0105	1.23E+02	0.0031
Segment 9	4.06E+01	0.0094	1.00E+00	0.0036	1.30E-02	0.0233	4.16E+01	0.0091

Source: BSC 2003 [DIRS 166596], Table 6.1-7.

Table B-28. Dose Rates on Radial Surface 1 m from Waste Package: Average BWR SNF (Concrete)

Axial Location (Surface 50)	Gamma		Neutron		Sec. Gamma		Total	
	Dose Rate (rem/h)	Relative Error						
Segment 1	1.97E+01	0.0055	3.49E-01	0.0029	5.76E-03	0.0128	2.01E+01	0.0054
Segment 2	2.53E+01	0.0051	4.06E-01	0.0027	6.07E-03	0.0126	2.57E+01	0.0050
Segment 3	3.25E+01	0.0043	4.75E-01	0.0022	6.32E-03	0.0103	3.30E+01	0.0042
Segment 4	4.23E+01	0.0027	6.18E-01	0.0014	6.97E-03	0.0069	4.29E+01	0.0026
Segment 5	4.76E+01	0.0026	7.58E-01	0.0012	7.59E-03	0.0065	4.84E+01	0.0026
Segment 6	4.86E+01	0.0026	8.03E-01	0.0011	7.79E-03	0.0065	4.94E+01	0.0025
Segment 7	4.67E+01	0.0027	7.57E-01	0.0012	7.52E-03	0.0065	4.75E+01	0.0026
Segment 8	3.77E+01	0.0031	6.09E-01	0.0013	6.90E-03	0.0072	3.83E+01	0.0031
Segment 9	2.54E+01	0.0068	4.74E-01	0.0026	6.17E-03	0.0115	2.58E+01	0.0067

Source: BSC 2003 [DIRS 166596], Table 6.1-8.

Table B-29. Dose Rates on Radial Surface 2 m from Waste Package: Average BWR SNF (Concrete)

Axial Location (Surface 51)	Gamma		Neutron		Sec. Gamma		Total	
	Dose Rate (rem/h)	Relative Error						
Segment 1	1.52E+01	0.0062	3.09E-01	0.0026	5.34E-03	0.0109	1.55E+01	0.0061
Segment 2	1.74E+01	0.0055	3.36E-01	0.0025	5.61E-03	0.0108	1.78E+01	0.0054
Segment 3	2.01E+01	0.0047	3.67E-01	0.0021	5.67E-03	0.0097	2.05E+01	0.0046
Segment 4	2.48E+01	0.0030	4.25E-01	0.0014	5.99E-03	0.0068	2.52E+01	0.0030
Segment 5	2.89E+01	0.0029	4.89E-01	0.0012	6.29E-03	0.0064	2.94E+01	0.0029
Segment 6	2.98E+01	0.0027	5.11E-01	0.0012	6.46E-03	0.0065	3.03E+01	0.0027
Segment 7	2.77E+01	0.0029	4.87E-01	0.0013	6.35E-03	0.0067	2.82E+01	0.0029
Segment 8	2.22E+01	0.0034	4.21E-01	0.0014	6.04E-03	0.0069	2.26E+01	0.0033
Segment 9	1.71E+01	0.0066	3.69E-01	0.0025	5.74E-03	0.0119	1.75E+01	0.0065

Source: BSC 2003 [DIRS 166596], Table 6.1-9.

Table B-30. Dose Rates on Segments of Axial Surfaces: Average BWR SNF (Concrete)

Axial Location	Gamma		Neutron		Sec. Gamma		Total	
	Dose Rate (rem/h)	Relative Error						
Top of Waste Package (Surface 41)								
Segment 10	5.78E+01	0.0042	6.15E-01	0.0057	1.04E-02	0.0405	5.84E+01	0.0041
Segment 11	3.42E+01	0.0034	4.32E-01	0.0042	1.07E-02	0.0242	3.46E+01	0.0033
Segment 12	1.22E+01	0.0040	2.77E-01	0.0022	5.63E-03	0.0083	1.24E+01	0.0039
1 m from Waste Package top (Surface 54)								
Area equal to Waste Package top surface	1.72E+01	0.0045	2.27E-01	0.0041	4.84E-03	0.0156	1.74E+01	0.0044
Segment 12	6.94E+00	0.0054	1.89E-01	0.0025	4.71E-03	0.0085	7.13E+00	0.0053
2 m from Waste Package top (Surface 55)								
Area equal to Waste Package top surface	8.99E+00	0.0087	1.62E-01	0.0049	4.49E-03	0.0166	9.15E+00	0.0085
Segment 13	3.80E+00	0.0041	1.51E-01	0.0016	4.43E-03	0.0062	3.96E+00	0.0040
Bottom of Waste Package (Surface 19)								
Segment 14	9.01E+01	0.0141	1.47E+00	0.0052	1.33E-02	0.0304	9.16E+01	0.0139
Segment 11	5.61E+01	0.0107	9.49E-01	0.0039	1.23E-02	0.0193	5.71E+01	0.0105
Segment 12	1.38E+01	0.0070	4.23E-01	0.002	6.32E-03	0.0077	1.42E+01	0.0068
1 m from Waste Package bottom (Surface 52)								
Area equal to Waste Package bottom surface	2.77E+01	0.0102	3.90E-01	0.0035	5.65E-03	0.0143	2.81E+01	0.0100
Segment 12	9.52E+00	0.0081	2.77E-01	0.0023	5.27E-03	0.0081	9.81E+00	0.0079
2 m from Waste Package bottom (Surface 53)								
Area equal to Waste Package bottom surface	1.38E+01	0.0131	2.41E-01	0.0042	4.84E-03	0.0144	1.41E+01	0.0129
Segment 13	4.82E+00	0.0057	1.94E-01	0.0015	4.83E-03	0.0059	5.02E+00	0.0055

Source: BSC 2003 [DIRS 166596], Table 6.1-10.

B.2.2 Maximum Source

Tables B-31 through B-35 present surface dose rates averaged over segments of the radial and axial surfaces of the 44-BWR waste package with the 30.48-cm (12-in) thick concrete structure located 3 m (9.8 ft) away (see Figures B-3 and B-4 for segment and surface locations). The neutron intensity peaking factor used in the calculation is 2.82 (BSC 2003 [DIRS 166596], Section 5.2.1).

Table B-31. Dose Rates on Inner Surface of Inner Vessel: Maximum BWR SNF (Concrete)

Axial Location (Surface 111)	Gamma		Neutron		Total	
	Dose Rate (rem/h)	Relative Error	Dose Rate (rem/h)	Relative Error	Dose Rate (rem/h)	Relative Error
Segment 1	1.53E+04	0.0014	2.89E+01	0.0046	1.53E+04	0.0014
Segment 2	2.83E+04	0.0011	3.69E+01	0.0042	2.84E+04	0.0011
Segment 3	4.58E+04	0.0011	5.78E+01	0.0031	4.58E+04	0.0011
Segment 4	4.16E+04	0.0016	1.29E+02	0.0015	4.18E+04	0.0016
Segment 5	4.08E+04	0.0017	1.61E+02	0.0013	4.10E+04	0.0017
Segment 6	4.09E+04	0.0017	1.65E+02	0.0013	4.11E+04	0.0017
Segment 7	3.28E+04	0.0021	1.61E+02	0.0013	3.30E+04	0.0021
Segment 8	3.23E+04	0.0021	1.30E+02	0.0015	3.24E+04	0.0021
Segment 9	1.65E+04	0.0043	6.56E+01	0.0034	1.65E+04	0.0043

Source: BSC 2003 [DIRS 166596], Table 6.2-1.

Table B-32. Dose Rates on Waste Package Outer Radial Surface: Maximum BWR SNF (Concrete)

Axial Location (Surface 4)	Gamma		Neutron		Total	
	Dose Rate (rem/h)	Relative Error	Dose Rate (rem/h)	Relative Error	Dose Rate (rem/h)	Relative Error
Segment 1	5.10E+02	0.0022	7.91E+00	0.0043	5.18E+02	0.0022
Segment 2	1.04E+03	0.0015	9.88E+00	0.0039	1.05E+03	0.0015
Segment 3	1.60E+03	0.0015	1.45E+01	0.003	1.61E+03	0.0015
Segment 4	8.41E+02	0.0035	2.95E+01	0.0015	8.71E+02	0.0034
Segment 5	7.84E+02	0.0039	3.63E+01	0.0013	8.20E+02	0.0037
Segment 6	7.87E+02	0.0038	3.72E+01	0.0013	8.24E+02	0.0036
Segment 7	7.94E+02	0.0038	3.65E+01	0.0013	8.30E+02	0.0036
Segment 8	7.74E+02	0.0038	2.99E+01	0.0015	8.04E+02	0.0037
Segment 9	4.44E+02	0.0068	1.63E+01	0.0033	4.61E+02	0.0066

Source: BSC 2003 [DIRS 166596], Table 6.2-2.

Table B-33. Dose Rates on Radial Surface 1 m from Waste Package: Maximum BWR SNF (Concrete)

Axial Location (Surface 50)	Gamma		Neutron		Total	
	Dose Rate (rem/h)	Relative Error	Dose Rate (rem/h)	Relative Error	Dose Rate (rem/h)	Relative Error
Segment 1	2.38E+02	0.0034	5.69E+00	0.0026	2.44E+02	0.0033
Segment 2	2.88E+02	0.0031	6.61E+00	0.0024	2.95E+02	0.0030
Segment 3	3.31E+02	0.0030	7.74E+00	0.002	3.39E+02	0.0029
Segment 4	3.39E+02	0.0026	1.00E+01	0.0012	3.49E+02	0.0025
Segment 5	3.18E+02	0.0030	1.24E+01	0.001	3.30E+02	0.0029
Segment 6	3.13E+02	0.0031	1.30E+01	0.001	3.26E+02	0.0030
Segment 7	2.99E+02	0.0032	1.23E+01	0.001	3.12E+02	0.0031
Segment 8	2.49E+02	0.0035	9.94E+00	0.0012	2.59E+02	0.0034
Segment 9	1.75E+02	0.0070	7.69E+00	0.0023	1.83E+02	0.0067

Source: BSC 2003 [DIRS 166596], Table 6.2-3.

Table B-34. Dose Rates on Radial Surface 2 m from Waste Package: Maximum BWR SNF (Concrete)

Axial Location (Surface 51)	Gamma		Neutron		Total	
	Dose Rate (rem/h)	Relative Error	Dose Rate (rem/h)	Relative Error	Dose Rate (rem/h)	Relative Error
Segment 1	1.45E+02	0.0047	5.03E+00	0.0024	1.50E+02	0.0045
Segment 2	1.61E+02	0.0043	5.45E+00	0.0023	1.67E+02	0.0042
Segment 3	1.78E+02	0.0043	5.95E+00	0.0019	1.84E+02	0.0041
Segment 4	1.94E+02	0.0028	6.93E+00	0.0013	2.01E+02	0.0027
Segment 5	2.03E+02	0.0030	7.95E+00	0.0011	2.11E+02	0.0029
Segment 6	1.97E+02	0.0030	8.32E+00	0.0011	2.05E+02	0.0029
Segment 7	1.81E+02	0.0033	7.92E+00	0.0011	1.89E+02	0.0031
Segment 8	1.46E+02	0.0038	6.85E+00	0.0013	1.53E+02	0.0036
Segment 9	1.18E+02	0.0074	5.98E+00	0.0023	1.24E+02	0.0071

Source: BSC 2003 [DIRS 166596], Table 6.2-4.

Table B-35. Dose Rates on Segments of Axial Surfaces: Maximum BWR SNF (Concrete)

Axial Location	Gamma		Neutron		Total	
	Dose Rate (rem/h)	Relative Error	Dose Rate (rem/h)	Relative Error	Dose Rate (rem/h)	Relative Error
Top of Waste Package (Surface 41)						
Segment 10	9.92E+02	0.0021	9.89E+00	0.0052	1.00E+03	0.0020
Segment 11	5.89E+02	0.0017	7.05E+00	0.0038	5.96E+02	0.0017
Segment 12	1.80E+02	0.0022	4.52E+00	0.002	1.84E+02	0.0021
1 m from Waste Package top (Surface 54)						
Area equal to Waste Package top surface	2.80E+02	0.0022	3.70E+00	0.0037	2.84E+02	0.0021
Segment 12	1.01E+02	0.0028	3.08E+00	0.0023	1.04E+02	0.0027
2 m from Waste Package top (Surface 55)						
Area equal to Waste Package top surface	1.40E+02	0.0040	2.64E+00	0.0045	1.42E+02	0.0039
Segment 13	4.68E+01	0.0025	2.46E+00	0.0014	4.92E+01	0.0024
Bottom of Waste Package (Surface 19)						
Segment 14	8.81E+02	0.0111	2.42E+01	0.0047	9.05E+02	0.0108
Segment 11	5.81E+02	0.0082	1.53E+01	0.0035	5.96E+02	0.0080
Segment 12	1.13E+02	0.0068	6.91E+00	0.0018	1.19E+02	0.0064
1 m from Waste Package bottom (Surface 52)						
Area equal to Waste Package bottom surface	2.67E+02	0.0084	6.36E+00	0.0033	2.73E+02	0.0082
Segment 12	9.07E+01	0.0070	4.49E+00	0.0021	9.52E+01	0.0066
2 m from Waste Package bottom (Surface 53)						
Area equal to Waste Package bottom surface	1.28E+02	0.0109	3.89E+00	0.0039	1.32E+02	0.0106
Segment 13	4.08E+01	0.0052	3.16E+00	0.0014	4.40E+01	0.0049

Source: BSC 2003 [DIRS 166596], Table 6.2-5.

BSC

Engineering Change Notice

1. QA: QA
2. Page 1 of 1

Complete only applicable items.

000-00C-DSU0-02800-000-00B-ECN1

3. Document Identifier: 000-00C-DSU0-02800-000-00B	4. Rev.: 00B	5. Title: Commercial SNF Waste Package Design Report	6. ECN: 1
---	-----------------	---	--------------

7. Reason for Change:
Per LP-3.12Q-BSC Design Calculations and Analyses Section 5.1 [2]c,

"The decision of the DEM, PCSA Manager, Criticality Manager, or PCA Manager to issue calculations or analyses with a "committed" status will be based on an experienced assessment of the likelihood that the results of the calculation or analysis will change, and the degree of impact those changes will have on designs that support the regulatory submittals or procurement activities, based on the design bounding conservatism."

The status designation of *Commercial SNF Waste Package Design Report* (000-00C-DSU0-02800-000-00B) can be changed to "Committed" as the results are not expected to change in such a manner that will affect support of regulatory submittals.

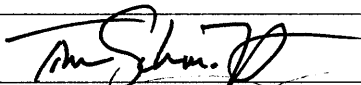
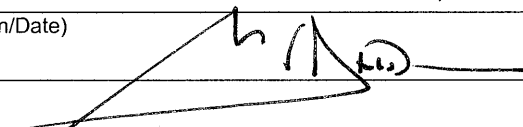
8. Supersedes Change Document: Yes If, Yes, Change Doc.: _____ No

9. Change Impact:

Inputs Changed: <input type="checkbox"/> Yes <input checked="" type="checkbox"/> No	Results Impacted: <input type="checkbox"/> Yes <input checked="" type="checkbox"/> No
Assumptions Changed: <input type="checkbox"/> Yes <input checked="" type="checkbox"/> No	Design Impacted: <input type="checkbox"/> Yes <input checked="" type="checkbox"/> No

10. Description of Change: (Address any "Yes" answers)
Add a "Committed" option in Block 7. On the cover sheet and change the "Document Status Designation" from Preliminary to "Committed". Block 7 on the cover sheet should read as follows

7. Document Status Designation: <input type="checkbox"/> Preliminary <input checked="" type="checkbox"/> Committed <input type="checkbox"/> Final <input type="checkbox"/> Cancelled

11. Originator: (Print/Sign/Date) Tim Schmitt	 8/12/05
Checker: (Print/Sign/Date) Michael Mullin	 8/12/05
Approved: (Print/Sign/Date) Michael J. Anderson	 8/12/05